ROBERT GORDON UNIVERSITY•ABERDEEN

# OpenAIR@RGU

## The Open Access Institutional Repository at Robert Gordon University

http://openair.rgu.ac.uk

### Citation Details

**Citation for the version of the work held in 'OpenAIR@RGU':**

**CHEONG-KI, C., 1981. An investigation of eddy diffusivities of momentum and heat in circular pipes. Available from *OpenAIR@RGU*. [online]. Available from: http://openair.rgu.ac.uk**

**Copyright**

Items in 'OpenAIR@RGU', Robert Gordon University Open Access Institutional Repository, are protected by copyright and intellectual property law. If you believe that any material held in 'OpenAIR@RGU' infringes copyright, please contact openair-help@rgu.ac.uk with details. The item will be removed from the repository while the claim is investigated.

# AN INVESTIGATION OF EDDY DIFFUSIVITIES OF MOMENTUM AND HEAT IN CIRCULAR PIPES

Thesis by

CHAN CHEONG-KI

In Partial Fulfilment of the Requirements
for the Degree of Doctor of Philosophy
of the Council for National Academic Awards.

Robert Gordon's Institute of Technology, Aberdeen
and University of Glasgow, Glasgow.

July, 1981

## ABSTRACT

The theoretical analysis of the present work was based on a thermodynamic approach, using the method of inference. An analysis was made to find the macroscopic turbulence transport properties from the description of microscopic behaviour of entities of varying shape, size and velocity. Momentum and energy transport in a turbulent fluid were investigated and expressions for the eddy diffusivities of momentum and heat proposed. Communication theory has been successfully used as a means for the interpretation of turbulence parameters.

Velocity profiles in simple shear flows, obtained with the present analysis, were compared with those found by others, both experimentally and theoretically. An overall heat transfer similarity parameter was derived with the assumption of a constant turbulent Prandtl number.

Measurement of mean velocity, microscale, turbulence intensity and eddy diffusivities of momentum and heat were obtained in a water tunnel. Results were obtained for Reynolds numbers from $2 \times 10^5$ to $9 \times 10^5$. Pipes were roughened internally with paint mixed with fine particles and roughness ratio r/k ranging between $7.2 \times 10^3$ and $2.5 \times 10^5$ with absolute roughness height between 4μm and 10μm.

In the light of the present analysis, it is concluded that the new and more realistic approach to turbulence phenomenon is a useful concept for predicting turbulence transport properties, as well as heat transfer characteristics of a simple shear flow.


This is to declare that, while registered as a candidate for the degree of Ph.D. (C.N.A.A.), the author has not been a registered candidate for another award of the C.N.A.A., or of a University during the research programme. The work described in the thesis is the result of investigations conducted by the candidate during the research study, except where specific reference is made to other investigators.


Chan Cheong-Ki.

Postgraduate Studies

Laser Anemometer Course,
Imperial College, London.

## ACKNOWLEDGEMENT

The author wishes to express his most sincere thanks to his supervisors, Dr. P.G. Walburn, Mr. J.G. Black and Dr. W. Hanbury for all their help, advice and comments. Particularly to Dr. Walburn who provided the suggestions, criticisms and patience during the course of this project. Tremendous thanks are owed to Mr. J.R. Tyldesley, the late external supervisor who provided much of the original ideas and encouragement before his sudden death in February 1980.

Gratitude is also owed to Mr. M.C. Hately, of the School of Electrical and Electronic Engineering who offered a great deal of help regarding some of the electronic instrumentation; to Mr. R. Dunk, the Technician who helped in the manufacture and install-:ation of part of the experimental facilities, and to Mr. A. Rennie, the Senior Technician and some of his other technical staff who provided the general technical help throughout the years of the project. Also, the author is very grateful to Mr. H.P. Lui, who helped in producing the photographs in this report, and to Mrs. M. Booth, for her care and patience in the typing of this thesis in its final form.

Outwith the Institute, the financial assistance given by the Scottish Education Department is gratefully acknowledged. Finally, the author wishes to acknowledge the friendliness and concern given to him by his fellow students (postgraduates and undergraduates) while in Aberdeen and at Robert Gordon's Institute of Technology in particular without which the carrying out of the project would have been less rewarding.

TABLE OF CONTENTS

## LIST OF SYMBOLS

| | |
|---|---|
| a,b | distances |
| a,b,c | semi-principal axes of ellipsoidal entity |
| A | area |
| A,B,C | numerical constant |
| c | numerical constant |
| Cp | specific heat |
| d | size of the eddy |
| D | diameter of the pipe |
| $E_T$ | total energy per unit volume |
| f | friction factor |
| f | variable quantity as used in Reynolds rules of averages |
| $f_D$ | doppler frequency |
| F | diffusivity ratio (equation 3.77) |
| F | force |
| g | lateral correlation coefficient |
| g | variable quantity as used in Reynolds rules of averages |
| h | heat transfer |
| i,I | angle of incidence |
| $j_H$ | non-dimensional j factor for heat transfer as defined by Colburn (equation 2.13) |
| k | average roughness height |
| k | constant |
| k | thermal conductivity |
| K,K' | constants |
| $\ell$ | mixing length |
| m | mass |
| M | momentum |
| N | number of sample points |
| N | number of zeros of u fluctuations per unit time |
| Nu | Nusselt number |
| p | pressure |
| P | probability distribution |
| Pe | Peclet number |
| Pr | Prandtl number |

| | |
|---|---|
| $Pr_t$ | turbulent Prandtl number |
| q | enthalpy flux |
| q | heat transfer rate |
| q | transferable quantity in the mixing length theory |
| Q | energy flux |
| Q | heat source strength |
| r,R | angle of refraction |
| r | radius of the eddy |
| r | radius of the pipe |
| R | shape and size function of the eddy |
| Re | Reynolds number |
| S | entropy |
| St | Stanton number |
| t | time |
| T | period of oscillation |
| T | temperature |
| Tr | temperature difference between the eddy and the surrounding fluid |
| u | velocity in the x-direction |
| $u_{\delta 1}$ | velocity at the edge of the laminar sublayer |
| $u_\tau$ | friction velocity |
| $\overline{U}=(u,v,w)$ | mean velocity of fluid |
| Ue | internal energy per unit volume |
| v | velocity in the y-direction |
| $\overline{V}=(U,V,W)$ | absolute velocity of the eddy |
| $\overline{V}r=(Ur,Vr,Wr)$ | velocity of the eddy relative to the mean fluid velocity |
| w | velocity in the z-direction |
| w | vorticity |
| y | distance from the wall |
| $\alpha, \alpha'$ | Langrangian multiplier |
| $\beta, \beta'$ | temper of variable distribution |
| $\gamma$ | numerical constant as defined by Dipprey and Sabersky (equation 2.21) |
| $\delta$ | boundary layer thickness |
| $\varepsilon$ | turbulent exchange coefficient as defined by Boussinesq |

| | |
|---|---|
| $\varepsilon_H$ | eddy diffusivity of heat |
| $\varepsilon\mu$ | eddy viscosity |
| $\varepsilon_\nu$ | eddy diffusivity of momentum |
| $\eta$ | refractive index |
| $\Theta$ | angle |
| $\Theta$ | distortion factor |
| $\lambda$ | distance travelled by the entity |
| $\lambda$ | microscale |
| $\lambda$ | resistance factor |
| $\lambda$ | wavelength of laser beam |
| $\lambda^*$ | mean distance travelled by the entity |
| $\Lambda$ | diffusion function as defined by Reichart (equation 2.6) |
| $\mu$ | dynamic viscosity |
| $\nu$ | kinematic viscosity |
| $\xi$ | distance as defined by the correlation coefficient |
| $\Pi$ | similarity parameter as used in the Buckingham method |
| $\rho$ | density |
| $\tau$ | time |
| $\tau$ | shear stress |
| $\Phi$ | dissipation |

Subscripts

| | |
|---|---|
| b | bulk |
| e | exit |
| f | fluid |
| i,j,k | three components of the cartesian co-ordinates as referred to x,y,z respectively |
| m | mean |
| o | initial condition |
| o | wall condition |
| r | eddy quantity relative to mean fluid quantity |
| s | smooth surface |
| t | total or overall |
| w | wall |

Superscripts

| | |
|---|---|
| ' | fluctuating quantity |
| - | mean quantity |
| * | maximum value of |
| * | non-dimensional quantity |

LIST OF TABLES

LIST OF FIGURES

APPENDICES

## 1. INTRODUCTION

Similarities between a collection of molecules in a gas and the motion of a turbulent fluid have enabled many researchers in obtaining useful concepts for turbulence phenomena which were related to those found in dealing with the transport properties of a gas. Models proposed by Prandtl {1} and Reynolds {2} were typical concepts for predicting bulk behaviour of heat and momentum transport of turbulent fluid flow. Although their utility in engineering design is well known, one of the basic problems associated with the accurate prediction of transport phenomena in a turbulent fluid is that, even for a simple flow, the Prandtl's mixing length and Reynolds' momentum flux vary through the flow field.

In the flow of a perfect gas, the bulk behaviour is the result of a large number of individual fluctuating motions. In this instance, the development of statistical thermodynamics provide a framework within which predictions of the combined effect of molecular motion can be made from the knowledge of individual molecules. In fluid turbulence, there exists more complex phenomena than molecular motion in a perfect gas.

One difficulty in making a thermodynamic approach to turbulence is that of defining a suitable parameter equivalent to the temperature of molecular motion. However, the method of Information Theory allows us to be obtained a statistical parameter for the turbulent fluctuations which is equivalent to the temperature of molecular fluctuations. The usual methods of statistical thermodynamics are difficult to employ because there exists no permanent entity comparable with the molecule. Turbulent fluid also has the characteristic that there exist particles of fluid of random size and shape moving relative to the average motion. Hence, the statistical analysis must include a random scale function and a random velocity function. In order to be of practical value, the scale functions have to be determinable throughout the flow field.

The validity of this analysis can only be judged by comparing the end product with experimental results. Nevertheless, a theory of

turbulence is likely to be most acceptable in engineering applic-
:ations, if the basic concept is that of a flux of entities rather
than an artificial mixing length or a correlation function.

## 2. LITERATURE REVIEW

### 2.1 Theory of turbulence

It was shown by Bradshaw {3} that quite small velocity fluctuations can produce large changes in flow resistance and other properties. A fluctuation with zero mean, superimposed on the mean velocity, produces a mean momentum flux of its own, proportional to the mean square of the fluctuating velocity. This is due to the fact that the momentum flux is the product of mass flow rate and velocity and the fluctuation contributes to both. This non-linearity of the relation between velocity and momentum flux appears in the Navier-Stokes equations, and has been the basic cause of their mathematical difficulty.

In turbulent flow, it is usually assumed that the instantaneous velocity components satisfy the Navier-Stokes equations. By substituting the expressions for the instantaneous velocity components into the Navier-Stokes equations of an incompressible fluid and taking the mean values of these equations according to the Reynolds rules of averages, a set of Reynolds equations of motion for turbulent flow of an incompressible fluid may be obtained, as shown in Appendix 1. The additional terms over the Navier-Stokes equations are due to the Reynolds stresses or turbulence stresses, $\tau_{ij}$. These stresses are the representation of the rate of transfer of momentum across the corresponding surface because of the turbulent velocity fluctuations. The solutions of the Reynolds equations will represent properly the turbulent flow.

However, one of the main difficulties in the theoretical investigation of turbulent flow is the necessity to find additional relationships between the characteristics of turbulence and those of the mean flow. This is due to the fact that there are more unknowns than the number of independent Reynolds equations. In order to obtain some definite results from these equations, further hypotheses about Reynolds stress must be made.

Hinze {4} showed that, in comparing the turbulence stresses in the equation of motion with the corresponding stresses caused by viscosity effects, it could be assumed that the turbulence stresses behave like viscous stresses and were directly proportional to the velocity gradient. This was an assumption made by Boussinesq {5}, in as early as 1877, who introduced in the theory of turbulence a turbulent exchange coefficient $\varepsilon$, such that for a simple mean flow,

$$\rho\overline{u'v'} = \overline{\tau_{xy}} = \varepsilon_\mu \cdot \frac{\partial \bar{u}}{\partial y} \qquad (2.1)$$

where $\varepsilon_\mu$ was called the turbulent or eddy viscosity. The overall shear stress may then be written as

$$\tau = (\mu + \varepsilon_\mu) \cdot \frac{\partial \bar{u}}{\partial y} \qquad (2.2)$$

However, Pai {6} pointed out that, in general, the Boussinesq hypothesis was a failure because for every new problem in fluid dynamics, a completely new expression for $\varepsilon$ was required.

A successful semi-empirical theory of turbulence was Prandtl's mixing length theory {7} in which Prandtl introduced the similarity of the turbulent theory with the kinetic theory of gases. In the mixing length theory, a length $\ell$ was introduced similar to the mean free path in the kinetic theory of gases so that certain quantities in the turbulent flow were assumed to be preserved during the turbulent mixing process throughout this length. Thus, this length was called a mixing length. There were various mixing length theories based on different models in which different quantities were assumed to be preserved and a brief review of the mixing length theory is shown in Appendix 2.

The main advantage of the mixing length theory over Boussinesq's theory is that it is generally easier to make a plausible assumption for $\ell$ than for $\varepsilon$. However, one of the defects of the mixing length theory is that the mixing length deduced from the measurements of the mean flow is not very small but of the same order of magnitude as the dimension of the mean flow. Also, neither Prandtl's momentum

transport theory nor Taylor's vorticity transport theory {8} describe the mechanism according to which the lumps of fluid adapt their transferable property to their new environments.

Von Karman, in what was known as his similarity hypothesis {9}, attempted to find relations between the turbulent shear stress and the mean velocity distribution which was independent of any special model such as those of Prandtl or Taylor. Von Karman made the following assumptions:

(a) the turbulence mechanism was independent of viscosity except in the immediate neighbourhood of the walls.

(b) the local flow pattern was statistically similar in the neighbourhood of every point and only the time and length scales were different.

The second assumption indicated a constant correlation between the different components of the velocity fluctuations. From these, von Karman found that for parallel mean flow,

(1) $|u'| \sim |v'| \sim \ell \frac{d\bar{u}}{dy}$ where $\ell$ was a characteristic length.

(2) $\tau = \rho . \ell^2 . \left(\frac{d\bar{u}}{dy}\right)^2$

(3) $\ell = k . \left|\frac{d\bar{u}}{dy}\right| \Big/ \left|\frac{d^2\bar{u}}{dy^2}\right|$ where k was a universal constant.

Thus, the von Karman formula for shear stress might be expressed as:

$$\tau = k^2 . \rho . \left(\frac{d\bar{u}}{dy}\right)^4 \Big/ \left(\frac{d^2\bar{u}}{dy^2}\right)^2 \qquad (2.3)$$

The most important deduction from von Karman's similarity hypothesis was the universal velocity distribution for the flow in circular pipes. With the absence of pressure gradient along the main flow direction, the universal velocity distribution or logarithmic profile may be obtained by replacing the shear stress $\tau$ with its value

on the wall, $\tau_o$ and integrating equation (2.3) as

$$\bar{u} = \frac{1}{k} \frac{\tau_o}{\rho} \cdot \log (y/\delta) \qquad (2.4)$$

where $\delta$ is a constant determined by the value of $\tau_o$, $\rho$ and $\nu$. More generally, the above may be expressed as

$$u^* = A + B \log y^* \qquad (2.5)$$

where $u^* = \bar{u}\sqrt{\tau_o/\rho}$

and $y^* = y\sqrt{\tau_o/\rho}\ /\nu$

One defect of the result is that the boundary conditions on the wall are not satisfied. The logarithmic velocity profile gives an infinite velocity at the wall. Usually one can only say that the result of such a theory does not hold true for a laminar sublayer and a viscous layer which are near the wall.

In the theories advanced by Boussinesq, Prandtl, Taylor and von Karman, a deductive method was followed. A hypothesis was made concerning the turbulence shear stress or concerning the turbulent diffusion coefficient. From it and with the aid of the equations of motion and continuity, and with assumed similarity conditions, velocity distributions were deduced. Reichardt objected to this method, pointing out that relatively easily measurable quantities such as mean velocities were derived on the basis of more or less questionable hypotheses. Also, the usual scatter of the experimental data used for comparison made any decision in favour of one hypothesis or another difficult.

As against the deductive method, Reichardt {10}, {11} proposed an inductive method based on directly measurable quantities. He assumed that a turbulent-transport process was a statistical process exactly analogous to molecular-transport process. By considering simple two dimensional free turbulence, Reichardt proposed the momentum-transfer law,

$$\overline{uv} = - \Lambda \frac{\partial \bar{u}^2}{\partial y} \qquad (2.6)$$

In the above equation, $\Lambda$ has the dimension of length, but mathematically it has the meaning of a diffusion constant; physically, it has no definite meaning. Although $\Lambda$ may be a function of x and y, Reichardt assumed that it was a function of x only, determined by the width of the mixing zone. The momentum-transfer law may be interpreted as the rate of transfer of u-momentum in the y direction is proportional to the change of the momentum flux $\overline{u^2}$ in that direction.

Although Reichardt's theory was somewhat more logical than the mixing length theory, the result could hardly be expected to predict an accurate distribution of the turbulent fluctuations and to throw light on the physics of turbulent production phenomena, because it was based on the measurement of the mean velocity. It became just another semi-empirical phenomenological theory for the determination of mean velocity distribution in free turbulence flow.

Even though the above theories had successfully predicted the mean velocity distributions in many practical problems, the final and logical solution of the turbulence problem required the applic-:ation of methods of statistical mechanics. In order to develop successfully a statistical theory of turbulence, it is necessary to define some quantities to describe the turbulence. Taylor {12}, {13} successfully developed a statistical theory of turbulence which was applicable to continuous movements and satisfied the equations of motion. The important new idea introduced by Taylor was that of the studying of correlation, or coefficient of correlation between the fluctuating quantities in the turbulent flow. The theory has been further developed by von Karman {14}, Kolmogoroff {15}, Heisenberg {16}, Bathchelor {17} and others.

However, to define a random function, it is not sufficient to give the correlation function and the spectral function. It is also necessary to prescribe the probability distribution of the random function and the joint probability distribution of the values of the random function at different times and different positions in the space. A complete statistical specification of a turbulent motion

thus requires a vast array of information. Since turbulent fluctuations are random in nature, it is permissible to apply the rules of probability calculus to them. Although the analysis of turbulence is much more complicated than most of the problems in statistical mechanics, it has been shown by Kempé de Fériet {18} that the theory of random stationary functions gave many useful theoretical results for the velocity field, especially in incompressible homogeneous turbulence. Thus the theory of random stationary functions provides a powerful tool for the investigation of the kinematics of turbulence.

As turbulence produces additional rates of transport of quantities other than momentum, such as temperature fluctuations, there exists similar analysis for heat transfer where the total or overall heat transferred in a turbulent fluid may be expressed as:-

$$\frac{q}{A} = k.\frac{\partial \overline{T}}{\partial y} - \rho.Cp.\overline{v'T'} \qquad (2.7)$$

where $(q/A)$ is the total heat flux and $\rho.Cp.\overline{v'T'}$ is the enthalpy flux. As suggested by Rohsenow and Choi {19}, the enthalpy flux may be expressed, similar to the momentum flux, as:-

$$\rho Cp\ \overline{V'T'} = -\rho Cp.\varepsilon_H.\frac{\partial \overline{T}}{\partial y} \qquad (2.8)$$

where $\varepsilon_H$ is the eddy diffusivity of heat. Hence, the total heat flux may be written as:-

$$\frac{q}{A} = (k + \rho.Cp.\varepsilon_H)\frac{\partial \overline{T}}{\partial y} \qquad (2.9)$$

$\rho Cp\varepsilon_H$ may be interpreted as the eddy conductivity.

Unlike $\mu$ and k, the eddy viscosity and eddy conductivity are not properties of the fluid and are dependent on the turbulence characteristics of the flow. In nearly all cases of interest, such as flow over bodies, in tubes and ducts and between parallel plates

Reynolds stresses and other turbulent transport rates are much larger than viscous stresses and other molecular transport rates, which adds to the importance of turbulence phenomenon.

Among many methods that proposed to predict the turbulent heat transfer were those of Dittus & Boelter {20}, McEligot et al {21}, Martinelli {22} and Kinney & Sparrow {23}. However, the validity of all these methods were limited as to the range of Prandtl numbers mainly due to their unsatisfactory theory on the eddy diffusivity of heat. Cebeci {24}, based on Prandtl's mixing length concept, proposed a model for the eddy diffusivity of heat for external boundary layer flows. His results agreed well with available experimental data over a wide range of Reynolds and Prandtl numbers. Following Cebeci's analysis, Na & Habib {25} extended it to the investigations of heat transfer in turbulent pipe flow. Their results compared quite well with experimental temperature distribution over a wide range of Prandtl numbers. However, their prediction of turbulent Prandtl number disagreed with measurements of McEligot & Picket et al {26}, {27} who suggested that the reason lies in the empirical determination of adjustable constants by Na & Habib as they relied on uncertain experimental data.

In studying transport phenomena in turbulent flows, it is reasonable to ask whether the transport processes of different quantities such as momentum, heat and turbulence energy can be analogous. If an analogy existed between any pair of quantities, similar relations would be obtained for these quantities. It might even be possible to express the parameters determining the transport of one quantity in terms of the parameters determining the transport of the other quantity. The question of the existence of analogies was, therefore, raised very early and had been answered more or less satisfactorily on the basis of existing theories.

Osborne Reynolds was one of the earliest scientists to recognise the existence of a relationship between heat transfer and skin friction. According to his theory {2} , the movement of heat between a surface and a fluid followed the same laws as the movement

of momentum between the surface and the fluid, whether by conduction or convection. By assuming the thermal diffusivity equal to the kinematic viscosity and also the equality of eddy diffusivities of heat and momentum, Reynolds proposed the following equation which is known as the Reynolds analogy:-

$$\frac{h}{\rho Cp.\overline{U}} = St = {}^{f}/_{2} \qquad (2.10)$$

where h is the heat transfer coefficient; f is the friction factor and St is the Stanton number which is the ratio of heat production to heat transfer by convection.

Although Reynolds analogy agreed well with turbulent heat transfer data on fluids which had a Prandtl number close to 1, it failed for $Pr \neq 1$. Furthermore, it did not take account of the velocity distribution across the pipe. In 1910, Prandtl {1} extended Reynolds work by considering the velocity distribution in the laminar sublayer and obtained a relationship which involved the ratio of the average velocity to the velocity at the edge of the laminar sublayer. Applying the Reynolds analogy for the turbulent core, Prandtl obtained the equation which has generally been referred to as Prandtl analogy:-

$$\frac{h}{\rho Cp\overline{U}} = St = \frac{f/2}{1+\frac{u_{\delta 1}}{\overline{U}}(Pr-1)} \qquad (2.11)$$

where $u_{\delta 1}$ is the velocity at the edge of the laminar sublayer.

Prandtl analogy was based on the assumption of clear cut division of the flow into a laminar boundary layer and a turbulent core. Further research into the mechanism of turbulent flow has brought the recognition of the existence of an intermediate layer in which the molecular and turbulent transport phenomena were of the same order of magnitude. Von Karman {28} obtained a further improvement of Prandtl analogy on this basis by making use of the universal velocity distribution. The resulting equation for the

Stanton number was:-

$$St = \frac{f/2}{1+5\sqrt{f/2}\left[(Pr-1) + \ell n\,(1 + 5/6\,(Pr-1))\right]} \qquad (2.12)$$

A useful empirical means of correlating convection heat transfer data and showing the relationship to the friction factor was developed by Colburn {29} who proposed the j factor. Colburn investigated a large number of convection heat transfer and pressure drop data and found that a correlation was obtainable, thus making it possible to predict the heat transfer coefficient from the friction factor. Colburn analogy gave the following expression:-

$$St = j_H.Pr^{-2/3} = f/2.Pr^{-2/3} \qquad (2.13)$$

where $j_H$ is the j factor for heat transfer as defined by Colburn.

A graphical comparison of the analogies of Reynolds, Prandtl, von Karman, and Colburn is shown in Figure 1, where the Nusselt number is plotted versus the Reynolds number at constant values of the Prandtl number. The top curves are for a Prandtl number of 10 and the lower curves for a Prandtl number of 0.01. When the Prandtl number is unity, all equations become identical. All equations agree well at high Prandtl numbers. At low Prandtl numbers, there is wide divergence of the various analogies, those of Prandtl and von Karman giving much lower values of the Nusselt number. These results would indicate that, for fluids with a high Prandtl number, the empirical equations satisfactorily predict the heat transfer coefficient. For low Prandtl number fluids, the large difference between empirical equations suggests that the present empirical relationships are not suitable.

The use of the analogy between momentum transfer and heat transfer for predicting heat transfer from momentum transfer depends on the relationship between the eddy diffusivities of heat and momentum, i.e. $\varepsilon_H$ and $\varepsilon_\nu$. Most investigators assume them to be equal, as Reynolds {2}, Prandtl {1}, von Karman {28} and Colburn {29}did; however, recent experimental work has shown they are not equal.

Therefore, a general relationship between $\varepsilon_H$ and $\varepsilon_\nu$ is needed so that the analogy between heat transfer and momentum transfer will be most useful.

Although a number of workers have used Reynolds and Prandtl analogies to predict the eddy diffusivity ratio, their results were found to be unsatisfactory. Jenkins {30} altered Prandtl's mixing length concept by allowing the moving particles to change their energy and momentum while in flight. Diffusivities predicted by Jenkins were known to be in error of 20% even for Prandtl number of the order of unity. At high Prandtl numbers, his prediction posed no upper limit for diffusivity ratio as the Prandtl number increased.

Deissler {31}, {32} using a modified mixing length theory and also a method based on correlation coefficients, produced reasonable prediction for diffusivity ratio in the low Prandtl number range. However, his theory required experimentally determined constants. Rohsenow and Cohen {33} modified Deissler's analysis by considering a spherical eddy travelling in a fluid whose temperature varied linearly with time. They produced a diffusivity ratio for very low Prandtl number range. Apart from not taking into account the effect of Reynolds number or turbulence intensity, their prediction gave infinite value of heat transfer coefficient as the Prandtl number increased.

Azer and Chao {34} based on the same analysis as Jenkin's concept and assumed a continuous change of momentum and energy during the flight of an eddy. Their prediction is valid in the case of pipe flow only. Also, they provided two separate expressions for the ratio of diffusivity for different Prandtl number regime. From his measurements in boundary layer air flows, Rotta {35} proposed a simple expression for diffusivity ratio across the boundary layer. However, the trend that $Pr_t$ decreases with the wall distance from the value of 0.9 at the wall to 0.5 near the outer edge of the boundary

layer is in opposition to the measurements of Quarmby & Quirk {36} for pipe flow. Jischa & Ricke {37},{38} proposed a second order closure model for the diffusivity ratio. Apart from having two different expressions for different Reynolds number regime, it also has two empirical constants.

Prior to the above analyses, Taylor in his Classical Vorticity Transport Theory {8} produced a unique value for the diffusivity ratio of 2.0. This is contrary to the large amount of available experimental data and the more up-to-date analysis that it depends on the Prandtl number.

Tyldesley & Silver {39}, {40} used an approach different from the mixing length concept or one based upon correlation coefficients. Their predicted values of diffusivity ratio was found to be well compared with those experimental data supplied by Stromquist {41}, Trefethen {42}, Seban & Doughty {43}, Mizushima & Sasano {44} and Isokoff & Drew {45}. Tyldesley & Silver's analysis was based on the concept that the fluid consisted of eddies or entities of variable shapes, sizes and velocities. A reasonably simply model for the prediction of turbulent transport properties was proposed. Their concept seemed to give a more realistic description of the flow of turbulence. The present work is based on the concept by Tyldesley & Silver whilst attempting to predict momentum and heat transport.

## 2.2 Flow in smooth and rough pipes

An extensive investigation on frictional resistance due to roughened surface was carried out by Nikuradse {46}. In his experiments, circular pipes were internally coated with sand grains of uniform size. Roughness ratios (r/k) ranging from 15 to 507 were used to correlate the relationship between friction coefficient or resistance factor and Reynolds number. He found rather abrupt transition from "smooth" law at low speed to "rough" law at high speed. A one-equation model for resistance factor with surface roughness was then proposed as:-

$$\lambda = (1.74 + 2 \log {}^{r}/k)^{-2} \qquad (2.14)$$

Prior to these investigations, Heywood {47} and others had carried out measurements of resistance factor on galvanized steel pipe and wrought iron pipe with roughness ratios between 28 and 70. Their results could only be explained by a much more gradual transition between the two resistance laws. Unlike Nikuradse and Heywood, Colebrook & White {48} used pipes with non uniform roughness and obtained similar experimental data as Heywood.

Although Nikuradse's investigation was thorough and widely accepted, it did not deal with the effect of roughness on heat transfer. As indicated by Bradshaw {49}, there remained a controversy as to whether or not roughening the surface of a pipe would increase heat transfer for a given pumping power. A partial explanation for this lack of information may lie in the difficulty involved in obtaining accurate heat transfer measurements and in the fact that for a complete study of heat transfer phenomena, the influence of the Prandtl number has to be studied.

A number of workers such as Kay & Nedderman {50} and Goldstein {51} have suggested that a similarity parameter $k^* = \frac{U_\tau . k}{\nu}$ existed in flow through rough pipes such that, for a certain kind of roughness, if $k^*<4$ or 5, the surface might be considered to be hydraulically smooth. If $k^* >100$, the surface might be considered completely rough. In the case where 4 or $5 < k^* < 100$, the effects of roughness and of viscosity were of equal importance.

Over the years, it has long been recognised that the heat transfer coefficient in an incompressible fluid over a smooth surface might be expressed as:-

$$Nu = A.Re^{B}.Pr^{C} \qquad (2.15)$$

where A, B and C were numerical constants. Different workers in the field have proposed different values for A, B and C. Schlichting {52} , Colladay {53} and Curle & Davies {54} all proposed values of A, B and C as 0.332, 0.5 and 0.33 respectively while Davies {55} proposed

values of 0.26, 0.6 and 0.3. With flows in circular pipes, Reynolds and Perkins {56} suggested different values of A, B and C for different Prandtl number regime. For $Pr > 20$, their suggested values of A, B and C were 0.0118, 0.9 and 0.3 respectively. For $1.0 < Pr < 20$, they proposed 0.0155, 0.83 and 0.5 whereas for $0.5 < Pr < 1.0$, their suggested values were 0.022, 0.8 and 0.6 respectively. In addition, for $Pr < 0.5$, they proposed a new expression for heat transfer as:-

$$Nu = 4.82 + 0.0185.Pe^{0.827} \qquad (2.16)$$

Although the different sets of numerical constants varied a great deal, the predicted heat transfer coefficients were quite similar in value. In addition, Sleicher & Rouse {57} suggested a correlation for the ranges $0.1 < Pr < 10^5$ and $10^4 < Re < 10^6$,

$$Nu = 5 + 0.015\ Re^m.Pr^n \qquad (2.17)$$

where $m = 0.88 - 0.24/(4 + Pr)$ and $n = 0.33 + 0.5 \exp(0.6Pr)$.

As the effect of wall roughness on the turbulence flow pattern is negligible if the relative roughness is sufficiently low, one may expect that the transport of heat in a flow past a rough wall with low relative roughness will be like the transport of heat in a flow past a smooth wall, except perhaps for a slight effect associated with the increased surface area of the rough wall. However, pipes which are sufficiently rough would increase heast transfer coefficients.

Davies {55} suggested that, in rough pipes, the eddies set up in the wake of each roughness element penetrated into the viscous sub-:layer where much of the resistance to heat flow normally occurred. Eckert {58} indicated that, because of the small laminar sublayer, the shearing stress at the wall for turbulent flow depended much on the roughness of the wall whereas, in laminar flow, the roughness had only a small influence. This could be explained as an increase in shearing stresses when the roughness was not filled out by the laminar sublayer. Reynolds {59} attempted to explain this by the presence of a recirculating flow within a cavity in the roughness layer. Heat across the layer, either entering the recirculating flow or to be carried to the outer flow, could only be transferred by diffusion at the solid boundary.

Hinze {4} suggested that with increasing roughness, there was an increasing effect on the flow pattern; among other things, the effective thickness of the viscous sublayer would decrease. The decrease affected the transfer of heat across the boundary layer, for the roughness caused disturbances in the viscous sublayer which promoted turbulence transport. Rotta {60}, using Nikuradse's experimental results, deduced a relationship between viscous sublayer and surface roughness as shown in Figure 2, and showed that for $\frac{U_\tau k}{\nu} > 55$, the effective thickness of the viscous sublayer became zero.

It has been found experimentally that roughness increased the rate of heat transfer by up to three or four times. Davies {55} showed that the heat transfer coefficient over a rough surface might be given by:-

$$Nu = 0.08 \cdot \sqrt{f/2} \cdot RePr^{0.5} \qquad (2.18)$$

It was suggested that if the pipe was screw-threaded $\sqrt{f/2}$ varied as $(k/D)^{0.3}$ but for sand-roughened pipes, the power of (k/D) would be 0.15. Although different assumptions were used during the derivation of smooth and rough pipe coefficients, the values of f/2 over the entire range from completely smooth to fully rough pipes might be valid in the same equation. Kolar {61} found that, in practice, as a first approximation, the empirical equation:-

$$Nu = 0.05 \cdot \sqrt{f/2} \cdot Re\ Pr^{0.5} \qquad (2.19)$$

gave quite a good representation of the heat transfer into fluids in both smooth and rough pipes.

One of the first studies of heat transfer in rough pipes was conducted by Cope {62} in 1941. The roughness ratios achieved in his experiments were between 8 and 45. His experimental results showed that the effect of surface roughness of the kind tested was positively detrimental to the efficiency of a pipe as a medium for heat transmission. Zukauskas & Slauciauskas {63} attempted to explain this by suggesting that the increase in drag outweighed the increase in heat transfer as the roughness was increased.

Most rough surface heat transfer studies in the past have used air as the test fluid not only because of its practical importance, but also because its Prandtl number was nearly unity. The effects of roughness on aerodynamic heating and boundary layer transition have been studied by Dunn {64}. Heat transfer studies by Bourgoyne et al {65}, Kemeny & Cyphers {66}, Sheriff & Gumley {67} and Walker & Rapier {68} in conjunction with the United Kingdom Atomic Energy Commission have provided experimental data for heat transfer coefficients in turbulent flow in rough annuli with air.

Nunner {69} carried out heat transfer and pressure drop measurements in roughened pipe flow. During his tests, artificial roughness was created by fixing different ringforms on the surface of the pipe. Roughness ratios obtained were between 2 and 80. Nunner then proposed an expression for rough surface heat transfer as:-

$$Nu = \frac{Re.Pr\ .\ f/2}{1 + 1.5\ Re^{-1/8}.\ Pr^{-1/6}\ (Pr.\ f/f_s - 1)} \qquad (2.20)$$

where $f/f_s$ was the ratio of rough to smooth friction factors at the same Reynolds number. In deriving the above equation, Nunner postulated that the viscous wall layer behaves almost exactly the same way in a rough pipe as in a smooth one at the same Reynolds number. Therefore, only the resistance of the turbulent core was affected by roughness.

Another expression for heat transfer which was frequently quoted was that developed by Martinelli {22} as:-

$$Nu = \frac{Re.\ Pr\ \sqrt{f/2}}{5\cdot\left[\ Pr + \ell n\ (1+5\ Pr) + \tfrac{1}{2}\ell n\left(\frac{Re}{60}\cdot\sqrt{\frac{f}{2}}\right)\right]} \qquad (2.21)$$

This equation differs from that derived by Martinelli for smooth pipes only by the omission of the temperature ratio $(Tw - Tc)/(Tw-Tb)$ in the numerator. Martinelli suggested that the above equation might apply to rough pipes as the effect of roughness entered the equation simply through the increase in fraction factor. The omission of the temperature ratio had relatively little effect as this term was usually just slightly less than 1.0 and rarely fell below 0.8.

As suggested by Gomelauri {70} that with the above two expressions, the effect of Prandtl number was not properly predicted. Also a unique relationship between Nu and f independent of roughness forms was proposed to the contrary of the findings of Dipprey & Sabersky {71} and others. Dipprey & Sabersky provided a set of experimental data on the friction as well as heat transfer characteristics of rough surfaces for a relatively wide range of Reynolds numbers, roughness ratios and Prandtl numbers. They proposed a heat transfer similarity law based on heat transfer to water as:-

$$Nu = \frac{Re.Pr.\ f/2}{1 + \sqrt{\frac{f}{2}} \cdot \left\{ \gamma \cdot \left[ Re. \sqrt{\frac{f}{2}} \cdot (k/D) \right]^{0.2} Pr^{0.44} - 8.48 \right\}} \quad (2.22)$$

where $\gamma$ was a numerical constant that depended on the roughness form and roughness ratio was expressed as:-

$$\frac{k}{D} = \exp\left[ \left( 3.0 - \frac{1}{\sqrt{f/2}} \right) / 2.5 \right]$$

The above equation refers to conditions in the 'fully rough' flow regime. They suggested that, for granular close-packed roughness, $\gamma = 5.19$ and for two dimensional roughness such as that investigated by Nunner, $\gamma$ might be taken as 6.37. Arguments in support of the above similarity law were well presented.

Gowen et al {72}, {73} also provided detailed experimental results on turbulent heat transfer to both smooth and rough pipe flows. During their investigations, temperature profiles, friction factors and heat transfer coefficients have been measured with pipes of roughness ratio between 11 and 48. A semi-theoretical equation based on the temperature profiles obtained was presented and shown to predict Nunner's results adequately, although it underestimated the results of Dipprey & Sabersky. The effects of roughness on free surface flows over smooth and rough boundaries were investigated by Blinco & Parenthiades {74}. They found that the relative turbulence intensity depended quite strongly on Reynolds number and increased strongly with increasing roughness.

Fujii et. al.{75} introduced extensive experimental results on natural convection with the influence of surface roughness. Although chiefly concerned with natural convection, they also suggested that the rough surface in the forced convection would reduce the mean velocity and the heat transfer coefficient would be increased just as much to compensate the loss of the kinetic energy when compared under the same pressure drop. Ramakrishma et al {76} attempted a theoretical approach and provided a direct relationship between friction coefficient and free convective heat transfer with different roughness ratios. However, the prediction was only valid for fluids whose Prandtl numbers were close to unity.

More recently, Cebeci & Chang {77} proposed a differential method with near wall mixing-length equations based on contributions by Rotta {78}. A higher order closure model was presented by Adams & Hodge {79} who used an integral form of the turbulent kinetic energy with a term added to represent the generation of turbulence which occurs in the wakes behind roughness elements. Hatton & Walklate {80} and Wassel & Mills {81} also used the mixing length models for the prediction of heat transfer in roughened pipes. A near-wall mixing-length equation used for the prediction of skin friction and heat transfer in conjunction with a wall temperature step and a turbulent Prandtl number distribution was proposed by Ligrani et al {82}, {83}, along with the same mixing length equation for the outer regions of smooth wall boundary layer.

With the present survey, it is evident that analyses and investig-:ations so far have yet to provide a thorough theoretical and experi-:mental criterion for predicting heat and momentum transfer under the influence of surface roughness. Furthermore, correlations based only on the heat transfer coefficient cannot generally and adequately predict heat transfer rate from rough surfaces because such correlations ignore the effect of roughness on the detailed structure of the resistance to heat transfer. As indicated earlier, the concept proposed by Tyldesley & Silver gave a more realistic description of the flow of turbulence - it is thus possibly more realistic to study the effect of roughness on heat transfer using the concept proposed by Tyldesley & Silver.

## 2.3 Experimentation

It was suggested by Nikuradse {84} that turbulence would be fully developed at a distance of 25 ∿40 diameters downstream of an abrupt change of pipe diameters. However, Logan & Jones {85} showed that, in rough tubes, transition from a developed smooth to a developed rough velocity profile required only 8 ∿ 10 diameters. Sleicher & Tribus {86} reviewed studies of several investigators and concluded that 5 ∿10 diameters were required for development of constant heat transfer coefficients.

Until recently, most of the investigations on heat transfer were confined to the heat transfer near the wall or in the boundary layer where the temperature gradients were large. As indicated by Kinney & Sparrow {87}, this has led to extensive experimental and analytical predictions to wall heat transfer. However, there has been little or no experimental investigation on the heat transfer to fluid flow with internal heat generation.

One of the earliest experimental and analytical works on internal heat generation heat transfer was carried out by Poppendiek{88} who assumed equal diffusivities of momentum and heat. Measurements were made of the fully developed wall-to-bulk temperature differences within an electrically heated fluid. Comparison between his experimental data and analysis was only fair, as the scatter in his data was about 30%. Miller {89} carried out tests on turbulent heat transfer in an adiabatic pipe with internal heat generation, but his results were not published. In addition, considerable uncertainty was reported as due to heat loss along the electrodes.

Recent experimental work by Inman {90} was performed for an internally heat generating fluid in the laminar flow regime. Axial wall temperature measurements along the adiabatic test section were in good agreement with the predictions of laminar analysis. However, measurements in the turbulent flow regime were not reported. Similar investigations based on the classical eddy diffusivity model were carried out by Petukhov and Genin {91}, Siegel & Sparrow {92} and Michiyoshi & Nakajima {93}. However, all the above analyses led to exact solutions for the heat transfer coefficient or wall temperature

that were too involved for engineering computations.

Danckwerts {94} followed by Thomas et al {95},{96} used a different approach which made use of the principle of surface renewal. As their analysis was derived on the basis of the assumption that eddies moved into direct contact with the wall, the application was restricted to moderate Prandtl numbers. Also, assumption that eddies could be considered as semi-infinite further restricted the analysis to the evaluation of wall temperature for cases in which internal heat generation was involved. Habib & Na {97} and Na & Chiou {98} carried out a theoretical analysis to turbulent heat transfer in pipes with internal heat generation. The results from their theoretical studies agreed reasonably well with available experimental data for moderate to low Prandtl numbers.

A method for generating a uniform heat source to fluid flow was introduced by Wilson {99} in as early as 1904. With his method, heated fluid could be injected into the main flow through a small injector and the injected fluid might be considered as a moving point source of heat, provided that the injector size was sufficiently small. An expression for the eddy diffusivity of heat might be expressed as:-

$$\rho C_p \varepsilon_H = \frac{Q}{4\pi \Delta T (x-x_o)} - k \qquad (2.23)$$

where Q was the heat source strength and $\Delta T$ was the rise in temperature with respect to the distance $(x-x_o)$. The method was found to be in error mainly due to the effect of finite boundaries. Although an analysis using Green's function might be carried out, as suggested by Carslaw & Jaeger {100}, to modify the above expression, such analysis was complex and therefore unnecessary for experimental verification. Sheriff et al {101},{102}, {103}carried out experimental investigation using the above expression. Their results of eddy diffusivity of heat were found to be underestimates. This was thought to be due to the finite boundaries in pipe flow.

Until recently, the most universal device for studying turbulent flows was a hot-wire anemometer. With the advent of lasers, the possibilities of the development of more advanced devices were opened up. In 1964, Yeh & Cummins {104} success-:fully measured velocity profiles in a fluid by examining the frequency shift in monochromatic coherent radiation scattered from particles in the fluid. The analytical description of Laser Doppler Anemometry was first shown by Rudd {105} as an uncontra-:dictory method on the basis of a doppler or interference technique. Many investigators such as Foreman et al {106}, Pike et al {107}, Welch & Tomme {108} and Lumley et al {109} have applied this technique to the measurement of mean square fluctuating velocities and instantaneous velocities in the turbulent flow of gases and liquids.

As listed by Durst & Zare {110}, a large number of articles were available on the various aspects of LDA. Many papers dealt with the specific applications of optical or electronic apparatus available. Durst & Whitelaw{111} carried out measurements of mean velocities, turbulence intensities and shear stresses in air jet flow by turning the two input laser beams through $90^{o}$, thus measuring the two velocity components. Bourke et al {112}, {113} measured the Reynolds shear stresses in water flow using two frequency trackers and an analogue correlator. It was shown that the above measurements of velocity and turbulence intensity compared favourably with those of hot wire measurements.

With laser doppler anemometry, it is necessary that particles of appropriate sizes are suspended in the flow for light scattering. With air or gas flow, it is usual to use some form of atomiser or spray for seeding of particles. Melling & Whitelaw {114} discussed the criterion which limited particle characteristics and assessed the available method for particle generation. However, as mains water generally contains enough contamination in the way of particles, seeding in water flow is usually not necessary.

Bates {115} carried out a number of tests on water flow using the LDA on a ten inch perspex pipe and obtained results of velocities, turbulence intensities, boundary layer thickness and skin friction coefficients. It was shown that the LDA system was suitable and useful in the measurements of properties of turbulent flows. Bates {116} continued his investigations by analysing his results on a PDP 11 minicomputer and found some discrepancies between his analogue and digital results.

As suggested by Van Atta {117}, one method of reducing the error of digital technique was by substantially increasing the sample size and sample rate or frequency. Yanta et al {118}, {119} developed a statistical analysis system incorporating a digital data processor in which the data were punched onto cards to be analysed later on a large computer. With a statistical definition of turbulence and its mean square fluctuations, they found that, as shown in Figure 3, for an accuracy of 1%, the number of data points needed to obtain velocity measurement was given by:-

$$N = 40000 \left( \frac{\sqrt{\overline{u'^2}}}{\overline{u}} \right)^2 \qquad (2.24)$$

A similar analysis was carried out to predict the number of data points needed to obtain accurate measurements of turbulence intensity. As shown in Figure 4, they found the number to be independent of flow conditions.

Whiffen & Meadows {120} and Smith & Meadows {121} used an improved system where the data was stored via a minicomputer onto disc before subsequently processed on a large computer. Blake {122} developed a frequency analysis system based upon a computing counter linked to the photomultiplier via a preamplifier and bandpass filter. A digital magnetic tape was obtained from a data logging device connected to the counter and then analysed off-line on a computer. However, Bates & Hughes {123}, {124} showed that, provided the turbulence intensity in the flow was low, the output from a frequency tracker might be fed directly into a minicomputer and sampled in a controllable manner to yield the required statistical information.

A number of articles were available on the statistical analysis of LDA signals and the errors involved therein. Greated & Manning {125} , {126} derived mathematical expressions for the ambiguity broadening due to finite flight time based on a two dimensional model. George & Lumley {127}, {128} presented an exact theory for the effect of ambiguities on measurements and presented a criterion for minimising such doppler ambiguity.

Microscale is a measure of the average dimension of the eddies that are mainly responsible for the dissipation of energy. As indicated by Hinze {4} while discussing correlation coefficients, the microscale might be expressed as:-

$$g(y) \approx 1 - \frac{y^2}{\lambda^2} \qquad (2.25)$$

where g(y) was the lateral correlation coefficient defined by:-

$$g(y) = \frac{\overline{u(\xi).u(\xi+y)}}{\overline{u'(\xi).u'(\xi+y)}} \qquad (2.26)$$

$\lambda$ could then be obtained by plotting the correlation coefficients and fitting an osculating parabola as shown in Figure 5. As stated by Hinze, the accurate measurement of the correlation curve was not very simple, particularly at small values of y when the coefficient was close to unity.

A second measurement method was suggested by Townsend 129 who made use of Taylor's hypothesis and proposed:-

$$\frac{1}{\lambda} = \frac{1}{\overline{U}^2\,\overline{u'^2}} \cdot \overline{\left(\frac{\partial u}{\partial t}\right)^2} \qquad (2.27)$$

Thus, by introducing a differentiation circuit into the electronic system, $\lambda$ could be measured. Laufer {130} and Liepmann {131} proposed a zero-crossing method for the determination of microscale. The microscale could be obtained from the knowledge of the average number of zeros of the u fluctuations per unit time. They proposed the expression as:-

$$\lambda = \frac{\overline{U}}{\pi.N} \qquad (2.28)$$

where N was the number of zeros of u fluctuations per unit time. The zero-crossing technique was the simplest of the three techniques to perform, although it was found by Philip {132} that this method still needed modification.

## 2.4 Summary

The present literature survey has indicated that, although there have been numerous researchers investigating the various aspects of turbulence flow, there remained to be found a thorough and realistic criterion for the prediction of momentum and heat transfer. It would be more satisfying to have a theory that allows the turbulent eddy shape, size and velocity to change with respect to time. As suggested by Roshko {133}, understanding of the physical processes actually occurring in turbulent flows is indispensable for progress towards an analytical description of them. Even short of that, knowledge of these processes is helpful for understanding and coping with practical problems in which turbulent flow is prominent. It would also be more appropriate to study the effect of roughness on heat and momentum transfer with an approach that describes the detailed structure of the resistance to heat transfer.

Experimentally, the method as introduced by Wilson and described in the last section for the generation of a heat source was found to be appropriate. The laser doppler anemometry technique was found to be suitable for the measurement of turbulence character-:istics. Digital techniques have been shown to provide simpler and more controllable methods for turbulence measurements, particularly with the advance of present-day digital computers.

## 3. THEORETICAL ANALYSIS AND DEVELOPMENTS

The theoretical analysis was based largely on the concept proposed by Tyldesley & Silver {39},{40}. In their work, the basic idea of entity concept was presented and eddy diffusivities of momentum, heat and mass were proposed as dependent on two variables, the entity scale and velocity. The ratio of eddy diffusivity of momentum and heat, when compared with other reserchers' experimental data, were found to be well predicted. However, no rigorous derivation of the expressions were presented. Neither were the relationships between the entity scale and velocity clearly defined.

The present work makes a rigorous presentation of the theoretical concept of entity model' of turbulence. In discussing the two important parameters of the entity concept, conditions for which Tyldesley & Silver's predicted eddy diffusivities would hold, were discussed. Also, the thermodynamic relationship between the two random variables, R and $\overline{V}r$ was presented. Solutions to the momentum and energy equations under simple flow situations were proposed. Furthermore, overall heat transfer characteristics in a simple pipe flow were investigated using the turbulent Prandtl number, originally proposed by Tyldesley & Silver.

The present analysis was based on a thermodynamic approach, using the method of statistical inference to provide a first order theory. The transport properties of a turbulent fluid were investigated using a simple model to represent the detailed fluid behaviour which was attributed to the motions of fluid entities of varying size, shape and velocity. An analysis was made to find the effect on the whole system, of interaction and transport between the individual entities. Information theory has been successfully used as a means for the interpretation of turbulence parameters. Using the present analysis, it has been possible to predict characteristics of turbulence shear flow not vastly different from those found in practice, with only a minimum amount of information.

## 3.1 Transport equations and eddy diffusivities

### 3.1.1 Conservation of momentum transport

Consider that u, v and w are the x, y and z components of the fluid velocity $\overline{U}$. For a stationary control surface $dS_X$ in the fluid, the rate at which momentum is transported across this surface in the x-direction is given by:-

$$\dot{M}x = \dot{m}u = \rho u.u \; dS_X \qquad (3.1)$$

Similarly, for control surfaces $dS_Y$ and $dS_Z$ in the fluid, the rate at which momentum are transported across these surfaces respectively in the x-direction are:-

$$\dot{M}y = \rho u.v \; dSy \qquad (3.2)$$

$$\dot{M}z = \rho u.w \; dS_Z \qquad (3.3)$$

It was shown by Bradshaw {3} that a probability distribution may be defined such that Pu d u is the probability that u lies between u-½du and u+½du. Such a probability distribution satisfies the following conditions:-

$$\int_{-\infty}^{\infty} Pu\ du = 1$$

$$\int_{-\infty}^{\infty} u\ Pu\ du = \langle u \rangle$$

and $$\int_{-\infty}^{\infty} u^n\ Pu\ du = \langle u^n \rangle$$

where < > denotes the expected value of. Similarly, joint probability distributions Puv and Puw may also be defined such that Puv dudv is the probability that u lies between u-½du and u+½du at the same time that v lies between v-½dv and v+½dv; Puw dudw is the probability that u lies between u-½du and u+½du at the same time that w lies between w-½dw and w+½dw. Such probability distributions satisfy:-

$$\int_{-\infty}^{\infty} P_{uv}\ du = Pv$$

$$\int_{-\infty}^{\infty}\int_{-\infty}^{\infty} P_{uv}\ dudv = 1$$

$$\int_{-\infty}^{\infty}\int_{-\infty}^{\infty} P_{uv}\ u^m v^n dudv = \langle u^m v^n \rangle$$

and $$\int_{-\infty}^{\infty} P_{uw}\ du = P_w$$

$$\int_{-\infty}^{\infty}\int_{-\infty}^{\infty} P_{uw}\ dudw = 1$$

$$\int_{-\infty}^{\infty}\int_{-\infty}^{\infty} P_{uw}\ u^m\ w^n\ dudw = \langle u^m w^n \rangle$$

Hence, the expected values of rate at which momentum are transported across the surfaces $dS_x$, $dS_y$ and $dS_z$ are:-

$$\dot{<M_x>} = \int_{-\infty}^{\infty} Pu^2 .\ \rho u^2\ dS_x\ .\ du$$

$$\dot{<M_y>} = \int_{-\infty}^{\infty}\int_{-\infty}^{\infty} Puv\ \rho uv\ dS_y \cdot dudv$$

and $$\dot{<M_z>} = \int_{-\infty}^{\infty}\int_{-\infty}^{\infty} Puw\ \rho uw\ dS_z \cdot dudw$$

If a control volume dV is formed by the surfaces $dS_x$, $dS_y$ and $dS_z$, the rate at which momentum is transported across the volume in the x-direction is thus the sum of the momentum flux through the boundary surfaces. Hence,

$$\dot{<M>} = \dot{<M_x>} + \dot{<M_y>} + \dot{<M_z>}$$

$$\therefore \quad \dot{<M>} = dSx\,dSy\,dSz \left\{ \int_{-\infty}^{\infty} Pu\rho u^2 du\ dS_x + \int_{-\infty}^{\infty}\int_{-\infty}^{\infty} Puv\rho uv\ dudv\ dS_y + \int_{-\infty}^{\infty}\int_{-\infty}^{\infty} Puw\ \rho\ uw\ dudw\ dS_z \right\} \qquad (3.4)$$

Within the control volume, the rate of change of momentum in the x-direction is given by $\int_V \frac{\partial(\rho u)}{\partial t}\ dV$. Again, the expected value of the rate of change of momentum in the x-direction is:

$$\int_V \frac{\partial <u>}{\partial t}\ \rho.dV = \int_V \frac{\partial}{\partial t} \cdot \int_{-\infty}^{\infty} Pu.\rho u du\ dV$$

For conservation of momentum transport to be satisfied:-

$$\int_V \frac{\partial <u>}{\partial t}\ .\rho\ dV + \dot{<M>} = 0$$

$$\therefore \quad \int_V \frac{\partial}{\partial t} \int_{-\infty}^{\infty} Pu\rho u\ du\ dV + \int_S \left\{ \int_{-\infty}^{\infty} Pu\ \rho u^2\ du\ dSx + \int_{-\infty}^{\infty}\int_{-\infty}^{\infty} Puv\ \rho uv\ dudv\ dS_y + \int_{-\infty}^{\infty}\int_{-\infty}^{\infty} Puw\ \rho uw\ dudw\ dSz \right\} = 0 \qquad (3.5)$$

Using Green's theorem for transforming a surface integral into a volume integral, equation (3.5) becomes:-

$$\frac{\partial}{\partial t}\left[\int_{-\infty}^{\infty} Pu.\rho u\ du\right] + \frac{\partial}{\partial x}\left[\int_{-\infty}^{\infty} Pu.\ \rho u^2\ du\right]$$

$$+ \frac{\partial}{\partial y}\left[\int_{-\infty}^{\infty} P_{uv}\ \rho uv\ dudv\right] + \frac{\partial}{\partial z}\left[\int_{-\infty}^{\infty} P_{uw}\rho uw\ dudw\right]$$

$$= 0$$

Hence $\frac{\partial}{\partial t}[\rho\langle u\rangle] + \frac{\partial}{\partial x}[\rho\langle u^2\rangle] + \frac{\partial}{\partial y}[\rho\langle uv\rangle] + \frac{\partial}{\partial z}[\rho\langle uw\rangle] = 0$

(3.6)

Consider the flow of turbulence such that $u = \langle u\rangle + u'$, $v = \langle v\rangle + v'$ and $w = \langle w\rangle + w'$. Again, by applying the Reynolds rules of average, we get:-

$$\langle u^2\rangle = \langle u\rangle^2 + \langle u'^2\rangle$$

$$\langle uv\rangle = \langle u\rangle\langle v\rangle + \langle u'v'\rangle$$

$$\langle uw\rangle = \langle u\rangle\langle w\rangle + \langle u'w'\rangle$$

$\therefore$ equation (3.6) becomes:-

$$\frac{\rho\partial\langle u\rangle}{\partial t} + \langle u\rangle\ \frac{\partial\rho}{\partial t} + \langle u\rangle\ \frac{\partial}{\partial x}(\rho\langle u\rangle) + \rho\langle u\rangle\ \frac{\partial\langle u\rangle}{\partial x}$$

$$+ \langle u\rangle\ \frac{\partial}{\partial y}(\rho\langle v\rangle) + \rho\langle v\rangle\ \frac{\partial\langle u\rangle}{\partial y} + \langle u\rangle\ \frac{\partial}{\partial z}(\rho\langle w\rangle)$$

$$+ \rho\langle w\rangle\ \frac{\partial\langle u\rangle}{\partial z} + \frac{\partial}{\partial x}(\rho\langle u'^2\rangle) + \frac{\partial}{\partial y}(\rho\langle u'v'\rangle)$$

$$+ \frac{\partial}{\partial z}(\rho\langle u'w'\rangle) = 0 \qquad (3.7)$$

By considering the conservation of mass over the control volume dV in a similar manner as above, an equation of mass conservation or continuity may be obtained as:-

$$\frac{\partial\rho}{\partial t} + \frac{\partial}{\partial x}(\rho\langle u\rangle) + \frac{\partial}{\partial y}(\rho\langle v\rangle) + \frac{\partial}{\partial z}(\rho\langle w\rangle) = 0 \qquad (3.8)$$

Therefore, equation (3.7) may be expressed as:-

$$\rho\frac{\partial\langle u\rangle}{\partial t} + \rho\langle u\rangle \frac{\partial\langle u\rangle}{\partial x} + \rho\langle v\rangle \frac{\partial\langle u\rangle}{\partial y} + \rho\langle w\rangle \frac{\partial\langle u\rangle}{\partial z}$$

$$+ \frac{\partial}{\partial x}(\rho\langle u'^2\rangle) + \frac{\partial}{\partial y}(\rho\langle u'v'\rangle) + \frac{\partial}{\partial z}(\rho\langle u'w'\rangle)$$

$$= 0 \qquad (3.9)$$

Putting $\sigma_{xx} = \rho\langle u'^2\rangle$

$$\sigma_{xy} = \rho\langle u'v'\rangle$$

$$\sigma_{xz} = \rho\langle u'w'\rangle$$

$$\therefore \quad \frac{\partial\langle u\rangle}{\partial t} + \langle u\rangle \frac{\partial\langle u\rangle}{\partial x} + \langle v\rangle \frac{\partial\langle u\rangle}{\partial y} + \langle w\rangle \frac{\partial\langle u\rangle}{\partial z}$$

$$= -\frac{1}{\rho}\cdot\left\{\frac{\partial}{\partial x}\sigma_{xx} + \frac{\partial}{\partial y}\sigma_{xy} + \frac{\partial}{\partial z}\sigma_{xz}\right\} \qquad (3.10)$$

The above equation represents the equation of conservation of momentum in the x-direction and is analogous to the Reynolds equation with the $\sigma$ terms anlaogous to Reynolds stresses. Similar equations may also be obtained for the conservation of momentum in the y and z-directions. In general, the momentum equations may be expressed in tensor notation, as:-

$$\frac{\partial\langle u_i\rangle}{\partial t} + \langle u_j\rangle \frac{\partial\langle u_i\rangle}{\partial x_j} = -\frac{1}{\rho}\frac{\partial}{\partial x_j}\sigma_{ij} \qquad (3.11)$$

## 3.1.2 Conservation of energy transport

Using a similar type of analysis as in the previous section, an energy transport equation may be obtained as:-

$$\frac{\partial}{\partial t}\langle E_T\rangle + \frac{\partial}{\partial x_i}(\langle E_T\rangle\langle U_i\rangle) + \frac{\partial}{\partial x_i}\langle Q_i\rangle$$

$$+ \frac{\partial}{\partial x_i}(\langle U_j\rangle\langle\sigma_{ij}\rangle) = 0 \qquad (3.12)$$

where $E_T = \frac{1}{2}\rho(u^2 + v^2 + w^2)$ is the total energy of the fluid per unit volume. $Q_i$ is the energy flux due to the turbulent motion and $\sigma_{ij}$

is the shear stress.

$$E_T = \tfrac{1}{2}\rho(u^2 + y^2 + w^2)$$

$$= \tfrac{1}{2}\rho(\langle u\rangle^2 + u'^2 + 2\langle u\rangle u' + \langle v\rangle^2 + v'^2 + 2\langle v\rangle v'$$

$$+ \langle w\rangle^2 + w'^2 + 2\langle w\rangle w')$$

$$\therefore \quad \langle E_T\rangle = \tfrac{1}{2}\rho(\langle u\rangle^2 + \langle v\rangle^2 + \langle w\rangle^2 + \langle u'^2\rangle + \langle v'^2\rangle + \langle w'^2\rangle)$$

Putting $\langle E_T\rangle = \frac{1}{2}\rho\langle U\rangle^2 + \langle Ue\rangle$ where $\frac{1}{2}\rho\langle U\rangle^2$ represents the kinetic energy per unit volume of the fluid motion and $\langle Ue\rangle$ is the expected value of internal energy per unit volume of the fluid, equation (3.12) becomes:-

$$\frac{\partial}{\partial t}\left(\tfrac{1}{2}\rho\langle U\rangle^2\right) + \frac{\partial}{\partial t}\langle Ue\rangle + \langle u_i\rangle \frac{\partial}{\partial x_i}\left(\frac{\rho}{2}\langle U\rangle^2\right)$$

$$+ \langle U_i\rangle \frac{\partial}{\partial x_i}\langle Ue\rangle + \frac{\rho}{2}\langle U\rangle^2 . \frac{\partial}{\partial x_i}\langle U_i\rangle + \langle Ue\rangle \frac{\partial}{\partial x_i}\langle U_i\rangle$$

$$+ \frac{\partial}{\partial x_i}\langle Q_i\rangle + \sigma_{ij}\frac{\partial}{\partial x_i}\langle U_j\rangle + \langle U_j\rangle \frac{\partial}{\partial x_i}\sigma_{ij} = 0$$

implies,

$$\frac{\partial}{\partial t}\langle Ue\rangle + \langle Ui\rangle \frac{\partial}{\partial x_i}\langle Ue\rangle + \langle Ue\rangle \frac{\partial}{\partial x_i}\langle Ui\rangle + \frac{\partial}{\partial x_i}\langle Qi\rangle$$

$$+ \sigma_{ij}\frac{\partial}{\partial x_i}\langle U_j\rangle = -\left[\frac{\langle U\rangle^2}{2}\frac{\partial\rho}{\partial t} + \frac{\langle U\rangle^2}{2}.\rho\frac{\partial}{\partial x_i}\langle Ui\rangle\right.$$

$$+ \frac{\langle U\rangle^2}{2}\langle U_i\rangle\frac{\partial\rho}{\partial x_i} + \rho\frac{\partial}{\partial t}\frac{\langle U\rangle^2}{2} + \langle U_i\rangle.\rho.\frac{\partial}{\partial x_i}\frac{\langle U\rangle^2}{2}$$

$$\left. + Uj\ \frac{\partial\,\sigma ij}{\partial x_i}\right] \qquad (3.13)$$

Using the equations of mass transport (3.8) and momentum transport, it can be shown that the right-hand side of equation (3.13) is equal to zero, hence:-

$$\frac{\partial}{\partial t}\langle Ue\rangle + \frac{\partial}{\partial x_i}(\langle Ui\rangle\langle Ue\rangle) + \frac{\partial}{\partial x_i}\langle Qi\rangle + \sigma_{ij}\frac{\partial\langle u_j\rangle}{\partial x_i}$$

$$= 0$$

where the first two terms represent the rate of increase of energy in the turbulent fluid, $\frac{\partial \langle Qi \rangle}{\partial x_i}$ represents the energy diffusion and $\sigma_{ij} \frac{\partial \langle Uj \rangle}{\partial x_i}$ represents the dissipation due to turbulence fluctuations.

As the energy of the turbulent fluctuations is continuously dissipated into thermal energy, an additional dissipation term $\Phi$, has to be included in the above equation. So far, the fluid has been considered to be free from surface forces or momentum flux due to molecular viscosity. In order to include such effect, a viscous stress or a dissipation term due to viscous stresses must also be included. Hence, for a turbulent fluid, the momentum and energy transport equations may be expressed as:-

$$\frac{\partial \langle Ui \rangle}{\partial t} + \langle Uj \rangle \frac{\partial \langle Ui \rangle}{\partial x_j} = - \frac{1}{\rho} \left[ \frac{\partial \sigma i_j}{\partial x_j} + \frac{\partial \sigma'_{ij}}{\partial x_j} \right] \quad (3.14)$$

and

$$\frac{\partial}{\partial t} \langle Ue \rangle + \frac{\partial}{\partial x_i} \left( \langle U_i \rangle \langle Ue \rangle \right) + \frac{\partial}{\partial x_i} \langle Qi \rangle$$

$$+ \left( \sigma_{ij} + \sigma'_{ij} \right) \frac{\partial \langle Uj \rangle}{\partial x_i} = \Phi \quad (3.15)$$

Although the equations obtained above are similar to those obtained by more classical methods, the approach in deriving these equations is different. It is perhaps more customary to obtain the momentum and energy equation by assuming that the instantaneous velocity field satisfies the Navier-Stokes equation. However, the method used in the present analysis avoids this assumption and enables the problem of turbulence to be treated as the flow of a particular fluid having unusual transport properties. The more detailed than usual derivation demonstrated that the similarities which existed between the governing equations of the turbulent fluid transport and molecular transport of gases were not by chance, but were the result of the systems being indistinguishable when described by average or expected values of their variables.

In order to solve the momentum and transport equations, the internal behaviour of the fluid has to be described. Furthermore, the diffusion and dissipation terms have to be investigated and solved.

### 3.1.3 Dissipation of turbulent energy

In turbulent fluid flow, particles of fluid tend to combine together and move with a common velocity relative to the average motion of the fluid. These particles or eddies are of random size, shape and velocity in any particular region of the flow field and the average of these quantities varies with position. The intro-:duction of the entity shape and size presents difficulties when discussing its motion. However, this may be overcome by considering the slow motion of an ellipsoid of semi-principal axes (a,b,c) moving as a solid with average velocity $\overline{V}r = (Ur,Vr,Wr,)$ relative to the fluid average velocity $\overline{U} = (u,v,w)$. Providing the ellipsoid is small compared to the surrounding fluid and the relative velocity is not too high, the force acting on the ellipsoid, as shown by Lamb{134} and Landau & Lifshitz {135}, may be expressed as:-

$$F = 6\pi\mu R\ \overline{V}r \qquad (3.16)$$

where $R = R(a,b,c)$ is a function dependent on the shape and size of the ellipsoid. As the above expression was originally treated by Stokes, it has generally been referred to as the Stokes' formula.

Introduce a factor $\Theta$ such that $\Theta = R/r$ and when $a=b=c=r, \Theta = 1$. $\Theta$ may be regarded as a factor that accounts for the effect of distortion of the entity from a purely spherical shape. Considering the rate of energy dissipation due to the ellipsoidal entity,

$$\frac{d}{dt}\left(\tfrac{1}{2}\, m\, \overline{V}r^2\right) = -F.\overline{V}r$$

$$\therefore \quad \frac{4}{3}\pi r^3\Theta^3 .\ \rho .\ \frac{d}{dt}\left(\frac{\overline{V}r^2}{2}\right) = -6\pi\mu r.\Theta\overline{V}r^2$$

$$\therefore \quad \frac{d}{dt}\left(\frac{\overline{V}r^2}{2}\right) = -\frac{9}{2}\frac{\mu}{\rho}\cdot\frac{1}{r^2\Theta^2}\ \overline{V}r^2$$

Hence,

$$\left\langle \frac{d}{dt}\left(\frac{\overline{V}r^2}{2}\right)\right\rangle = -\frac{9}{2}\,\frac{\mu}{\rho}\left\langle \frac{\overline{V}r^2}{r^2\Theta^2}\right\rangle \qquad (3.17)$$

In order to proceed further, the correlation between velocity and the size of entities have to be known. Although most turbulent flows are inhomogeneous, the more important features of energy transport process are the same whether the flow is homo-:geneous or not. As indicated by Townsend {136}, if the time-:delay correlation function was converted to a structure function to give information about eddies of various sizes, the decrease of maximum autocorrelation with time was caused mostly by the random movements of eddy centres. If the random displacements were small compared with the eddy diameters, the change in the structure function would be produced substantially by simple translation by a convection velocity. In homogeneous turbulence, the convection velocity was constant for all sizes of eddies and equalled the mean flow velocity.

Taylor {137} suggested the structure function as:-

$$u_i(x,t) = u_i(x - u\tau,\ t+\tau) \qquad (3.18)$$

for not too large values of $\tau$. Townsend showed that the above relation was a good one if the random displacements of eddy centres in $\tau$ were small compared with the diameters of the smaller eddies. Velocity variations due to eddies of size d were completely uncorrelated for separation $\tau$ large compared with d/U.

The use of structure function to obtain information about eddy sizes is not restricted to homogeneous turbulence and it applies to all flows whose variations of mean velocity and fluctuating velocity are both small compared with the average velocity over the whole flow field. Nevertheless, the condition is not satisfied in turbulent jets and boundary layers as in these regions, the convection velocities of the large scale pattern of velocity may be considerably different from the local mean velocity.

Although the above argument was intended for obtaining the structure function, it may be deduced from the analysis that, providing the eddy velocity relative to the mean flow velocity is small and random displacements of eddies are small compared to the eddy sizes, the correlations between eddy size and its relative velocity is considered weak.

Hence equation (3.17) becomes:-

$$\frac{d}{dt}\left\langle \frac{\overline{V}r^2}{2} \right\rangle = -\frac{9}{2}\frac{\mu}{\rho}\frac{\langle \overline{V}r^2 \rangle}{\langle r^2\Theta^2 \rangle} \qquad (3.19)$$

which is a version of the well-known von Karman-Howarth equation {138} for the decay of energy with the term $\langle r^2\Theta^2 \rangle$ similar to the square of the microscale $\lambda$ . As dissipation of energy is equivalent to the rate of change of energy per unit volume, the dissipation term may be expressed as:-

$$\Phi = \rho\left\langle \frac{d}{dt}\left(\frac{\overline{V}^2}{2}\right)\right\rangle$$

Hence $$\Phi = -\frac{9}{2}\mu\frac{\langle \overline{V}r^2 \rangle}{\langle r^2\Theta^2 \rangle} \qquad (3.20)$$

### 3.1.4 Surface stresses in a turbulent fluid

So far, the eddies have been taken as an ellipsoid of semi-:principal axes (a,b,c) where R is a function of such axes. The factor $\Theta$ was used to indicate the shape distortion of the entity from a sphere. In flow situations remote from any physical boundary, it may be assumed that the turbulence is isotropic as the effect of a solid boundary which tends to generate disturbances is absent. It may then be assumed that in such a flow situation the eddies are of spherical shape. However, in flow situations not remote from physical boundary, isotropy may not be assumed and the ellipsoidal shape of the eddy has to be maintained.

For isotropic turbulence where a spherical entity is assumed, a=b=c=R=r and $\Theta$ =1. For nonisotropic turbulence, it may be assumed that the ellipsoid is in fact an elongated sphere with axes (a,a,b) and volume 4/3 $\pi a^2 b$.

As indicated in the last section, the correlation between eddy size and its relative velocity near a physical boundary might not be weak. Predictions obtained might not be as accurate as those for regions remote from physical boundaries. However, from the analysis that follows, it is apparent that a definite shape of an eddy is of minor importance in the analysis.

Consider an eddy of spherical shape as described above which has an average velocity along the x-axis and uniform in any plane perpendicular to the y-axis. In the case where the bulk flow is unidirectional with constant velocity gradient, the bulk velocity relative to some plane y=0 may be expressed as:-

$$\overline{U} = \left(y \frac{d\langle u\rangle}{dy}, 0, 0\right) \qquad (3.21)$$

With the absolute entity velocity taken as $\overline{V} = (U,V,W)$, components of forces acting on the entity are thus:-

$$Fx = 6\pi\mu.r \left(y \frac{d\langle u\rangle}{dy} - U\right)$$

$$Fy = -6\pi\mu r V$$

Considering the rate of change of momentum,

$$\frac{d}{dt}(m.U) = -6\pi\mu r \left(U - y\frac{d\langle u\rangle}{dy}\right)$$

$$\frac{d}{dt}(m.V) = -6\pi\mu r V$$

Hence,
$$\frac{dU}{dt} = -\frac{9\mu}{2\rho} \cdot \frac{1}{r^2} \left(U - y\frac{d\langle u\rangle}{dy}\right) \qquad (3.22)$$

$$\frac{dV}{dt} = -\frac{9\mu}{2\rho} \cdot \frac{1}{r^2} V \qquad (3.23)$$

If the initial conditions are $(U,V,W)_o = (Uo,Vo,Wo)$ when $y = 0$, it may be shown as in Appendix 3 that the solutions to the above equations are:-

$$U = Uo\,(1 - y/\lambda^*) + \frac{d\langle u\rangle}{dy}\left[\, y + \lambda^*\,(1-y/\lambda^*).\ln(1-y/\lambda^*)\,\right] \qquad (3.24)$$

$$V = Vo\,(1-y/\lambda^*) \qquad (3.25)$$

where $\lambda^* = Vo.\frac{2\rho r^2}{9\mu}$ is the mean distance travelled by the entity from the plane y = 0 before its momentum is entirely dissipated by viscous action.

Equations (3.24) and (3.25) represent the expected or average values of the velocity components of an entity which was created at time t = 0 in the plane y = 0. Equation (3.25) indicates that only the initial term is concerned with the value of Uo while the remaining terms are independent of Uo and give the effect of the velocity gradient $\frac{d\langle u\rangle}{dy}$ on the eddy velocity. As pointed out by Tyldesley & Silver {39} since the decay of entity of momentum is exponential, an infinite time is required for the entity to travel the distance $\lambda^*$. It thus represents a limit which will be rapidly approached but never actually achieved. Equation (3.24) also shows that the axial component of the entity momentum is influenced by the mean velocity gradient and thus give rise to a shear stress.

### 3.1.4.1 Shear stress due to momentum flux and eddy diffusivity of momentum

Since an entity is identified by its motion relative to the mean flow, it follows that entities are also created within the flow field. Consider the flux of entities crossing the plane y = 0 and, in particular, an entity that was created a distance $\lambda$ from the plane and is now crossing it. The entity velocities relative to the average fluid velocity are:-

$$Ur = \lambda\frac{d\langle u\rangle}{dy} - \left\{Uo(1-\lambda/\lambda^*) + \frac{d\langle u\rangle}{dy}\left[\,\lambda + \lambda^*(1-\lambda/\lambda^*)\ln(1-\lambda/\lambda^*)\right]\right\}$$

$$= -Uo\,(1-\lambda/\lambda^*) - \frac{d\langle u\rangle}{dy}\left[\,\lambda^*(1-\lambda/\lambda^*)\ln(1-\lambda/\lambda^*\,)\,\right]$$

$$Vr = -Vo\,(1-\lambda/\lambda^*)$$

Here, Uo and Vo are the values of Ur and Vr at the creation of the entity. The contribution to the kinetic shear stress from this entity may be expressed as:-

$$\sigma_{xy} = -\rho\langle Ur\ Vr\rangle$$

Hence, $\sigma_{xy} = -\rho\langle Uo\ Vo\ (1-\lambda/\lambda^*)^2\rangle - \rho\frac{d\langle u\rangle}{dy}\langle Vo\ \lambda^*(1-\lambda/\lambda^*)^2 \ell n(1-\lambda/\lambda^*)\rangle$

However, $\langle Uo\ Vo\ (1-\lambda/\lambda^*)\rangle$ may be taken as zero, providing the creation process favours neither positive nor negative values of Uo,

$$\therefore \quad \sigma_{xy} = -\rho\frac{d\langle u\rangle}{dy}\langle Vo\ \lambda^*\ (1-\lambda/\lambda^*)^2 \ell n(1-\lambda/\lambda^*)\rangle$$

$$= -\frac{2\rho^2}{9\mu}\ \frac{d\langle u\rangle}{dy}\langle Vo^2\ r^2\ (1-\lambda/\lambda^*)^2 \ell n(1-\lambda/\lambda^*)\rangle$$

$$\sigma_{xy} = -\frac{2\rho^2}{9\mu}\ \frac{d\langle u\rangle}{dy}\ \langle Vo^2\rangle\langle r^2\rangle\langle(1-\lambda/\lambda^*)^2 \ell n(1-\lambda/\lambda^*)\rangle \quad (3.26)$$

As there is continuous production and dissipation of entities and there is no mean flow in the transverse direction, the least prejudiced assignment of probability density to the value of $\lambda/\lambda^*$ when an entity crosses the plane y = 0 is that the density is uniform for all values of $\lambda/\lambda^*$ between 0 and 1. Thus, all values of $\lambda/\lambda^*$ between 0 and 1 are equally likely. Hence:-

$$\langle(1-\lambda/\lambda^*)^2 \ell n(1-\lambda/\lambda^*)\rangle = \int_0^1 (1-\lambda/\lambda^*)^2 \ell n(1-\lambda/\lambda^*)\ d\left(\frac{\lambda}{\lambda^*}\right)$$

$$= -\frac{1}{9}$$

$$\therefore \quad \sigma_{xy} = -\frac{2\rho^2}{9\mu}\ .\ \frac{d\langle u\rangle}{dy}\ .\ \langle Vo^2\rangle\ \langle r^2\rangle .\left(-\frac{1}{9}\right)$$

$$= \frac{2\rho^2}{81\mu}\ \langle r^2\rangle\langle Vo^2\rangle .\ \frac{d\langle u\rangle}{dy}$$

As shear stress due to momentum flux may also be expressed as $\sigma_{xy} = \varepsilon\mu\ \frac{d\langle u\rangle}{dy}$ where $\varepsilon\mu$ is the eddy viscosity

$$\therefore \quad \varepsilon\mu = \frac{2\rho^2}{81\mu}\ \langle r^2\rangle\langle Vo^2\rangle \quad (3.27)$$

The eddy diffusivity of momentum may be written as $\varepsilon_\nu = \varepsilon_\mu / c$, and hence may be expressed as:-

$$\varepsilon_\nu = \frac{2}{8T} \frac{\rho}{\mu} \cdot \langle r^2 \rangle \langle Vo^2 \rangle \qquad (3.28)$$

From the preceding analysis, the concept of eddy viscosity arises naturally from the description of an entity in turbulent fluid. Its value in any region of the fluid is dependent on the history of the entities traversing the region and, in this respect, it cannot be described as a local parameter.

### 3.1.4.2 Shear stress due to viscous forces

As discussed in section 3.1.2, the viscous effect in the turbulent fluid which gives rise to a viscous stress term must also be considered. This viscous stress term must be that of the average force per unit area of the entity as the entities cross the plane $y = 0$. The force acting on the spherical eddy is given by:-

$$F = 6 \pi \mu r \, Ur \qquad (3.29)$$

The projected area of a spherical entity is $\pi r^2$, hence the expected value of viscous stress may be given by:-

$$\sigma'_{xy} = \left\langle \frac{F}{\pi r^2} \right\rangle$$

$$= \left\langle 6 \mu \frac{Ur}{r} \right\rangle$$

Substituting the value of Ur as derived from the last section,

$$\sigma'_{xy} = \left\langle - 6 \mu \frac{1}{r} . \lambda^* (1-\lambda/\lambda^*) \ell n (1-\lambda/\lambda^*) \frac{d\langle u \rangle}{dy} \right\rangle$$

$$= - \frac{4}{3} \rho \langle r \rangle \langle Vo \rangle \langle (1-\lambda/\lambda^*) \ell n (1-\lambda/\lambda^*) \rangle \frac{d\langle u \rangle}{dy}$$

Again considering the probability density distribution:-

$$\langle(1-\lambda/\lambda^*)\ell n(1-\lambda/\lambda^*)\rangle = \int_0^1 (1-\lambda/\lambda^*)\ell n(1-\lambda/\lambda^*)d(\lambda/\lambda^*)$$

$$= -\frac{1}{4}$$

$$\therefore \sigma'_{xy} = \frac{1}{3}\rho \langle r\rangle\langle Vo\rangle . \frac{d\langle u\rangle}{dy}$$

Similarly to the shear stress due to momentum flux, the shear stress due to viscous forces may also be written as $\sigma'_{xy} = \varepsilon'\mu \frac{d\langle u\rangle}{dy}$ .

Hence $\varepsilon'\mu = \frac{1}{3}\rho \langle r\rangle \langle Vo\rangle$ (3.30)

or $\varepsilon'\nu = \frac{1}{3}. \langle r\rangle \langle Vo\rangle$ (3.31)

Comparing equation (3.27) with equation (3.30), it can easily be recognised that the shear stress due to momentum flux is much larger than that due to viscous forces as already indicated in section 2.1.

### 3.1.5 Thermal energy transport in a turbulent fluid and eddy diffusivity of heat

The process of thermal energy diffusion may be considered as carried out by the migration of entities between regions of differing energy. For consistency, an assumed uniformity of momentum within the entity implies an assumption of a uniformity of temperature. Hence, in thermal interactions, it is assumed that the entity has a uniform internal temperature. Consider a spherical entity of uniform internal temperature T surrounded by a turbulent fluid of temperature Tf, the heat transfer rate across the surface of the entity is given by:-

$$q = 4\pi r\, k\, (T - Tf) \qquad (3.32)$$

where k is the thermal conductivity of the fluid.

As in the case of momentum transfer, the interaction process is assumed to be quasistatic so that the above equation holds even when the temperature of the surrounding fluid is changing. Also, the heat transfer rate across the surface per unit volume of the entity may be considered as the heat flux density when the temperature gradient in the fluid is not large.

Hence, $$q = -4/3\ \pi r^3 . \rho Cp \frac{dT}{dt} \qquad (3.33)$$

Since the thermal energy flux must be from points at a high temperature to those at a lower temperature, thus the negative sign in equation (3.33). Comparing equations (3.32) and (3.33) gives:

$$\frac{dT}{dt} = -3\ \frac{k}{\rho Cp} . \frac{1}{r^2}\ (T - Tf) \qquad (3.34)$$

Similar to the argument for momentum transfer in section 3.1.4, where the temperature in planes perpendicular to the y-axis is uniform and the temperature gradient is constant, then the expected value of fluid temperature may be expressed as:-

$$\langle Tf \rangle = y \frac{d\langle Tf \rangle}{dy}$$

$$\therefore \quad \frac{dT}{dt} = -\frac{3\ k}{\rho Cp}\ \frac{1}{r^2}\ (T - y \frac{d\langle Tf \rangle}{dy}) \qquad (3.35)$$

If the initial condition is T = To when y = 0, it may be shown as in Appendix 4 that the solution to the above equation is:-

$$T = To(1-y/\lambda^*)^{a/b} + y \frac{d\langle Tf \rangle}{dy} + \frac{Vo}{(a-b)} \left[ (1-y/\lambda^*)^{a/b} - (1-y/\lambda^*) \right] \frac{d\langle Tf \rangle}{dy}$$

(3.36)

where $a = \frac{3\ k}{\rho Cp r^2}$ and $b = \frac{9\mu}{2\rho r^2}$

As T represents the internal temeprature of an entity, the temperature difference between the entity and the surrounding fluid as it crosses the plane y = 0 may then be expressed as:-

$$Tr = To(1-\lambda/\lambda^*)^{a/b} + \frac{Vo}{(a-b)} \left[ (1-\lambda/\lambda^*)^{\frac{a}{b}} - (1-\lambda/\lambda^*) \right] \frac{d\langle Tf \rangle}{dy}$$

As indicated in section 2.1, the enthalpy flux may be expressed as:-

$$q_H = \rho . Cp \langle Vr \cdot Tr \rangle$$

$$\therefore \quad q_H = -\rho Cp.\left\langle VoTo\,(1-\lambda/\lambda^*)^{\frac{a}{b}+1}\right\rangle - \rho Cp.\left\langle \frac{Vo^2}{(a-b)}\cdot\left[(1-\lambda/\lambda^*)^{\frac{a}{b}+1} - (1-\lambda/\lambda^*)^2\right]\frac{d\langle Tf\rangle}{dy}\right\rangle$$

Again, $\langle Vo\ To\ (1-\lambda/\lambda^*)^{\frac{a}{b}+1}\rangle$ may be taken as zero,.

Hence $$q_H = -\rho Cp.\left\langle \frac{Vo^2}{(a-b)}\left[(1-\frac{\lambda}{\lambda^*})^{\frac{a}{b}+1} - (1-\lambda/\lambda^*)^2\right]\frac{d\langle Tf\rangle}{dy}\right\rangle \qquad (3.37)$$

However, $$\frac{1}{a-b} = \frac{2\rho Cp.r^2}{(6k-9\mu Cp)}$$

and $$\frac{a}{b} = \frac{2k}{3\mu Cp} = \frac{2}{3Pr}$$

$$\therefore \quad q_H = \frac{2\rho^2Cp^2}{(9\mu Cp-6k)}\left\langle Vo^2\ r^2\left[(1-\lambda/\lambda^*)^{\frac{2}{3Pr}+1} - (1-\lambda/\lambda^*)^2\right]\frac{d\langle Tf\rangle}{dy}\right\rangle$$

$$= \frac{2\rho^2Cp^2}{(9\mu Cp-6k)}\ \frac{d\langle Tf\rangle}{dy}\ \langle Vo^2\rangle\langle r^2\rangle\left\langle (1-\lambda/\lambda^*)^{\frac{2}{3Pr}+1} - (1\lambda/\lambda^*)^2\right\rangle$$

Considering the probability density distribution,

$$\left\langle (1-\lambda/\lambda^*)^{\frac{2}{3Pr}+1} - (1-\lambda/\lambda^*)^2\right\rangle = \int_0^1 (1-\lambda/\lambda^*)^{\frac{2}{3Pr}+1} - (1-\lambda/\lambda^*)^2\, d(\lambda/\lambda^*)$$

$$= \frac{(3.Pr-2)}{6(1+3Pr)}$$

$$\therefore \quad q_H = \frac{\rho^2Cp}{9\mu}.\left(\frac{Pr}{1+3Pr}\right).\langle r^2\rangle\langle Vo^2\rangle\ \frac{d\langle Tf\rangle}{dy} \qquad (3.38)$$

As the enthalpy flux may also be expressed as:-

$$q_H = \rho.Cp.\varepsilon_H.\frac{d\langle Tf\rangle}{dy}$$

where $\varepsilon_H$ is the diffusion coefficient of thermal energy or the eddy diffusivity of heat.

$$\therefore \quad \varepsilon_H = \frac{\rho}{9\mu} \frac{Pr}{(1+3Pr)} \langle r^2 \rangle \langle Vo^2 \rangle \qquad (3.39)$$

A diffusion coefficient has been generated using the present analysis and its value is also dependent on the history of the entity traversing the region, as would be expected. The analogy between heat and momentum transport in turbulent flow may be investigated by considering the ratio of their eddy diffusivities. Using equations (3.28) and 3.39), the diffusivity ratio may be expressed as:-

$$\frac{\varepsilon_H}{\varepsilon_\nu} = \frac{4.5\ Pr}{(1+3\ Pr)} \qquad (3.40)$$

A non-dimensional similarity parameter given by the reciprocal of the above ratio is generally known as the turbulent Prandtl number, $P_{rt}$. Although, for flow in pipes, the turbulent Prandtl number varies across the section of the pipe, fairly adequate predictions of heat transfer may be made by the assumption of constant turbulent Prandtl number.

## 3.2 Interpretation of turbulence parameters

### 3.2.1 Distribution functions of the random variables

Up to now, two random variables R and $\overline{V}r$ have been used to describe the behaviour of a turbulent fluid. It has been shown that it was necessary and sufficient to use only these two variables to describe momentum and energy transport. In order to assess the probability distribution of these variables, information theory may be used to maximise the entropy of the analysis, subject to the given information.

In 1948, Shannon {139} presented a thorough account of his communication theory which provided the relationship between various independent random signals. As turbulence signals are generally random in nature, it gives a first indication that they may be analysed using Shannon's theory, or communication theory, in general. Jaynes {140} as well as Reza {141} proposed the method of least prejudiced or biased probability for random signal analysis. In fact, Tribus {142} showed that, in the case of a simple gas, the communication theory may be used to predict accurately its macroscopic behaviour.

In order to analyse the random variables in a turbulent flow, the method of Jaynes may be used. A summary of Jaynes' formalism is given in Appendix 5. In communication theory, the amount of information in an average message is given by the equation:-

$$S_i = -K \sum_i Pi \ \ell n \ Pi = -K \int_{-\infty}^{\infty} Pi \ \ell n \ Pi \ di \qquad (3.41)$$

where Pi is the probability of the occurrence of the event Ei and K is an arbitrary constant. The solution to the problem may be obtained by maximising the entropy Si subject to the given information.

Consider, firstly, the velocity variable of an entity $\overline{V}r$. The entropy of its distribution is thus given by:-

$$S_{\overline{V}r} = -K \int_{-\infty}^{\infty} P_{\overline{V}r} \ \ell n \ P_{\overline{V}r} \cdot d_{\overline{V}r} \qquad (3.42)$$

The probability distributions introduced in section 3.1.1 provide the constraints to the entropy, thus:

$$\int_{-\infty}^{\infty} P_{\overline{V}r} \cdot d_{\overline{V}r} = 1 \qquad (3.43)$$

$$\int_{-\infty}^{\infty} P_{\overline{V}r} \cdot \ \overline{V}r^2 \cdot d\overline{V}r = \langle \overline{V}r^2 \rangle \qquad (3.44)$$

Jaynes' method, as outlined in Appendix 5, suggests that $S_{\overline{V}r}$ is a maximum when

$$P_{\overline{V}r} = \exp\left[ -\alpha - \beta\overline{V}r \right]$$

where $\alpha$ and $\beta$ are referred to as Langrangian multipliers, and may be expressed as:-

$$\alpha = \ell n \left[ \int_{-\infty}^{\infty} e^{-\beta \bar{V}r^2} \, d\,\bar{V}r \right]$$

Using a table of definite integrals, $\int_{-\infty}^{\infty} e^{-ax^2} dx = \sqrt{\frac{\pi}{a}}$

$$\therefore \alpha = \tfrac{1}{2} \ell n \left( \frac{\pi}{\beta} \right)$$

and $$P_{\bar{V}r} = \left( \frac{\pi}{\beta} \right)^{-\frac{1}{2}} . e^{-\beta \bar{V}r^2}$$

Applying the above to the constraint equation (3.44),

$$\langle \bar{V}r^2 \rangle = \int_{-\infty}^{\infty} \left( \frac{\pi}{\beta} \right)^{-\frac{1}{2}} . \quad e^{-\beta \bar{V}r^2} \, \bar{V}r^2 \, d\bar{V}r$$

Again, from a table of integrals, $\int_{-\infty}^{\infty} e^{-ax^2} . x^2 dx = \frac{1}{2a} \sqrt{\frac{\pi}{a}}$

$$\therefore \quad \langle \bar{V}r^2 \rangle = \left( \frac{\beta}{\pi} \right)^{\frac{1}{2}} \frac{1}{2\beta} \cdot \left( \frac{\pi}{\beta} \right)^{\frac{1}{2}}$$

$$\text{or} \quad \langle \bar{V}r^2 \rangle = \frac{1}{2\beta} \qquad (3.45)$$

Hence, the square of the relative entity velocity may be expressed in terms of a variable $\beta$ which is identified as the "temper" of the velocity distribution. It may be seen that, from equation (3.45), $\beta$ is inversely proportional to the internal energy of the turbulent flow.

Consider now the variable R that describes the shape and size of the entity. The entropy of its distribution is also given by:-

$$S_R = - K' \int_{-\infty}^{\infty} P_R \ \ell n \ P_R \ dR \qquad (3.46)$$

As the creation process of an entity favours neither the positive nor negative direction, it may be assumed that the following constraints hold,

$$\int_{-\infty}^{\infty} P_R \, d_R = 1 \tag{3.47}$$

$$\int_{-\infty}^{\infty} P_R \, R^2 \, dR = \langle R^2 \rangle \tag{3.48}$$

Using identical argument as previously for the velocity distribution, the square of the entity size distribution may be expressed as:-

$$\langle R^2 \rangle = \frac{1}{2\beta'} \tag{3.49}$$

where $\beta'$ represents the 'temper' of the entity size distribution.

### 3.2.2 Relationship between the 'tempers'

Two new variables have been introduced during the investigation of the distribution functions. In order to obtain a relationship between the tempers $\beta$ and $\beta'$, further analysis using Jaynes' formalism has to be carried out. For a system with two independent random variables, the entropy of the system has a maximum when each individual random variable has a maximum entropy. The entropies of $\overline{V}r$ and R are given by:-

$$S_{\overline{V}r} = -K \int_{-\infty}^{\infty} P_{\overline{V}r} \, \ell n \, P_{\overline{V}r} \, d_{\overline{V}r}$$

$$S_R = -K' \int_{-\infty}^{\infty} P_R \, \ell n \, P_R \, dR$$

Substituting the probability distributions into their respective entropy equations yields:-

$$S_{\overline{V}r} = -K \int_{-\infty}^{\infty} \left(\frac{\pi}{\beta}\right)^{-\frac{1}{2}} e^{-\beta \overline{V}r^2} \cdot \left[ -\tfrac{1}{2} \ell n \left(\frac{\pi}{\beta}\right) - \beta \overline{V}r^2 \right] d\overline{V}r$$

$$= \frac{K}{2} \left[ \ell n \left(\frac{\pi}{\beta}\right) + 1 \right]$$

and $S_R = \frac{K'}{2}\left[ \ell n \left(\frac{\pi}{\beta'}\right) + 1 \right]$

Since for any function f(x,y) to be at a maximum, its gradient $\nabla f(x,y)$ must be equal to zero. Hence $\frac{\partial S_{\overline{V}r}}{\partial \beta} + \frac{\partial S_R}{\partial \beta'} = 0$ is the condition for the maximum entropy of the system.

$$\therefore \quad \frac{K}{2\beta} + \frac{K'}{2\beta'} = 0$$

$$\text{or} \quad \frac{\beta}{\beta'} = -\frac{K}{K'} = C \qquad (3.50)$$

where C is again an arbitrary constant.

It has just been shown that, if $\overline{V}r$ and R are the only two variables necessary for the description of turbulent flow, in discussing the maximum entropy of the system or the expected values of the variables, the ratio of the tempers of the distributions is a constant. So far, the momentum and energy transport in a turbulent fluid have been considered. The diffusion and dissipation process have been investigated in particular and found to be related to a simple parameter, the temper of its probability distribution. The analysis is reasonably simple, however, the validity of the analysis or, more precisely, the validity of the assumption taken during the analysis, depends on its capability in solving the momentum and energy equations.

## 3.3 Solutions to the momentum and energy equations

### 3.3.1 Simple flows remote from solid boundaries

Mean velocity profile for the case of a simple shearing flow in a region away from solid boundary may be investigated using the results obtained in previous sections. Consider that the mean flow is steady, its velocity component is in the x-direction only and the turbulent fluctuations are functions of y only, the momentum and energy transport equations become:-

$$-\frac{1}{\rho}\frac{d}{dy}\left(\sigma_{xy} + \sigma'_{xy}\right) + \frac{1}{\rho}\frac{dP}{dx} = 0 \qquad (3.51)$$

and $$\frac{d\langle Qx\rangle}{dy} + \left(\sigma_{xy} + \sigma'_{xy}\right)\frac{d\langle u\rangle}{dy} = \Phi \qquad (3.52)$$

As shown in sections 3.1.4.1, 3.1.4.2 and 3.1.5,

$$\sigma_{xy} = \frac{2}{81}\frac{\rho^2}{\mu}\langle r^2\rangle\langle Vo^2\rangle\frac{d\langle u\rangle}{dy} \qquad (3.53)$$

$$\sigma'_{xy} = \frac{1}{3}\rho.\langle r\rangle\langle Vo\rangle\frac{d\langle u\rangle}{dy} \qquad (3.54)$$

$$\text{and} \quad Q = \frac{\rho^2}{9}\frac{Cp}{\mu}\left(\frac{Pr}{1+3\ Pr}\right).\langle r^2\rangle.\langle Vo^2\rangle\frac{d\langle Tf\rangle}{dy} \qquad (3.55)$$

As already discussed in section 3.1.3, the analysis that followed was the same whether the shape of an entity was taken to be a sphere or an ellipsoid. The only parameter needed to be altered is the term $r^2$ or $R^2$ into $r^2\Theta^2$. Hence without the loss of generality, $\langle r^2\rangle$ and $\langle Vo^2\rangle$ may be expressed as:-

$$\langle r^2\rangle = \frac{1}{2\beta'} \quad \text{and} \quad \langle Vo^2\rangle = \frac{1}{2\beta}$$

where $\beta$ is the temper of the velocity distribution at the initial condition. Similar to equations (3.45) and (3.49), the expected values of the velocity and size of an entity may be deduced and expressed as:-

$$\langle \overline{V}r\rangle = \frac{1}{\beta} \quad \text{and} \quad \langle r\rangle = \frac{1}{\beta'}$$

where $\beta$ and $\beta'$ are the tempers of the $\overline{V}r$ and R distributions. Hence equations (3.53) - (3.55) become:-

$$\sigma_{xy} = \frac{2}{81}\frac{\rho^2}{\mu}\cdot\frac{1}{2\beta'}\cdot\frac{1}{2\beta}\cdot\frac{d\langle u\rangle}{dy}$$

$$\sigma'_{xy} = \frac{1}{3}\cdot\frac{1}{\beta'}\cdot\frac{1}{\beta}\cdot\frac{d\langle u\rangle}{dy}$$

$$\text{and} \quad Q = \frac{\rho^2 Cp}{9\mu}\cdot\left(\frac{Pr}{1+3\ Pr}\right)\cdot\frac{1}{2\beta'}\cdot\frac{1}{2\beta}\frac{d\langle Tf\rangle}{dy}$$

As indicated in section 3.2.1 $\beta$ is inversely proportional to the internal energy or the temperature of the turbulent fluid, and it may be deduced that:-

$$\langle Tf\rangle \propto \frac{1}{\beta}$$

$$\text{or} \quad \frac{d\langle Tf\rangle}{dy} = K.\frac{d\left(\frac{1}{\beta}\right)}{dy}$$

Introducing a set of constants such that

$$\psi_1 = \frac{\rho^2}{162\mu} \cdot C$$

$$\psi_2 = \frac{\rho}{3} C$$

$$\psi_3 = \frac{\rho^2 . Cp}{36\mu} \cdot \left(\frac{Pr}{1+3Pr}\right) . C . K$$

where C is the constant as derived in equation (3.50). Therefore, equations (3.51) and (3.52) become:-

$$-\frac{1}{\rho}\frac{d}{dy}\left[\frac{\psi_1}{\beta^2} \cdot \frac{d<u>}{dy} + \frac{\psi_2}{\beta^2}\frac{d<u>}{dy}\right] + \frac{1}{\rho}\frac{dP}{dx} = 0 \qquad (3.56)$$

and

$$\frac{d}{dy}\left(\frac{\psi_3}{\beta^2} \cdot \frac{d\left(\frac{1}{\beta}\right)}{dy}\right) + \left[\frac{\psi_1}{\beta^2}\frac{d<u>}{dy} + \frac{\psi_2}{\beta^2}\frac{d<u>}{dy}\right]\frac{d<u>}{dy} = \Phi \qquad (3.57)$$

A simple and perhaps rather trivial solution to the above equations is when there is no pressure gradient present in the flow field and $\beta$ is a constant. Hence, equation (3.56) implies,

$$-\frac{1}{\rho}\left(\frac{\psi_1}{\beta^2} + \frac{\psi_2}{\beta^2}\right) . \frac{d^2<u>}{dy^2} = 0$$

or

$$\frac{d^2<u>}{dy^2} = 0$$

giving

$$<u> = A\,y + B \qquad (3.58)$$

The above equation gives a linear velocity profile typical for that of Couette flow.

For a more general solution, with symmetry about the y-axis, it may be assumed that:-

$$\frac{1}{\beta} = \frac{1}{\beta_0}\left[1 + \left(\frac{y}{h}\right)^2\right]^{\frac{1}{2}}$$

where $\beta_0$ and h are constants introduced so as to non-dimensionalise $\beta$ and y respectively. Equation (3.56) gives:-

$$\frac{d}{dy}\left\{(\psi_1 + \psi_2).\frac{1}{\beta_o^2}\left[1 + \left(\frac{y}{h}\right)^2\right]\frac{d\langle u\rangle}{dy}\right\} = \frac{dP}{dx}$$

As $\frac{dP}{dx}$ is a function of x only, integrating the above yields:-

$$\frac{(\psi_1+\psi_2)}{\beta_o^2}.\left[1 + \left(\frac{y}{h}\right)^2\right]\frac{d\langle u\rangle}{dy} = \frac{dP}{dx}.y \qquad (3.59)$$

$$\therefore \quad \frac{d\langle u\rangle}{dy} = \frac{dP}{dx}.\frac{\beta_o^2}{(\psi_1+\psi_2)}.y.\left[1 + \left(\frac{y}{h}\right)^2\right]^{-1}$$

Expanding the expression $y\left[1 + (y/h)^2\right]^{-1}$ using Taylor's series and considering the region where $(y/h)<<1$, terms with higher than second order of $(y/h)$ may be neglected. Hence:-

$$\frac{d\langle u\rangle}{dy} = \frac{dP}{dx}.\frac{\beta_o^2}{(\psi_1+\psi_2)}.y$$

$$\langle u\rangle = \frac{dP}{dx}.\frac{\beta_o^2}{(\psi_1+\psi_2)}.\frac{y^2}{2} + K$$

with $\langle u\rangle_{y=0} = Uo$, the velocity profile is thus given by:-

$$\langle u\rangle = Uo + \frac{dP}{dx}.\frac{\beta_o^2}{(\psi_1+\psi_2)}.\frac{y^2}{2} \qquad (3.60)$$

The above equation gives a velocity profile for the core region of the flow under the influence of a pressure gradient. Hinze {143} provided experimental evidence to indicate that the mean velocity in the core region may be described by a velocity defect law of the form,

$$\langle u\rangle = Uo + A.y^n \qquad (3.61)$$

where A and n are constants determined by experimental data. The value of the exponent n generally lies between 1.4 and 2.1 which agrees fairly well with the above result.

### 3.3.2 Flow near a plane solid boundary

Although many of the assumptions taken in the present analysis indicate that it is not valid in a flow region near a solid boundary or in a turbulent jet, investigation is still attempted so as to explore the limitations to the analysis.

Near a plane solid boundary, isotropic turbulence may not be assumed and it is unlikely that representation of an eddy with a sphere will be satisfactory. It is likely that an eddy is better described by an ellipsoidal shape having symmetry about an axis perpendicular to the boundary. This stretching of the eddies was also suggested by the experiments of Comte-Bellot {144}.

Consider an ellipsoidal eddy having semi-principal axes (a,a,b) at a distance y from the limiting boundary of the turbulent region. The symmetric scale b will depend on both a and y, hence b may be expressed as a function of a and y:-

$$b = b(a,y) \tag{3.62}$$

It is assumed that a distance h can be found such that for $y >> h$, the eddies are again spherical. As the wall is approached, the ratio b/a decreases monotonically, tending to zero as y tends to zero. Hence, the parameter b may be expressed as:-

$$b = ay/h \tag{3.63}$$

such that at $y = h$, $b = a$ and as y tends to zero, b also tends to zero.

It was shown by Lamb {134} that, to a reasonable degree of approximation, the force acting on the ellipsoidal eddy of axes (a,a,b) may be taken to be independent of b and expressed as:-

$$F = 6 \pi \mu a . Vr$$

The mass of the ellipsoid does, however, depend on the value of b and can be expressed as:-

$$m = \rho . \frac{4}{3} \pi a^2 b = \rho \frac{4}{3} \pi a^3 . \frac{y}{h}$$

Considering the rate of energy dissipation due to the ellipsoidal entity:

$$\frac{d}{dt} \left( \tfrac{1}{2} m \overline{Vr}^2 \right) = -F . \overline{Vr}$$

$$\therefore \quad \frac{d}{dt} \left( \frac{\overline{Vr}^2}{2} \right) = -\frac{9}{2} \frac{\mu}{\rho} . \frac{h}{y} \frac{\overline{Vr}^2}{a^2} .$$

Hence $$\left\langle \frac{d}{dt} \left( \frac{\overline{Vr}^2}{2} \right) \right\rangle = -\frac{9}{2} \frac{\mu}{\rho} . \frac{h}{y} . \frac{\langle \overline{Vr}^2 \rangle}{\langle a^2 \rangle} \qquad (3.64)$$

As already discussed in section 3.1.1, the expected value of $a^2$ may be expressed in terms of its distribution as in equation (3.49), therefore:-

$$\langle a^2 \rangle = \frac{1}{2\beta'}$$

Using results obtained from equations (3.45) and (3.50), the dissipation term $\Phi$ may be obtained as:-

$$\Phi = -\frac{9\mu}{2} \frac{h}{y} . C \qquad (3.65)$$

The above equation indicates that dissipation is inversely proportional to the distance from the wall, which is a reasonable conclusion.

It was shown by Laufer {145} that, in turbulent flow near the walls of a channel, the energy diffusion term is small compared with the production and dissipation terms. Again, considering the mean flow to be steady and unidirectional, the momentum and energy equations become:-

$$\frac{1}{\rho}\ \frac{d}{dy}\left[\ \sigma_{xy}\ +\ \sigma'_{xy}\ \right]\ =\ 0 \qquad (3.66)$$

and $$\left[\ \sigma_{xy} + \sigma'_{xy}\ \right].\ \frac{d\langle u\rangle}{dy}\ =\ \Phi\ =\ -\frac{9\mu}{2}\ .\ \frac{h}{y}.C \qquad (3.67)$$

Equation (3.66) yields:-

$$(\sigma_{xy} + \sigma'_{xy})\ =\ C'$$

Hence:-

$$C'\ \frac{d\langle u\rangle}{dy}\ =\ -\ \frac{9\mu}{2}\ \frac{h}{y}\ C$$

$$\langle u\rangle\ =\ -\ \frac{9\mu}{2}\ h.\ \frac{C}{C'}\ \ell n\ y\ +\ K'$$

or $$\langle u\rangle\ =\ -\ \frac{9\mu}{2}\ h.K.\ell n\ y\ +\ K' \qquad (3.68)$$

The above equation gives a logarithmic velocity profile near a plane solid boundary. The analysis described above compares well with both experimental evidence and other researchers' analysis for regimes near the wall, as well as away from the wall (i.e. the law of the wall and the power law respectively). The only parameter differences in the analysis for the two flow situations is the different shapes in the eddies in the two regions.

## 3.4 Heat Transfer in circular pipes

Most analyses of heat transfer in turbulent flow assume the equality of eddy diffusivities of heat and momentum. However, modern versions of the analogy between heat and momentum transfer state that, for any particular fluid, the ratio of eddy diffusivity of heat to the eddy diffusivity of momentum is in general a function of Prandtl number. Analysis in section 3.1 has resulted in the presentation of a turbulent Prandtl number given by:-

$$\frac{1}{Pr_t} = \frac{\varepsilon_H}{\varepsilon_\nu} = \frac{4.5\ Pr}{(1+3\ Pr)} \qquad (3.69)$$

Although the turbulent Prandtl number varies across the section of the pipe, it has been indicated that fairly adequate predictions of heat transfer may be made by the assumption of a constant turbulent Prandtl number.

The momentum and heat transfer equations across the pipe may be expressed as:-

$$\frac{\tau_o}{\rho}\left(1 - \frac{y}{r_o}\right) = (\nu + \varepsilon_\nu)\ \frac{d\bar{u}}{dy} \qquad (3.70)$$

and

$$\left(\frac{q}{A}\right)_o\left(1 - \frac{y}{r_o}\right) = -(k + \rho\ Cp\ \varepsilon_H)\frac{dT}{dy} \qquad (3.71)$$

The above equations may be integrated across the pipe to obtain temperature distributions as a function of y. To carry out the integrations, universal velocity distributions are used. As shown by McAdam {146}, the manipulation led to the temperature distributions as:-

$$y^* < 5 \ : \ (T_o - T) = \frac{(q/A)_o}{\rho . Cp\sqrt{\tau o/\rho}} . Pr . y^* \qquad (3.72)$$

$$5 < y^* < 30: \ (T_1 - T) = \frac{5(q/A)_o}{Prt . \rho Cp . \sqrt{\tau_o/\rho}}\ \ell n\left[1 + P_{rt} . Pr\left(\frac{y^*}{5} - 1\right)\right] \qquad (3.73)$$

$$30 < y^* \ : \ (T_2 - T) = \frac{1.25(q/A)_o}{P_{rt} . \rho Cp\sqrt{\tau_o/\rho}} \cdot \frac{F}{2} . \ell n\ \left(\frac{Re}{60}\right)\sqrt{\frac{f}{2}} \qquad (3.74)$$

where the suffices 0, 1 and 2 denote conditions at $y^*=0$, $y^* = 5$, and $y^* = 30$ respectively and F is the diffusivity ratio given by:-

$$F = \frac{\varepsilon_H}{\varepsilon_H + k/\rho Cp}$$

Adding the above equations across the pipe yields:-

$$(T_o - T_c) = \frac{5(q/A)_o}{Pr_t \cdot \rho Cp \sqrt{\tau_o/\rho}} \cdot \left[ Pr_t \cdot P_r + \ell n\,(1+5\,Pr_t\,P_r) + \frac{F}{2} \cdot \ell n\,(\frac{Re}{60}) \cdot \sqrt{\frac{f}{2}} \right] \qquad (3.75)$$

The heat transfer parameter of the flow, Nusselt number, may be expressed as:-

$$Nu = \frac{h\,D}{k} = \frac{D}{(T_o - T_m)} \left(\frac{\partial T}{\partial y}\right)_o$$

Hence,
$$Nu = \frac{Pr_t \sqrt{\frac{f}{2}}\ Re.\ Pr}{\left(\frac{T_o - T_m}{T_o - T_c}\right) .5.\left[ Pr_t \cdot P_r + \ell n\,(1+5Pr_t Pr) + \frac{F}{2} \cdot \ell n\left(\frac{Re}{60}\right) \sqrt{\frac{f}{2}} \right]}$$

where
$$\frac{T_o - T_m}{T_o - T_c} = \frac{1}{\pi r^2} \int_0^{ro} \frac{u}{U} \frac{To - T}{T_o - T_c}\ 2\pi r\ dr \qquad (3.76)$$

As the eddy diffusivity ratio, F, is given by:-

$$F = \frac{\varepsilon_H}{(\varepsilon_H + k/\rho Cp)} \qquad (3.77)$$

and over a large part of the flow, $\varepsilon_H >> k/\rho Cp$, it may be assumed F = 1. Comparing with Martinelli's experimental results indicates that the above assumption is reasonable for Pe $>10^5$. Values of F for less restricted values of Pe are shown in Table 1(a). Also, values of (To-Tm)/(To-Tc) are shown in Table 1(b). Hence, using equation (3.69), the heat transfer parameter, Nu, may be expressed as:-

$$Nu = \frac{(\frac{1+3Pr}{4.5}) .\ Re. \sqrt{\frac{f}{2}}}{\left(\frac{To-Tm}{To-Tc}\right) .5.\left[ \frac{1+3Pr}{4.5} + \ell n\,(1 + \frac{5+15Pr}{4.5}) + \tfrac{1}{2}\,\ell n\,(\frac{Re}{60}) \cdot \sqrt{\frac{f}{2}} \right]} \qquad (3.78)$$

where $\sqrt{f/2}$ may be obtained experimentally or from empirical relations proposed by Drew et al {147} as,

$$f = 0.0014 + 0.125.Re^{-0.32} \qquad (3.79)$$

for Reynolds numbers between 3,000 and 3,000,000 or

$$f = 0.046.Re^{-0.2} \qquad (3.80)$$

over a limited range of Raynolds numbers between 5,000 and 200,000.

Nusselt numbers obtained using the above equation (3.78) are slightly higher than those obtained using the assumption of equal eddy diffusivities. This trend is as expected and thus further supports the investigation of a non-unity turbulent Prandtl number.

## 3.5 Concluding Remarks

The entity concept proposed by Tyldesley and Silver has been thoroughly presented. In particular, the relationships between the two random variables in the analysis, R and $\overline{V}r$, have been investigated. Further development of the entity concept has enabled solutions to the momentum and energy equations to be made under simple flow conditions. The main limitation to the analysis was the assumption of isotropic turbulence.

It seems that the present type of approach is capable of describing the behaviour of a turbulent fluid to a degree of accuracy comparable with other theories in common use. It is more satisfying to be able to discuss the structure of turbulence using an analysis closely related to the well established formalism of statistical thermodynamics.

In the analysis, Shannon's communication theory which was originally proposed for investigating the electronic communication signals has been successfully used for the interpretation of turbulence parameters. Therefore, the communication theory becomes a powerful tool in studying turbulence phenomena. The comparative simplicity of the model and the subsequent analysis

makes application to problems in turbulence tractable and it seems likely that it will be possible to describe the behaviour of turbulent fluid in most problems for which a laminar solution is possible.

It is concluded here that the described model of turbulence is a useful concept for predicting the transport behaviour in simple turbulent flow. However, the general limitation of a concept derived from a 'varied mixing-length' or 'eddy diffusivity' model is that of its simplicity, and thus only capable of predicting simple shear flows.

# 4. EXPERIMENTAL FACILITIES

In order to enable a study of turbulent transport properties, a water circuit which was originally designed by Philip {132} and subsequently modified was used. The circuit was of the open-return type, consisting of four pipelines of different diameters. As part of the turbulence measurements were to be made using a DISA Laser Doppler Anemometer, the working sections were designed to be of clear perspex pipes to allow the admission of laser beams through the flow.

The test sections could also be removed and replaced with artificially roughened pipes. In the middle of each test section, an injector was fitted to allow the injection of pre-heated fluid into the main flow so as to carry out direct heat transfer measure-:ments.

## 4.1 Main structure of Water Tunnel

The main recirculating section of the test rig was made of 76 mm internal diameter polypropylene pipes and fittings. Polypropylene was chosen for its resistance to attack from most fluids and chemicals, thus allowing the rig to be used with various fluids in the future. A schematic diagram of the tunnel is shown in Figure 6. As the material is resistant to most chemicals, it could not be joined by glueing or using solvents as with other plastic pipes. The best jointing method was found to be the fusion welding technique.

Water was stored in a main sump-tank of $1m^3$ capacity. A galvanised tank coated with bitumen paint was used, so as to keep the contamination of water to a minimum. The return line into the sump tank had an 'elephant's foot' fitted and there was a baffle in the middle of the tank. These helped in destroying the momentum of the fluid, thus ensuring a calm and airfree suction for the pump.

The main circulating pump was a WEIR SNA3 MONOGLIDE type, single stage centrifugal pump, capable of delivering a maximum flow rate of 30 litres/sec at 17 metres head. This pump was found to be

adequate in providing the level of flow rate desired in the test section. Although the perspex pipes in the working section could sustain pressure of up to 5 bars, some of the joints were found to be weaker. A butterfly valve immediately downstream of the pump was installed, so as to relieve some of the pressure on the perspex working sections of the rig. In each of the four main branches, a butterfly valve was fitted so that each, and any number of lines, might be selected or closed. The flow returned via a main control gate valve to the sump tank. Control of the flow rate was carried out using the main butterfly valve as well as by opening or shutting lines other than the one being used for measurements.

An orifice plate situated upstream of the four branches was used to monitor the bulk fluid flow rate. This measuring device, as designed in accordance with BS1042 {148}, was found to be necessary so that flow rates and hence velocities measured using the Laser Doppler Anemometer could be checked.

## 4.2 Perspex working section

The central test section was manufactured from clear, extruded acrylic tubes. Four different diameters were used, namely 25 mm, 38 mm, 50 mm and 63 mm nominal internal diameters. Flanges and spigots were fitted in all the joints in the perspex sections to ensure a smooth transition of flow past the joints. 'TENSOL' cement was used to join all the perspex pipes.

As indicated by Nikuradse {84}, a minimum entry of 25 diameters was required for fully developed turbulent flow, a minimum of 35 diameters downstream of the beginning of the working section was reached before an injector was placed into the main stream. The injector was used for the injection of pre-heated fluid for direct heat transfer measurements. There were entry ports for ten thermo-:couples downstream and one upstream of the injector, so that axial temperature distributions could be obtained downstream of the injector. The thermocouple entry ports were perspex saddles made from similar sheet as the pipe flanges. They were drilled and tapped for a plug

and included a small well for a rubber grommet under the threaded hole. The centre of each plug was drilled so that a thermocouple could be inserted and firmly held by screwing onto the grommet. One view of the perspex section is shown in Figure 7. The injector which was a 1 mm internal diameter stainless steel hypodermic tube was also glued onto one of the saddles.

It was essential that all the perspex sections were kept clean and polished, because any scratch or dirt on the perspex surface could impair the setting up and operation of the laser doppler anemometry.

## 4.3 Injection Circuit

An injection system with a flow-meter was incorporated so that flow rate of up to 0.75 litre/min through a 1 mm internal diameter injector could be achieved and measured. This could produce velocities of up to 15 m/s through the injector. The fluid for injection was contained in a 100 litre capacity, fully insulated tank. The temperature of the fluid was controlled by means of a variable thermostat via a contactor. The capacity of the tank contained sufficient fluid for a continuous injection of up to 2 hours at maximum flow rate, thus allowing sufficient time to carry out a series of temperature measurements.

As mentioned in the last section, the injector was manufactured from 1 mm internal diameter stainless steel hypodermic tubing. The injector was fitted to the perspex test section by means of a saddle similar to those used for the thermocouple entries. A copper tube extended back from the injector for approximately 10 cm and ended in a tee fitting to which a nylon tube from the injection pump could be fitted. The other junction of the tee was fitted with another thermocouple entry, so that the temperature of the heated fluid entering the injector could be measured. The area around the tee junction and the entire copper tubing was covered with insulating material, so that deviation from the temperature measured at the tee junction and the temperature of heated fluid entering the injector was negligible.

The prime mover of the injection circuit was a small gun metal gear pump driven by a 0.4 kW D.C. motor, which was, in turn, controlled by an electronic variable potentiometer type speed control. The flow rate was measured by means of a variable area flowmeter. The fittings in the circuit were connected by means of nylon tubings and 'ENOTS' type couplers. The flowmeter was calibrated relative to the injector size in terms of flow velocity, rather than flow rate, so that injection velocity could be directly adjusted to be the same as the bulk fluid velocity at the test section.

## 4.4 Roughened pipes

To study fully the effects of surface roughness on heat transfer, it is required to separate the regions such that $k^*<5$, $5<k^*<55$ and $k^*>55$. Although it is generally accepted that the turbulence flow pattern is not affected by the surface roughness in the case that $k^*<5$, as indicated in section 2.2, the increase in surface area of the rough wall inside the laminar sublayer could still affect the heat transfer slightly.

The full effects of surface roughness on the heat transfer were not studied with the present work, as this would require extensive experimental work. Instead, the experimental investigation was confined to roughness height such that $k^*<5$. This would provide the first critical experimental assessment of the theoretical analysis carried out in section 3.

In order to make such an investigation, internal surfaces of perspex pipes were coated with a thin layer of paint. Before coating, the paint was mixed with fine particles of less than 125 μm diameter. To obtain different relative roughness on the pipe wall, different quantities of particles were mixed. The method of coating was very similar to that of Nikuradse {46} except that, in his work, lacquer and sand grain were used. As perspex material is resistant to paint, special adhesive chemical was added to the paint by the manufacturer/

so that, when coated, the paint formed a permanent layer on the pipe surface.

As mentioned earlier, because the test sections had to be clear, so as to allow the admission of laser beams, two stripes of draughting tapes of 10 mm and 20 mm wide were adhered to the internal surface of the perspex pipe longitudinally before coating. After the paint was dried, the tapes were peeled off, leaving the test section with two parallel sections clear. A cross-section of one of such coated pipes as well as a picture are shown in Figures 8 and 9 respectively. The roughness height of each pipe was measured accurately using a RANK 'TALYSURF' roughness measuring system. Typical outputs of such roughness measurements are shown in Figure 10(a) - 10(c). The diameters of each pipe were measured accurately using micrometers and the relative roughness ratios derived from these measurements. The relative roughness ratio, r/k, obtained for the experimental investigation was between $7.2 \times 10^3$ and $2.5 \times 10^5$ with absolute roughness height between 4μm and 10μm. This level of roughness height was not sufficient to be projected beyond the laminar sublayer, so that $k^* < 5$.

# 5. EXPERIMENTAL TECHNIQUES

## 5.1 Velocity and turbulence intensity measurements

The measurements of velocity and turbulence characteristics during the present work were carried out using a DISA 55L Laser Doppler Anemometer. Laser doppler anemometry is a highly advanced system for scientific measurements of local flow velocity and possesses outstanding advantages in flow measurement.

The most notable advantage is the non-contact probing, which does not disturb the flow. Only light is needed to be transmitted to the point of interest and the light from a laser can be focused onto a very small volume where the velocity is required. The consequent resolution, typically 20 — 100$\mu$m exceeds that obtainable by any other method. As it is a high resolution fast response technique, it is in the field of turbulence that its potentialities are fully realised. On the other hand, this technique is not well suited for measurement of bulk flow as this requires an integration over a cross-section.

One of the main limitations of the laser doppler technique is its dependence on the presence of particles or seedings in the flow. However, measurements in water flow is far less of a problem than air flow, as mains water generally contains sufficient contamination in the way of particles for laser doppler anemometry, so that seeding is usually not required. A list of the advantages and disadvantages of the laser doppler technique was suggested by Drain {149} and is shown in Table 2.

### 5.1.1 Principle of LDA

In any form of wave propagation, frequency changes can occur owing to movement of the source, receiver, propagating medium, or intervening reflector or scatter. These shifts of frequency are generally called 'Doppler' shifts after the Austrian physicist who first considered the phenomenon in 1842.

In order to utilize the measuring principle based on the Doppler effect, a monochromatic light source emitting coherent light waves must be used to produce the incident beam to the flow. The laser fulfils these requirements of the light source and, with its high intensity, is well suited for this purpose . When the laser beam passes through the flow, the light is scattered by particles suspended in the fluid. The scattered light contains information about the velocity which is interpreted by optoelectronic means.

The optical and optoelectronic equipments used in laser anemometry are, besides the laser itself, a beam splitter, lenses, apertures, a filter and a photodetector These components may be arranged for different modes of operation, namely the reference beam mode, the differential-doppler mode and the dual beam mode. During the course of the present experimental work, the differential-doppler mode was chosen as it has a considerable signal to noise advantage over the other modes. Also, with this mode, scattered light may be collected over a wide aperture, whereas with the reference beam technique, the useful aperture is extremely restricted.

A simple differential doppler arrangement is illustrated in Figure 11. The two illuminating beams derived from the laser are focused onto a small region conveniently by a single lens. Scattered light from this region is focused onto the photodetector. Since light scattered from the beams reaches the detector simultaneously, a beat is obtained of a frequency equal to the difference in Doppler shifts corresponding to the two angles of scattering. It may be shown that the beat frequency is independent of the receiving direction and is given by:-

$$fD = \frac{2u}{\lambda} . \sin \frac{\theta}{2} \qquad (5.1)$$

where u is the velocity of particles passing through the measuring volume, $\lambda$ is the wave length of the laser light and $\theta$ is the angle between the two illuminating beams.

Hence, the velocity of particles through the measuring volume or, in fact, the velocity of the flow, is thus:-

$$u = \frac{fD \cdot \lambda}{2 \sin \frac{\theta}{2}} \qquad (5.2)$$

As the region where the two beams cross is full of interference fringes as shown in Figure 12, the modulation of the intensity at the photodetector is simply due to the variation in the illumination of particles as they cross light and dark fringes. For this reason, the technique is sometimes called the 'intensity modulation' or the 'real fringe' method.

### 5.1.2 Measurements using LDA

The laser doppler anemometry equipment used in the experimental study consisted of a SPECTRA PHYSICS 15 mW Helium-Neon laser, a DISA 55L optical unit, a photomultiplier, a high voltage supply, a doppler signal processor with a preamplifier, a frequency tracker and a meter unit, and an ADVANCE 44 digital voltmeter. The output signal from the signal processor was linked directly to a DEC PDP 11/10 computer. A schematic diagram of the LDA measurement chain is shown in Figure 13.

The laser beam was passed into the optical unit housing where it was split by means of a biprism into two beams of equal intensity, one passing through the biprism, and the other being deflected through $90^{o}$ as in Figure 11. The other beam was then deflected again by means of an adjustable surface mirror so that it ran parallel to the original beam, but separated from it. The two beams were then focused onto an intersection point by means of a plano-convex lens at the front of the housing. In order to ensure that the two beams intersected perfectly, a test objective was used to project the intersection volume onto a screen as in Figure 14. Adjustment of the intersection was made via the two adjustment screws on the mirror housing of the optical unit. These screws turned the glass wedge plates adjusting the direction of one of the beams. With correct intersection adjustment, the screen showed two overlapping spots with interference fringes.

The beams were introduced into the flow and positioned using a traversing mechanism. Together with the experimental rig, a special gantry and traverse mechanism was built to enable the

measuring volume to be traversed across the flow without disturbing the fine adjustments. Such a traversing mechanism is shown in Figure 15. The photomultiplier was then set focused onto the measuring volume. It simply detected the doppler shift of the light scattered from the measuring volume and amplified it to an acceptable level for the electronic instrumentation. The high voltage required for the photomultiplier cathode was supplied by the high voltage unit with the anemometry.

The output from the photomultiplier tube was passed to the preamplifier in the signal processor via the high voltage unit. The signal was amplified and filtered before passing to the frequency tracker. The tracker followed the doppler frequency and gave a D.C. output voltage directly proportional to the frequency. Apart from displaying this frequency on the meter unit, it was also sent in parallel to two BNC sockets on the front of the meter panel. The output from the meter unit was monitored on a digital voltmeter as well as connected to the minicomputer for on-line data sampling.

### 5.1.3 Computer Link

The processing of results by digital means was carried out by a DEC PDP 11/10 computer. The small digital computer has 16 K store, part of which was used to support the programming language, BASIC. The voltage output from the frequency tracker was collected using the AR11 analogue/digital converter unit in the computer. Data was stored and then analysed when sampling was completed. Using BASIC to control the sampling, it was found that the largest and fastest optimised sample size and rate was 1200 at 2.5 kHz. As a sample size of 1200 was found to be insufficient for the investigation, the ensembled or time averaged technique which made an average over repeats of an experiment was used to sample 1200 data ten times, assuming that conditions remained constant during the process, thus making the total number of samples 12,000.

The analogue input of the AR11 operated in a bipolar mode between -2.5V and +2.5V. As the output from the tracker was 0 - 10 V, it was necessary to include a voltage divider in the system.

With the output of the AR11 between 0 and 1024 non-dimensionally, the AR11 together with the voltage divider had to be calibrated. The calibration was carried out using a frequency generator and the signal processor in its manual mode as a DC supply. The calibration with subsequent least square fit of the data produced a first order polynomial for converting the AR11 digital output into a voltage for the calculation of doppler frequency. This calibration was checked from time to time to ensure stability of the voltage divider.

### 5.1.4 Calibration of measurement chain

The accuracy of the LDA depends on an accurate measurement of beam separation angle, which may be obtained simply from careful measurement of the optical set-up geometrically. However, the accuracy and reliability of the whole measurement chain requires verification.

First of all, calibration tests were carried out to obtain the optimised sample size for accurate measurements of velocity and turbulence intensity. Figure 16 shows the results of some such tests. It indicated that, with a sample size of 12,000 or more, results converged with an error band of less than 2%. Hence, a sample size of 12,000 was chosen for the main tests.

Having established the number of samples required for accurate velocity measurements, tests were carried out to verify the accuracy of the measurement chain. As the LDA only allowed the measurements of velocity at a point, a velocity traverse had to be carried out and integrated over the cross-section to obtain the mean bulk fluid velocity. As suggested by Boadway & Karahan {150}, refraction at optical surfaces changes the paths of the laser beams, thus moving both their point of intersection and the angle between the beams. It was therefore necessary to evaluate the actual distance of the beam intersection from the inside of the pipe wall relative to the virtual distance of the beam intersection. This is shown in Appendix 6.

As mentioned in section 4.1, an orifice plate was used to monitor the bulk fluid flow rate. Using the BS 1042 {148}, pressure drop across the orifice plate was used to calculate the flow rate and hence the mean velocity of the flow. Figure 17 shows the results of such a velocity traverse. The mean velocity calculated from the velocity traverse measurements compared well with that obtained from orifice plate results. The 4% discrepancy between the two indicated that the entire measurement chain may be considered accurate to within 4%. Computer programs for the above calibration tests are listed in Appendices 7 and 8.

## 5.2 Microscale measurements

Microscale is a measure of the average dimension of the eddies that are mainly responsible for the dissipation of energy. It may also be considered as a measure of the dimension of eddies which, at the same intensity, produce the same dissipation as the turbulence considered. The measurement of microscale was carried out using a method based on the zero-crossing technique proposed by Laufer {130} and Liepmann {131}.

With the zero-crossing technique, the microscale of turbulence was given by:-

$$\lambda = \frac{\overline{U}}{\pi . N} \qquad (5.3)$$

where $\overline{U}$ was the mean velocity and N was the average number of zeros of the u fluctuations per unit time. The derivation of this expression assumed u to be a pure harmonic such that:-

$$u = u^* \sin \frac{2\pi t}{T} \qquad (5.4)$$

Although Laufer and Liepmann suggested that the expression was also true for a real turbulence, a number of the high frequency fluctuations were bound to be ignored due to the nature of turbulence characteristics. However, it may be shown that the number of maxima and minima of u fluctuations per unit time is equal to the number of zeros with a harmonic wave form. Furthermore, counting the number of maxima and

minima, or the inflexion counting technique, also takes the high frequency fluctuations of the turbulent signal into account.

The evaluation of microscale was carried out with the measurement chain as described in section 5.1.2 using the inflexion counting technique. A computer program, as shown in Appendix 9, was written which compared the slopes of two consecutive pairs of results and incremented every time it changed sign. A lack of available experimental data on microscale has prevented a direct verification of the method. However, values of microscales obtained during the tests were found to be about 1 ∿2 mm, which was considered to be of the correct order of magnitude.

## 5.3 Temperature

In order to carry out temperature measurements, thermocouples situated upstream and downstream of the injector were used. One thermocouple was placed in the injection circuit just before the injector, so as to measure the temperature of the injection fluid.

The thermocouples were PYROTENAX TIOHT7 nickel chromium/ :constantan insulated thermocouples with a bonded hot junction. The thermocouple e.m.f. were sampled with a SOLARTRON 3230 data transfer unit coupled to a DVM and driven by a TS 50/3232 low level scanner, as shown in Figure 18. Although the data transfer unit was capable of sampling at a rate of 25 Hz, the teletype printer which was used for outputting the data, had a much slower printing speed. Hence, the sample rate during the temperature measurements had to be greatly reduced to approximately 2Hz.

Twelve thermocouples in all were used for temperature measure- :ments and were calibrated individually in an oil bath for the range of $15^{o}C \sim 80^{o}C$. A second order polynomial was derived for each thermo- :couple, using the method of least square. The computer program written for the derivation is listed in Appendix 10. Coefficients of each polynomial are shown in Table 3.

One of the thermocouples was placed in the injection circuit to monitor the temperature of the injection fluid. Although the area just before the injector was insulated, temperature loss along the stainless steel hypodermic injector due to convection still existed and resulted in the thermocouple giving a higher reading. In order to verify this loss against theoretical prediction, another thermocouple consisting of fine copper/constantan wires of 0.16 mm diameter was placed inside the injector just before the injection point, so as to measure an accurate temperature of injection fluid. This thermocouple was also calibrated between $15^{o}C \sim 80^{o}C$ and results found to be almost identical to that provided in BS 1828 [151]. Figure 19 shows the result of such calibrations.

Tests have shown that the temperature loss along the injector was well predicted by the theoretical analysis as outlined in Appendix 11. Therefore, during the main experiments, the fine wire thermocouple was not used, so as not to restrict the injection flow rate. Injection temperature was thus evaluated from readings obtained using the thermocouple situated before the injector.

## 5.4 Heat Transfer

Apart from obtaining heat transfer measurements from velocity and turbulence intensity measurements as described in section 3.1.5, heat transfer measurements were also deduced from temperature distribution along the centreline after the injection of heated fluid. By keeping the injector size as small as possible, the injected fluid could be considered as a moving point source of heat.

With a continuous point source of heat at the centre of the pipe, the rise in temeprature along the centreline may be expressed as:-

$$(T-T_o) = \frac{Q}{4\pi k_t.(x-x_o)} \qquad (5.5)$$

where Q is the heat source strength, $k_t$ is the total diffusivity of heat and $(x-x_o)$ is the distance from the injector. Re-arranging equation (5.5), the eddy diffusivity of heat may be expressed as:-

$$\varepsilon_H = \frac{\overline{U} \cdot d^2}{16} \cdot \frac{\Delta\Theta}{\Delta T} \cdot \frac{1}{(x - x_o)} - \frac{\nu}{Pr} \qquad (5.6)$$

where $\overline{U}$ is the mean velocity of injection fluid, d is the diameter of injector, $\Delta\Theta$ is the difference of ambient and injection temperation and $\Delta T$ is the temperature rise along distance $(x-x_o)$.

Along the axis of the flow, it may be assumed the eddy diffusivity of heat to be uniform with x. Therefore, for a particular flow condition, $\frac{\Delta\Theta}{\Delta T} \cdot \frac{1}{(x - x_o)}$ could be assumed constant. However, experimental results as in Figure 20 indicated that the slope of $\frac{\Delta\Theta}{\Delta T}/(x-x_o)$ failed to be constant in two regions. As already suggested by Sheriff & O'Kane {101} this could be caused by the assumptions of single point source of heat and infinite boundary not being satisfied. Particularly, in the region very near to the injector, momentum change in the injected fluid immediately after injection caused by the difference in temperature, density, viscosity and even velocity led to a finite distance or time required for developed flow. Also difference in temperature could lead to irregularity in flow pattern due to buoyancy effect. Further downstream, the effect of the pipe wall became apparent and thus affected the temperature difference.

The above problem was overcome by least square fitting a straight line through the points in the graph of $\frac{\Delta\Theta}{\Delta T}./_{(x-x_o)}$ vs distance from injector. Either point from the two extremes which lay outside a 5% error band was neglected and a new straight line fitted. The process was performed iteratively until all the points lay within the band. The slope of the final straight line was then used for the evaluation of eddy diffusivity of heat. A computer program, as listed in Appendix 12, which applied the above process and evaluated the eddy diffusivity of heat, was written for the analysis.

As the theoretical analysis in section 3.1.5 suggested that the eddy diffusivity of heat could be expressed as:-

$$\varepsilon_H = \frac{\rho}{9\mu} \frac{Pr}{(1+3Pr)} \langle r^2 \rangle \langle Vo^2 \rangle \qquad (5.7)$$

where $\langle r^2 \rangle$ is the expected value of the square of half the microscale and $\langle Vo^2 \rangle$ is the expected value of the square of the initial relative

entity velocity. The $\langle r^2 \rangle$ term was obtained as discussed in section 5.2. In the centre of the pipe, assumption of isotropy allowed the assumption of $\langle Vo^2 \rangle = \langle Uo^2 \rangle$ . Although $\langle Uo^2 \rangle$could not be measured directly using the LDA, it could be deduced from the instantaneously and mean velocity measurements as $u'=u-\bar{u}$. Hence $\langle Vo^2 \rangle$ was given by:-

$$\langle Vo^2 \rangle = \frac{\sum_{1}^{n}(u-\bar{u})^2}{N} \qquad (5.8)$$

As listed in Appendix 13, a computer program was written for the on-:line processing of velocity, turbulence intensity, microscale, entity velocity and hence the eddy diffusivity of heat.

## 5.5 Pressure measurements

As mentioned in sections 4.1 and 5.1.4, pressure drop across the orifice plate had to be obtained in order to verify the bulk flow rate. A NATIONAL SEMICONDUCTOR LX1603DF fluid filled differential pressure transducer was used for the measurements. Although the response of the transducer was rather slow, it was found to be well suited for monitoring bulk or mean pressure difference. The trans-:ducer was an electronic chip type, containing a bridge circuit and required only a 15V D.C. power supply. The transducer was calibrated using a vacuum pump and a mercury manometer. As shown in Figure 21, the calibration was found to be consistent with the design data supplied by the manufacturer.

# 6. RESULTS AND OBSERVATIONS

## 6.1 Velocity, turbulence intensity and microscale

A series of experiments was carried out to obtain the measurements of velocity, turbulence intensity and microscale. A longitudinal traverse of the pipe was undertaken to investigate the variation of the turbulence characteristics in the spatial direction. As all the measurements were taken at least 32 diameters downstream of the beginning of the perspex working section, turbulence was expected to be fully developed, hence, velocity, turbulence intensity and microscale measurements were expected to be constant in the spatial direction. As indicated in Table 4, the deviation of velocity, turbulence intensity and microscale measurements in the spatial direction was small and, in all cases, lie well within the error band as discussed in Appendix 14.

Velocity traverse in the radial direction across the pipe was also carried out. The velocity profile across the pipe, as shown in Figure 22, compared well with the power laws. Apart from the well-known 1/7 power law, as Reynolds number was generally greater than $10^5$, the 1/10 power was also plotted. The close agreement between experimental data and the power laws further indicated that the flow was fully developed in that region. Therefore, measurements in the present experimental work were taken 32 diameters downstream from the beginning of the working section.

There was no direct control of the level of turbulence intensity as it was only promoted by the sudden change of diameter at the beginning of the working section. Figure 23 showed that the turbulence intensities achieved in the tests were between 3% to 8%. Measurements of microscales were also taken and Figure 24 indicated that an increase of Reynolds number led to an increase of microscale. The relationship between initial eddy velocity, as also described by von Karman & Lin [152], and microscale was shown in Figure 25 and indicated that a larger energy dissipation eddy generally

had a greater initial eddy velocity. The microscales obtained during the experiment were found to be between 0.75 mm to 2.25 mm which was the correct order of magnitude to be expected.

Figures 22 - 25 also indicated that, within the error bands, the turbulence characteristics were not influenced by the relatively low roughness ratio. As expected, when $k^* < 5$, the pipes could be considered hydraulically smooth and turbulence characteristics such as velocity, turbulence intensity and microscale were not expected to vary with relative roughness ratio.

## 6.2 Eddy diffusivity of momentum and heat

Measurements of eddy diffusivity of momentum were obtained using the expression as discussed in section 3.1.4. Figures 26(a) and (b) showed the distribution of eddy diffusivity of momentum obtained along the centreline of pipes of two different diameters. The Reynolds number achieved for the tests were between $2 \times 10^5$ to $10^6$, thus representing a typical range of Reynolds number for turbulence flow. Results influenced by different roughness height were plotted. It could be seen that the small roughness height coated in the pipes had no effect on the eddy diffusivity of momentum, within the specified error band. As expected, the values of eddy diffusivity of momentum obtained were a few orders of magnitude larger than the kinematic viscosity of the fluid. Moreover, as both the microscales and initial eddy velocities increased with Reynolds number, the eddy diffusivity of momentum also increased sharply with Reynolds number.

Figures 27(a) and (b) showed the eddy diffusivity of heat obtained with the expressions as discussed in sections 3.1.5 and 5.4. It could be seen that the results obtained with the thermocouple readings were generally lower than those obtained with the LDA. Again, within the estimated error band, the roughness height had no effect on the eddy diffusivity of heat. Similar to that of the momentum transfer, the values of eddy diffusivity of heat, obtained with either the thermocouples or the LDA, were a few orders of magnitude larger than the molecular thermal diffusivity, $k/\rho Cp$, of the fluid.

# 7. ANALYSIS AND DISCUSSIONS

## 7.1 Principle of similarity in momentum and heat transfer

In order to analyse the experimental quantities of eddy diffusivity of momentum and heat, the principle of similarity was applied. The existence of similarity parameters discovered on the basis of the study of a model would apply, not only to the original system, but also to an infinite number of other systems, provided they were physically similar to the model.

As indicated by Gröber et al {153}, the method of similarity allowed the researchers to generalise the experimental results with the aid of the model rules. The determination of the model rules reduced itself to the establishment of dimensionless parameters which were in the form of products of powers of dimensioned quantities such as length, temperature and velocity. The dimensionless para-:meters of a given system can be determined in a number of ways. A well-known technique called the Buckingham $\Pi$ method was used in Appendix 15 to obtain a set of non-dimensional parameters which satisfied the principle of similarity in turbulent momentum and heat transfer. The similarity parameter could be expressed as:-

$$\Pi_1 = \frac{\varepsilon_H}{UD} \tag{7.1}$$

$$\Pi_2 = \frac{\varepsilon_H}{\nu} \tag{7.2}$$

$$\Pi_3 = \frac{\varepsilon_H}{k} . \rho Cp \tag{7.3}$$

$$\Pi_4 = \frac{\varepsilon_\nu}{U.D} \tag{7.4}$$

$$\Pi_5 = \frac{\varepsilon_\nu}{\nu} \tag{7.5}$$

It was interesting to note that both the ratios of $\Pi_2$ to $\Pi_1$ and $\Pi_5$ to $\Pi_4$ gave the familiar similarity parameter, the Reynolds number. Also, the ratio of $\Pi_4$ to $\Pi_1$ or $\Pi_5$ to $\Pi_2$ was, in fact, the turbulent Prandtl number. Since $\Pi_5$ was the ratio of the eddy diffusivity of momentum to the absolute viscosity and $\Pi_3$ was the ratio of eddy diffusivity of heat to the molecular diffusivity of heat, both $\Pi_3$ and $\Pi_5$ were expected to be very large. Lastly, the ratio of $\Pi_3$ to $\Pi_2$ gave another familiar similarity parameter, the Prandtl number.

As $\Pi_1$, $\Pi_2$ and $\Pi_3$ were closely related in the non-dimensional analysis of turbulent heat transfer, $\Pi_4$ and $\Pi_5$ were closely related in the non-dimensional analysis of turbulent momentum transfer, it would be sufficient to discuss only one of the parameters in each group.

Figure 28 shows the variation of $\Pi_5$ against Reynolds number. For each pipe configuration, it could be seen that the height of roughness elements had no effect on the ratio of eddy diffusivity of momentum to the absolute viscosity. It could also be seen that $\varepsilon_v/\nu$ increased sharply with Reynolds number with an approximate slope of 4.0.

The ratio of eddy diffusivity of heat to thermal diffusivity obtained using the LDA was shown in Figure 29. Similar to the diffusivity of momentum, $\frac{\varepsilon H}{k}$ .$\rho$Cp increased sharply with Reynolds number. As indicated in section 2.2 and 4.4 that while the roughness elements lie entirely within the laminar sublayer, the transport of heat in such roughened pipes would be like the transport of heat in smooth pipes, except for a slight effect associated with the increased surface area of the rough wall. However, within the estimated error band, no effect on the heat transfer could be seen.

Figure 30 shows the ratio of eddy diffusivity of heat to thermal diffusivity obtained using the thermocouples. As shown in Appendix 14, the heat transfer measurements obtained with the thermocouples had a narrower error band. This was shown to be the case as Figure 30

indicated less scattering in experimental data. However, no significant effect of the roughness elements on the heat transfer could be seen. Although the ratio of eddy diffusivity of heat to thermal diffusivity still increased with Reynolds number, the rate of increase was much smaller, compared with that obtained with the LDA with an approximate slope of 2.0. As suggested by Sheriff et al{101},{102} who carried out measurements with thermocouples using the similar technique that heat transfer data were likely to be underestimated due to finite boundaries of the pipe. Apart from the two different slopes deduced from the two different measurement techniques, the ratio of eddy diffusivity of heat to the thermal diffusivity obtained with the two techniques compared reasonably, particularly with lower Reynolds number.

## 7.2 Overall heat transfer

No overall heat transfer measurements were taken with the present work, as this would involve eddy diffusivity measurements across the pipe. However, as shown in section 3.4, overall heat transfer could be fairly adequately predicted by the assumption of a constant turbulent Prandtl number, $\varepsilon_\nu/\varepsilon_H$. Figure 31 shows the heat transfer similarity parameter, Nusselt number predicted using equation (3.78) as derived in section 3.4. Semi-empirical relations for Nu derived by other researchers such as Reynolds {2}, Martinelli {22}, Colburn {29} and Reynolds & Perkins {56}were also presented.

In order to make a comparison with other researchers' predictions, Prandtl numbers of 10, 1 and 0.01 were used. As expected, the Nusselt number predicted with the present work was slightly higher than that predicted by other semi-empirical relations. This could be mainly due to the assumption of constant turbulent Prandtl number across the pipe.

As most of the researchers proposed the heat transfer parameter of the form, $Nu = A\ Re^b.\ Pr^c$, it would also be possible to correlate the prediction obtained with equation (3.78) of section 3.4. Such correlation gave the heat transfer similarity parameter as:-

$$Nu = 0.0125.\ Re^{0.89} Pr^{0.27} \qquad (7.6)$$

The above relation has numerical constants fairly close to those proposed by Davies {55} and Reynolds & Perkins {56.}

## 7.3 Remarks and Comments

Since the internal surfaces of the pipes were not completely coated, as shown in Figures 8 and 9, pipes of different diameters were no longer geometrically similar. Hence k/**r**, although widely recognised as a similarity parameter, could only be used when r was constant. With the pipes coated with roughness elements of non-dimensional roughness height k*<5, the elements lie within the laminar sublayer, the change of roughness ratio was not expected to influence the momentum and heat transfer. Although the increase in surface area could still give rise to an increase in the heat transfer, this possible increase being slight and the estimated error band being around 20% to 40%, such increase was not evident.

Experimental data has shown that the turbulent momentum and heat diffusivities were a few orders of magnitude larger than their respective molecular diffusivities. Results obtained with the LDA were found to be higher than those obtained with the thermocouples, as expected. Another reason for this discrepancy could be due to the assumption taken in deriving the expression for eddy diffusivities in section 3. In their derivation, isotropic turbulence was assumed. Although this would be a reasonable assumption for the flow of turbulence along the centre of the pipe, small departure from isotropy would make the assumption of spherical eddy no longer valid. With the spherical eddy being stretched into a somewhat ellipsoidal eddy, it was expected that the expected value of the effective size of dissipation eddy be reduced. This would indicate an overestimate of the prediction of turbulence transport parameters when the flow was departed from local isotropy.

Experimental scatter for measurements taken in the pipes of smaller diameter was found to be greater than that taken in the pipes of larger diameter. This was expected as in a small pipe, the condition of

isotropy was less likely to be satisfied and, hence, led to a further overestimate of the turbulence transport parameters. A comparison between Figure 27(a) and (b) shows that the discrepancy between measurements with the LDA and thermocouples was greater with the pipe of smaller diameter. This further demonstrated the above argument as well as the suggestions of Sheriff et. al. {101}, {102} that finite boundaries of the pipe led to the eddy diffusivity of heat obtained with thermocouples being underestimated.

With the assumption of a constant turbulent Prandtl number which was itself a function of Prandtl number only, overall heat transport parameter was proposed with the present work. It was found to be reasonable, compared with predictions suggested by many other researchers. In accordance with most other workers, a simple relation for Nusselt number was also proposed as:-

$$Nu = 0.0125.Re^{0.89}.Pr^{0.27}$$

Also, the emergency of the above relation was based on a concept that attempted to describe the detailed behaviour of turbulence character-:istics and, hence, provided a more realistic and acceptable prediction for engineering applications.

The results of the experimental work have shown that the expressions for the eddy diffusivities of momentum and heat derived in section 3 were valid for the prediction of momentum and heat transfer. Experimental evidence obtained both with the LDA and thermocouples confirmed that roughness elements, while lying completely within the laminar sublayer, have no influence on the momentum and heat transfer. As the data reduction of the measurements were made using the theoretical expressions, this further indicated that the expressions derived theoretically in section 3 were valid. Particularly, the eddy transport of heat was shown to be dependent on the eddy scale and velocity parameters only and independent of temperature.

A single heat transfer similarity expression was proposed without restrictions on Prandtl number. As most other researchers' empirical predictions for heat transfer involve a number of equations for different

Prandtl number or Reynolds number regimes, the present universal heat transfer equation (3.78) has a significant advantage over the others. Limitations to the use of this equation are the level of turbulence intensity and isotropy, as the derivation of the equation required the turbulence intensity to be low and flow conditions to be isotropic. Departure from these conditions is likely to give overestimates to heat transfer rates.

## 8. CONCLUSIONS

With a basic concept of a flux of eddies of random shape, size and velocity, rather than an artificial mixing length or a correlation function, a thorough and realistic criterion for the prediction of momentum and heat transfer has been proposed. The analysis was based on a thermodynamic approach using the stochastical theory of turbulence. The macroscopic turbulence transport parameters were derived from the description of microscopic behaviour of eddies.

Jaynes and Shannon's communication theory, originally used for the investigation of electronic communication signals, has been successfully used for the interpretation of turbulence parameters. The comparative simplicity of the concept and its analysis made the derivation of an analytical solution to most problems in turbulence possible.

With the present investigation, the following conclusions could be made:-

(i) it is necessary and sufficient to express the eddy diffusivities of momentum and heat in terms of two independent parameters, entity velocity and scale.

(ii) using the analysis, velocity profiles for simple shear flows could be obtained.

(iii) ratio of eddy diffusivities or the turbulent Prandtl number could be predicted without the use of any adjustable constants.

(iv) overall heat transfer prediction could be obtained with a single equation for all ranges of Prandtl number.

However, a number of limitations still existed in the theoretical analysis. Departure from isotropic turbulence would result in the assumption of spherical eddies not satisfied and, hence, an over-:estimation of eddy transport parameters. Moreover, the assumption of weak correlations between eddy size and velocity would restrict the eddy velocity relative to the mean flow velocity to be small and indicated better prediction with lower turbulence intensity.

Also, with an eddy viscosity model of turbulence, only simple flows are likely to be predicted.

The laser doppler anemometer has been used for all turbulence measurements, except temperature, which was measured with thermocouples and a data scanner. The experimental techniques involved in the investigation have been shown to be satisfactory. However, with the method of roughening the pipes during the present investigation, pipes of different diameters were not geometrically similar, thus making the introduction of roughness ratio similarity more restricted than customary.

It could be said that a new and realistic approach to turbulent transport was thoroughly presented. The information or communication theory provided a useful means for studying turbulence phenomena. As a recommendation for future work, more refinement in the description of eddy shape could be made. Particularly near a plane solid boundary, the more detailed flow pattern will have to be investigated and analysed. Experimentally, distribution of eddy diffusivities could be measured across the pipe to derive a more accurate overall heat transfer similarity parameter. In roughening th epipes, geometrical similarity would have to be maintained as far as possible. Finally, the process of mass transfer in relation to heat and momentum transfer could also be investigated using the present concept.

## REFERENCES


1. Prandtl, L.: Eine Bezienhung zwischen Wärmeaustausch und Strömungswiderstand der Flüssigkeiten. Physisk Z, 11, 1072, 1910.

2. Reynolds, O.: On the extent and action of the heating surface of steam boilers. Scientific Papers of Osborne Reynolds, Cambridge, 1900.

3. Bradshaw, P.: An introduction to turbulence and its measurement. Pergamon Press Ltd., 1975.

4. Hinze, J.O.: Turbulence - An introduction to its mechanism and theory. McGraw-Hill Book Co., 1959.

5. Boussinesq, J.: Essai sur la théorie des eaux courantes. Mém prés par div savants à l'acad. sci., Paris, Vol. 23, 1877.

6. Pai, S.I.: Viscous flow theory, Vol. 2. D. Van Nostrand Co. Inc., 1957.

7. Prandtl, L.: The mechanics of viscous fluids. Aerodynamic Theory, Vol. 3, Div. G., edited by Durand, W.F., 1935.

8. Taylor, G.I.: The transport of vorticity and heat through fluid in turbulent motion. Proc. Royal Society A135, 1932.

9. Von Karman, Th.: Mechanische Aehnlichkeit und Turbulenz. Nach. Gesell. Wiss. Goettingen, Math. Phys. Klasse, Heft 5, 1930. NACA TM611, 1931.

10. Reichardt, H.: Ueber eine neue Theorie der freien Turbulenze. ZAMM Bd. 21, 1941. J. Royal Aero. Soc., 1943.

11. Reichardt, H.: Laws of free turbulence.
VDI. Forschungsheft 414, Deutscher Ingenieur Verlag, 1951.

12. Taylor, G.I.: Diffusion by continuous movements.
Proc. London Math. Soc. 20, 1920.

13. Taylor, G.I.: The statistical theory of turbulence.
Proc. Royal Soc. (London) A151, Part 1 IV, 1935.

14. Von Karman, Th.: The fundamentals of the statistical theory of turbulence.
J. Aero. Science, Vol. 4, 1937.

15. Kolmogoroff, A.N.: Dissipation of energy in locally isotropic turbulence.
C.R. Acad. Sci. USSR, Vol 31 & 32, 1941.

16. Heisenberg, W.: Sur statistischen Theorie der Turbulenz.
Z. Phys., 124, 1938.

17. Batchelor, G.K.: The theory of homogenous turbulence.
Cambridge University Press, 1953.

18. Kempé de Fériet, J.: Introduction to the statistical theory of turbulence. Correlation and spectrum.
Institute for Fluid Dynamics and Applied Mathematics, University of Maryland.
Lecture Series No.8, 1951.

19. Rohsenow, W.M. and Choi, H.Y.: Heat, mass and momentum transfer.
Prentice-Hall Inc., 1961.

20. Dittus, F.W. and Boelter, L.M.K.: Heat transfer in auto-:mobile radiators of the turbular type.
University of California, Publication in Engineering, Vol. 2, No.13, 1930.

21. McEligot, D.M., Ormand, L.W. and Perkins, H.C.: Internal low Reynolds-Number turbulent and transitional gas flow with heat transfer.
J. Heat Transfer, Trans. ASME, Vol. 88, 1966.

22. Martinelli, R.C.: Heat transfer to molten metals.
J. Heat Transfer, Trans. ASME, Vol. 69, 1947.

23. Kinney, R.B. and Sparrow, E.M.: Turbulent flow, heat transfer and mass transfer in a tube with surface suction.
J. Heat Transfer, Trans. ASME, Vol. 92, 1970.

24. Cebeci, T.: A model for eddy conductivity and turbulent Prandtl number.
Report No. MDC-J0747101, Douglas Aircraft Co., 1971.

25. Na, T.Y. and Habib, I.S.: Heat transfer in turbulent pipe flow based on a new mixing length model.
App. Sci. Res., Vol. 28, 1973.

26. McEligot, D.M., Pickett, P.E. and Taylor, M.F.: Measurements of wall region turbulent Prandtl numbers in small tubes.
Int. J. Heat Mass Transfer, Vol. 19, 1976.

27. Pickett, P.E., Taylor, M.F. and McEligot, D.M.: Heated turbulent flow of helium-argon mixtures in tubes.
Int. J. Heat Mass Transfer, Vol. 22, 1979.

28. Von Karman, Th.: Analogy between fluid friction and heat transfer.
J. Heat Transfer, Trans. ASME, Vol. 61, 1939.

29. Colburn, A.P.: A method of correlating forced convection heat transfer data and a comparison with fluid friction.
Trans. AIChE, Vol. 29, 1933.

30. Jenkins, R.: Variation of eddy conductivity with Prandtl modulus and its use in prediction of turbulent heat transfer.
Proc. Heat Transfer Fluid Mechanics Institute, Stanford University, 1951.

31. Deissler, R.G.: Analysis of fully developed turbulent heat transfer at low Peclet numbers in smooth tubes with application to liquid metals.
NACA Res. Mem. E52F05, 1952.

32. Deissler, R.G.: Turbulent heat transfer and temperature fluctuations in a field with uniform velocity and temperature gradients.
Int. J. Heat Mass Transfer, Vol. 6, 1963.

33. Rohsenow, W.M. and Cohen, L.S.:

MIT Heat Transfer Laboratory Report, 1960.

34. Azer, N.Z. and Chao, B.T.: A mechanism of turbulent heat transfer in liquid metals.
Int. J. Heat Mass Transfer, Vol. 1, 1960.

35. Rotta, J.C.: Turbulente Strömungen.
B.G. Teubner, 1972.

36. Quarmby, A. and Quirk, R.: Measurements of the radial and tangential eddy diffusivities of heat and mass in turbulent flow in a plain tube.
Int. J. Heat Mass Transfer, Vol. 15, 1972.

37. Jischa, M. and Rieke, H.B.: Turbulent heat transfer in duct flow.
Proceedings of the 6th Int. Heat Transfer Conference, 1978.

38. Jischa, M. and Rieka, H.B.: About the prediction of turbulent Prandtl and Schmidt numbers from modelled transport equations.
Int. J. Heat Mass Transfer, Vol. 22, 1979.

39. Tyldesley, J.R. and Silver, R.S.: The Prediction of the transport properties of a turbulent fluid.
Int. J. Heat Mass Transfer, Vol. 11, 1968.

40. Tyldesley, J.R. and Silver, R.S.: Transport phenomena in free turbulence flows.
Int. J. Heat Mass Transfer, Vol. 12, 1969.

41. Stromquist, W.K.: Effect of wetting on heat transfer characteristics of liquid metals.
U.S. Atomic Energy Commission Report, 1953.

42. Trefethen, L.: Heat transfer properties of liquid metals.
Oak Ridge National Laboratory, NP 1788, 1950.

43. Seban, R.A. and Doughty, D.L.: Heat transfer to turbulent boundary layers with variable free stream velocity.
J. Heat Transfer, Trans. ASME, Vol. 78 (1), 1956.

44. Mizushina, T. and Sasano, T.: The ratio of the eddy diffusivities for heat and momentum and its effect on liquid metal heat transfer coefficients.
Proc. Int. Heat Transfer Conference, ASME, 1961.

45. Isokoff, S.E. and Drew, T.B.: Heat and momentum transfer in flow of mercury.
General Discussions of Heat Transfer, I.Mech.E., 1951.

46. Nikuradse, J.: Laws of flows in rough pipes.
NACA TM 1292, 1950.
Translation of "Strömungsgesetze in rauhen Rohren."
VDI-Forschungsheft 361, 1933.

47. Heywood, F.: The flow of water in pipes and channels.
Minutes Proc. Institution of Civil Engineers, 219, 1924.

48. Colebrook, C.F. and White, C.M.: Experiments with fluid friction in roughened pipes.
Proc. Royal Society, A161, 1937.

49. Bradshaw, P.: Experimental fluid mechanics.
Pergamon Press Ltd., 1970.

50. Kay, J.M. and Nedderman, R.M.: An introduction to fluid mechanics and heat transfer.
Cambridge University Press, 1974.

51. Goldstein, S.: Modern developments in fluid dynamics, Vol. 2,
Dover Publication Inc., 1965.

52. Schlichting, H.: Boundary layer theory.
McGraw-Hill Book Co., 1968.

53. Colladay, R.S.: Turbine Cooling.
NASA SP290, 1975.

54. Curle, N. and Davies, H.J.: Modern fluid dynamics, Vol. 2.
Van Nostrand-Reinhold, 1971.

55. Davies, J.T.: Turbulent phenomena.
Academic Press, 1972.

56. Reynolds, W.C. and Perkins, H.C.: Engineering thermo-:dynamics.
McGraw-Hill Kogakusha Ltd., 1977.

57. Sleicher, C.A. and Rouse, M.W.: A convenient correlation for heat transfer to constant and variable property fluids in turbulent pipe flow.
Int. J. Heat Mass Transfer, Vol. 18, 1975.

58. Eckert, E.R.G.: Introduction to the transfer of heat and mass.
McGraw-Hill Book Co. Inc., 1950.

59. Reynolds, A.J.: Turbulent flows in engineering.
John Wiley & Sons, 1974.

60. Rotta, J.C.: Contribution to the calculation of turbulent boundary layers.
TMB 242, 1951.
Translation of "Beitran zur Berechnung der turbulenten Grenzchichten."
Ingenieur Archiv, Vol. 19 1951.

61. Kolar, V.: Heat transfer in smooth and rough tubes.
Int. J. Heat Mass Transfer, Vol.8, 1965.

62. Cope, W.F.: The friction and heat transmission coefficient of rough pipes.
Proc. I. Mech. E., Vol. 145, 1941.

63. Zukauskakas, A. and Slanciauskas, A.: Heat transfer in turbulent flow of fluid.
Thermophysics 5, 1973.

64. Dunn, M.G.: Effect of three dimensional roughness elements on boundary layer and aerodynamic heating.
J. Spacecraft Rockets, Vol.1, 1964.

65. Bourgoyne, T.B., Burnett, P. and Wilkie, D.: Forced convection heat transfer from surfaces roughened by transverse ribs.
U.K.A.E.A. TRG Report 781(W), 1964.

66. Kemeny, C.A. and Cyphers, J.A.: Heat transfer and pressure drop in an annular gap with surface spoilers.
J. Heat Transfer, Trans. ASME, Vol. 83(2),1961.

67. Sheriff, N. and Gumley, P.: Heat transfer and friction properties of surfaces with discrete roughness.
U.K.A.E.A. TRG Report 929, 1965.

68. Walker, V. and Rapier, A.C.: Fuel element heat transfer.
J. British Nuclear Energy Society, Vol. 2(2), 1963.

69. Nunner, W.: Wärmeübergang und Druckabfall in rauhen Rohren.
VDI-Forschungsheft 455, 1956.

70. Gomelauri, V.: Influence of two dimensional artificial roughness on convective heat transfer.
Int. J. Heat Mass Transfer, Vol. 7, 1964.

71. Dipprey, D.F. and Sabersky, R.: Heat and momentum transfer in smooth and rough tubes at various Prandtl numbers.
Int. J. Heat Mass Transfer, Vol. 6, 1963.

72. Gowen, R.A. and Smith J.W.: Turbulent heat transfer from smooth and rough surfaces.
Int. J. Heat Mass Transfer, Vol. 11, 1968.

73. Smith, J.W., Gowen, R.A. and Wasmund, B.D.: Eddy diffusivities and temperature profiles for turbulent heat transfer to water in pipes.
American Int. Chemical Engineers Symposium Series, 1967.

74. Blinco, P.H. and Parenthiades, S.E.: Turbulence characteristics in free surface flows over smooth and rough boundaries.
J. Hydraulics Research, Vol. 9(1), 1971.

75. Fujii, T., Fujii, M. and Takeuchi, M.: Influence on various surface roughness on the natural convection.
Int. J. Heat Mass Transfer, Vol. 16, 1973.

76. Ramakrishan, K., Seetharamu, K.N. and Sarma, P.K.: Turbulent heat transfer by free convection from a rough surface.
J. Heat Transfer, Trans. ASME.

77. Cebeci, T. and Chang, K.C.: Calculation of incompressible rough-wall boundary layer flows.
AIAA Journal, Vol. 16, 1978.

78. Rotta, J.C.: Turbulent boundary layers in incompressible flow.
Prog. Aerospace Science, Vol. 2, 1962.

79. Adams, J.C. and Hodge, B.K.: The calculation of compressible, transitional, turbulent and relaminarisational boundary layers over smooth and rough surfaces using an extended mixing-:length hypothesis.
AIAA 10th Fluid and Plasmadynamics Conference, 1977.

80. Hatton, A.P. and Walklate, P.J.: A mixing-length method for predicting heat transfer in rough pipes.
Int. J. Heat Mass Transfer, Vol. 19, 1976.

81. Wassel, A.T. and Mills, A.F.: Calculation of variable property turbulent friction and heat transfer in rough pipes.
J. Heat Transfer, Trans. ASME, Vol. 101, 1979.

82. Ligrani, P.M., Moffat, R.J. and Kays, W.M.: The thermal and hydrodynamic behaviour of thick, rough-wall turbulent boundary layers.
Stanford University, Thermosci, Div. Department of Mechanical Engineering, Report No. HMT-29, 1979.

83. Ligrani, P.M., Kays, W.M. and Moffat, R.J.: A heat transfer prediction method for turbulent boundary layer developing over rough surfaces with transpir-:ation.
Int. J. Heat Mass Transfer, Vol. 24, 1981.

84. Nikuradse, J.: Gesetzmässigkeiten der turbulenten Strömung in glatten Rohren. VDI-Forschungsheft 356, 1932.

85. Logan, E. and Jones, J.B.: Flow in a pipe following an abrupt increase in surface roughness. J. Bas. Engrg., Vol. 85(1), 1963.

86. Sleicher, C.A. and Tribus, M.: Recent advances in heat and mass transfer. McGraw-Hill Book Co., 1961.

87. Kinney, R.B. and Sparrow, E.M.: Turbulent pipe flow of an internally heat generating fluid. J. Heat Transfer, Trans. ASME, Vol. 88, 1966.

88. Poppendiek, H.F.: Forced convection heat transfer in pipes with heat sources within the fluid. Chemical Engineering Progress Symposium Series, J. Nuclear Engineering, Vol. 50, 1954.

89. Miller, G.L.: Experimental forced convection heat transfer with adiabatic walls and internal heat generation in a liquid metal. ASME Paper No.58-HT-17.

90. Inman, R.M.: Experimental study of temperature distribution in laminar tube flow of a fluid with internal heat generation. Int. J. Heat Mass Transfer, Vol. 5, 1962.

91. Petukhov, B.S. and Genin, L.G.: Heat transfer in tubes with internal heat sources in the fluid stream. Int. Chemical Engineering, Vol. 3, 1963.

92. Siegel, R. and Sparrow, E.M.: Turbulent flow in a circular tube with arbitrary internal heat sources and wall heat transfer. J. Heat Transfer, Trans. ASME, Vol. 81, 1959.

93. Michiyoshi, I. and Nakajima, T.: Heat transfer in turbulent flow with internal heat generation in concentric annulus fully developed thermal situation. J. Nuclear Science and Technology, Japan, Vol. 5, 1968.

94. Danckwerts, P.V.: Significance of liquid film coefficient in gas absorption.
I. & E.C., Vol. 43, 1951.

95. Thomas, L.C.: Temperature profile for liquid metals and moderate Prandtl number fluids.
J. Heat Transfer, Trans. ASME, Vol. 92, 1970.

96. Chung, B.T.F. and Thomas, L.C.: Turbulent heat transfer for pipe flow with prescribed wall heat fluxes and uniform heat sources in the stream.
J. Heat Transfer, Trans. ASME, Vol. 96, 1974.

97. Habib, I.S. and Na, T.Y.: Prediction of heat transfer in turbulent pipe flow in pipes with constant wall temperature.
J. Heat Transfer, Trans. ASME, Vol. 96, 1974.

98. Na, T.Y. and Chiou, J.P.: Turbulent heat transfer for pipe flow with uniform heat generation.
Wärme und Staffübertragung, Thermal and Fluid Dynamics, Vol. 12, 1979.

99. Wilson, H.A.: On convection of heat.
Proc. Cambridge Philosophical Society, Vol. 12, 1904.

100. Carslaw, H.S. and Jaeger, J.C.: Conduction of heat in solids.
Oxford University Press, 1959.

101. Sheriff, N. and O'Kane, D.J.: Eddy diffusivity of mass measurements for air in circular duct.
Int. J. Heat Mass Transfer, Vol. 14, 1971.

102. Sheriff, N., O'Kane, D.J. and Mather, B.: Measurement of eddy diffusivity of heat in sodium.
Proc. 4th International Heat Transfer Conference, 1970.

103. Sheriff, N. and O'Kane, D.J.: Sodium eddy diffusivity of heat measurements in a circular duct.
Int. J. Heat Mass Transfer, Vol. 24, 1981.

104. Yeh, Y. and Cummins, H.Z.: Localised fluid flow measurements with He-Ne laser spectrometer.
Applied Physics Letters, Vol. 4, 1964.

105. Rudd, M.J.: A new theoretical model for the laser doppler meter.
Journal of Physics:E, Vol. 2, 1969.

106. Foreman, J.W., Lewis, R.D. et. al.: Laser doppler velocimeter for measurement of localised fluid velocities in liquids.
Proc. IEEE, Vol. 54, 1966.

107. Pike, E.R., Jackson, D.F., Bourke, P.J. and Page, D.I.: Measurement of turbulent velocities from the doppler shift in scattered laser light.
Presentation American Phys. Society, 1967.

108. Welch, N.E. and Tomme, W.J.: Analysis of turbulence from data obtained with a laser velocimeter.
AIAA Paper No.67, 1967.

109. Lumley, J.L., George, W.K. and Kobashi, Y.: The influence of ambiguity and noise on the measure-:ment of turbulent spectra by dopper scattering.
Proc. Symposium on Turbulence measurement in Liquids, 1970.

110. Durst, F. and Zaré, M.: Bibligraphy of laser dopper anemometry literature.
DISA Information Centre, 1974.

111. Durst, F. and Whitelaw, J.H.: Measurements of mean velocity, fluctuating velocity and shear stress in air using a simple channel optical anemometer.
DISA Information, No. 12, 1971.

112. Bourke, P.J., Brown, C.G. and Drain, L.E.: Measurement of Reynolds shear stresses in water by laser anemometry.
DISA Information, No. 12, 1971.

113. Bourke, P.J., Drain, L.E. and Moss, B.C.: Measurement of spatial and temporal correlations of turbulence in water by laser doppler anemometry.
DISA Information, No. 12, 1971.

114. Melling, A. and Whitelaw, J.H.: Seeding of gas flows for laser anemometry.
DISA Information, No. 15, 1973.

115. Bates, C.J.: Experimental pipe flow using LDA.
DISA Information, No. 16, 1974.

116. Bates, C.J.: Flow measurement using a laser doppler anemometer.
Proc. Conference on Fluid Flow Measurements in The Mid 1970's, 1975.

117. Van Atta, C.W.: Sample techniques in turbulence measurements.
Annual Review of Fluid Mechanics, Vol. 6, 1974.

118. Yanta, W.J. and Smith, R.A.: Measurement of turbulent transport properties using laser doppler anemometry.
AIAA 11th Aerospace Sciences Meeting, 1973.

119. Yanta, W.J. and Lee, R.E.: Determination of turbulence transport properties with a laser doppler velocimeter and conventional time averaged mean flows and measurements at Mach 3.
AIAA 7th Fluid & Plasma Dynamics Conference, 1974.

120. Whiffen, M.C. and Meadows, D.M.: Two axes, simple particle laser velocimeter system for turbulence spectral analysis.
Proc. 2nd International Workshop on Laser Velocimetry, 1974.

121. Smith, D.M. and Meadows, D.M.: Power spectra from random time samples for turbulence measurements using a laser velocimeter.
Proc. 2nd International Workshop on Laser Velocimetry, 1974.

122. Blake, K.A.: New developments of the NEL laser velocimeter and the treatment of data.
Opto-Electron, Vol. 5, 1973.

123. Bates, C.J. and Hughes, T.D.R.: Real time statistical LDV system for the study of a high Reynolds number, low turbulence intensity flow.
J. Physics,E, Vol. 9, 1976.

124. Bates, C.J. and Hughes, T.D.R.: The effect of both sample size and sample rate on the statistical fluid flow parameters in a high Reynolds number, low turbulence intensity flow.
5th Biennial Symposium on Turbulence, 1977.

125. Greated, C.A.: An improved method of flow measurement in water.
La Houille Blanche, No. 6, 1969.

126. Greated, C.A. and Manning, R.: Water waves measured with a laser flowmeter.
La Houille Blanche, No. 6, 1970.

127. George, W.K.: Limitations on the measurement of unsteady flow velocities with a laser doppler velocimeter.
Proc. DISA Conference, 1972.

128. George, W.K. and Lumley, J.L.: Limitations on the measurement of turbulence using a laser doppler velocimeter.
ASCE National Water Resource Engineering Meeting, 1971.

129. Townsend, A.A.: The measurement of double and triple correlation derivatives in isotropic turbulence.
Proc. Cambridge Phil. Soc., Vol. 43, 1947.

130. Laufer, J.: Investigation of turbulent flow in a two dimensional channel.
NACA TR 1053, 1949.

131. Von Liepmann, H.W.: Die Anwendung eines Satzes über die Nullstellen Stochastischer Funktionen auf Turbulenzmessungen.
Helu. Phys. Acta, Vol. 2, 1949.

132. Philip, M.G.: Some investigation of turbulence in pipelines using a laser doppler anemometer and digital correlation.
RGIT Research Report, 1977.

133. Roshka, A.: Structure of turbulent shear flow: A new look.
AIAA Journal, Vol. 14, 1976.

134. Lamb, H.: Hydrodynamics.
Cambridge University Press, 1962.

135. Landau, L.D. and Lifshitz, E.M.: Fluid Mechanics.
Translated by Sykes, J.B. and Reid, W.H.
Pergamon Press, 1963.

136. Townsend, A.A.: The structure of turbulent shear flow. Cambridge University Press, 1976.

137. Taylor, G.I.: The spectrum of turbulence. Proc. Royal Society, A157, 1938.

138. Von Karman, Th. and Howarth, L.: On the statistical theory of isotropic turbulence. Proc. Royal Society, A164, 1938.

139. Shannon, C.E.: A mathematical theory of communication. Bell System Technical Journal, Vol. 27, 1948.

140. Jaynes, E.T.: Information theory and statistical mechanics. Phys. Rev., Vol. 106 & Vol. 108, 1957.

141. Reza, F.M.: An introduction to information theory. McGraw-Hill Book Co., 1961.

142. Tribus, M.: Thermostatics and thermodynamics. D. Van Nostrand Co., Inc., 1961.

143. Hinze, J.O.: Turbulent pipe flow. Proc. International Symposium of the National Scientific Research Centre, Maseille, Gordon and Brech, 1961.

144. Comte-Bellot, G.: Écoulement turbulent entre deux parois paralléles. Publications scientifiques et techniques du Ministére de l'Air, No. 419, 1965.

145. Laufer, J.: The structure of turbulence in fully developed pipe flow. NACA TN2954, 1953.

146. McAdams, W.H.: Heat transmission. McGraw-Hill Book Co., 1954.

147. Drew, T.B., Koo, E.C. and McAdams, W.H.:

Trans. AIChE., Vol. 28, 1932.

148. British Standards Institution. Methods for the measurements of fluid flow in pipes. Orifice plates, nozzles and venturi tubes. BS 1042. 1965.

149. Drain, L.E.: The laser doppler technique. J. Wiley & Sons, 1980.

150. Boadway, J.D. and Karahan, E.: Correction of laser doppler anemometer readings for refraction at cylindrical interfaces. DISA Information, No. 26, 1981.

151. British Standards Institution: International thermo-:couple reference tables (copper v. constantan). BS 1828, 1970.

152. Von Karman, Th. and Lin, C.C.: On the statistical theory of isotropic turbulence. Advances in Applied Mechanics, Vol. 2, 1951.

153. Grober, H., Erk, S. and Grigull, U.: Fundamentals of heat transfer. McGraw-Hill Book Co., 1961.

| AUTHOR | REFERENCE NO. |
|---|---|
| Adams, J.C. | 79 |
| Azer, N.Z. | 34 |
| Batchelor, G.K. | 17 |
| Bates, C.J. | 115, 116, 123, 124 |
| Blake, K.A. | 122 |
| Blinco, P.H. | 74 |
| Boadway, J.D. | 150 |
| Bourke, P.J. | 112, 113 |
| Bourgoyne, T.B. | 65 |
| Boussinesq, J. | 5 |
| British Standards Institution | 148, 151 |
| Bradshaw, P. | 3, 49 |
| Carslaw, H.S. | 100 |
| Cebeci, T. | 24, 77 |
| Chung, B.T.F. | 96 |
| Colburn, A.P. | 29 |
| Colebrook, C.F. | 48 |
| Colladay, R.S. | 53 |
| Comte-Bellot, G. | 144 |
| Cope, W.F. | 62 |
| Curle, N. | 54 |
| Danckwerts, P.V. | 94 |
| Davies, J.T. | 55 |
| Deissler, R.G. | 31, 32 |
| Dipprey, D.F. | 71 |
| Dittus, F.W. | 20 |
| Drain, L.E. | 149 |
| Drew, T.B. | 147 |
| Dunn, M.G. | 64 |
| Durst, F. | 110, 111 |

| AUTHOR | REFERENCE NO. |
|---|---|
| Eckert, E.R.G. | 58 |
| Fujii, T. | 75 |
| Foreman, J.W. | 106 |
| George, W.K. | 127, 128 |
| Goldstein, S. | 51 |
| Gomelauri, V. | 70 |
| Gowen, R.A. | 72 |
| Greated, C.A. | 125, 126 |
| Grober, H. | 153 |
| Habib, I.S. | 97 |
| Hatton, A.P. | 80 |
| Heisenberg, W. | 16 |
| Heywood, F. | 47 |
| Hinze, J.O. | 4, 143 |
| Inman, R.M. | 90 |
| Isokoff, S.E. | 45 |
| Jaynes, E.T. | 140 |
| Jischa, M. | 37, 38 |
| Jenkins, R. | 30 |
| Kay, J.M. | 50 |
| Kemeny, C.A. | 66 |
| Kempé de Fériet, J. | 18 |
| Kinney, R.B. | 23, 87 |
| Kolar, V. | 61 |
| Kolmogoroff, A.N. | 15 |

| AUTHOR | REFERENCE NO. |
|---|---|
| Lamb, H. | 134 |
| Landau, L.D. | 135 |
| Laufer, J. | 130, 145 |
| Ligrani, P.M. | 82, 83 |
| Logan, E. | 85 |
| Lumley, J.L. | 109 |
| Martinelli, R.C. | 22 |
| McAdams, W.H. | 146 |
| McEligot, D.M. | 21, 26 |
| Melling, A. | 114 |
| Michiyoshi, I. | 93 |
| Miller, G.L. | 89 |
| Mizushina, T. | 44 |
| Na, T.Y. | 25, 98 |
| Nikuradse | 46, 84 |
| Nunner, W. | 69 |
| Pai, S.I. | 6 |
| Petukhov, B.S. | 91 |
| Philip, M.G. | 132 |
| Pickett, P.E. | 27 |
| Pike, E.R. | 107 |
| Poppendiek, H.F. | 88 |
| Prandtl, L. | 1, 7 |
| Quarmby, A. | 36 |
| Ramakrishan, K. | 76 |
| Reichardt, H. | 10, 11 |
| Reynolds, A.J. | 59 |
| Reynolds, O. | 2 |

Table 1(a) Values of F for limited values of Pe

| Pe \ Re | $10^4$ | $10^5$ | $10^6$ |
|---|---|---|---|
| $10^2$ | 0.18 | 0.098 | 0.052 |
| $10^3$ | 0.55 | 0.45 | 0.29 |
| $10^4$ | 0.92 | 0.83 | 0.65 |
| $10^5$ | 0.99 | 0.985 | 0.980 |
| $10^6$ | 1.00 | 1.00 | 1.00 |

Table I(b) Values of (To-Tm)/(To-Tc) for values of Re and Pr

| Pe \ Re | $10^4$ | $10^5$ | $10^6$ | $10^7$ |
|---|---|---|---|---|
| 0 | 0.564 | 0.558 | 0.553 | 0.550 |
| $10^{-4}$ | 0.568 | 0.560 | 0.565 | 0.617 |
| $10^{-3}$ | 0.570 | 0.572 | 0.627 | 0.728 |
| $10^{-2}$ | 0.589 | 0.639 | 0.738 | 0.813 |
| $10^{-1}$ | 0.692 | 0.761 | 0.823 | 0.864 |
| 1.0 | 0.865 | 0.877 | 0.897 | 0.912 |
| 10 | 0.958 | 0.962 | 0.963 | 0.966 |
| $10^2$ | 0.992 | 0.993 | 0.993 | 0.994 |
| $10^3$ | 1.00 | 1.00 | 1.00 | 1.00 |

Table 2 Velocity Measurement by the Laser Doppler Technique

| Advantages | Disadvantages |
|---|---|
| Does not disturb the flow | Medium must be transparent |
| High spatial resolution | Artificial seeding may be needed |
| Fast response | Optical access is required |
| Response linear and easily calibrated | Not suitable for measurement of total flow as this requires a tedious integration over a cross-section |

Table 3. Polynomials for Thermocouples

| Thermocouple Number | A | B | C |
|---|---|---|---|
| 1 | -0.216324 | 17.1919 | -0.330355 |
| 2 | -0.220018 | 17.2620 | -0.451493 |
| 3 | -0.211522 | 17.1575 | -0.307668 |
| 4 | -0.218163 | 17.2232 | -0.417665 |
| 5 | -0.210146 | 17.1660 | -0.318308 |
| 6 | -0.218138 | 17.2077 | -0.342309 |
| 7 | -0.208166 | 17.1485 | -0.193740 |
| 8 | - | - | - |
| 9 | -0.207287 | 17.1727 | -0.343504 |
| 10 | -0.215007 | 17.2124 | -0.467030 |
| 11 | -0.212972 | 17.2206 | -0.471656 |
| 12 | -0.220443 | 17.2473 | -0.473862 |
| 13 | -0.213515 | 17.2076 | -0.438195 |
| 14 | -0.218622 | 17.2125 | -0.370868 |

Polynomial of each thermocouple is expressed as:-

$$T = A.V^2 + B.V + C$$

where V is the voltage output in millivolts,

and T is the temperature measured in $^{o}C$.

Table 4. Spatial Variation of Turbulence Characteristics

| V(m/s) | $\bar{V}$(m/s) | $\frac{V-\bar{V}}{\bar{V}} \times 100\%$ | V(m/s) | $\bar{V}$(m/s) | $\frac{V-\bar{V}}{V} \times 100\%$ |
|---|---|---|---|---|---|
| 6.11 | | 0.87 | 3.10 | | 1.27 |
| 6.07 | | 0.21 | 3.13 | | 0.32 |
| | 6.058 | | | 3.140 | |
| 6.06 | | 0.04 | 3.17 | | 0.96 |
| 5.99 | | 1.11 | 3.16 | | 0.64 |

| Tu(%) | $\bar{Tu}$(%) | $\frac{Tu-\bar{Tu}}{\bar{Tu}} \times 100\%$ | Tu(%) | $\bar{Tu}$(%) | $\frac{Tu-\bar{Tu}}{\bar{Tu}} \times 100\%$ |
|---|---|---|---|---|---|
| 4.25 | | 1.73 | 5.17 | | 3.45 |
| 4.31 | | 0.35 | 4.87 | | 2.55 |
| | 4.325 | | | 4.998 | |
| 4.36 | | 0.81 | 5.04 | | 0.89 |
| 4.38 | | 1.27 | 4.91 | | 1.75 |

| $\delta$ (mm) | $\bar{\delta}$(mm) | $\frac{\delta-\bar{\delta}}{\bar{\delta}} \times 100\%$ | $\delta$ (mm) | $\bar{\delta}$ (mm) | $\frac{\delta-\bar{\delta}}{\bar{\delta}} \times 100\%$ |
|---|---|---|---|---|---|
| 1.263 | | 0.34 | 0.577 | | 3.55 |
| 1.261 | | 0.18 | 0.600 | | 0.29 |
| | 1.259 | | | 0.598 | |
| 1.265 | | 0.50 | 0.620 | | 3.64 |
| 1.246 | | 1.01 | 0.596 | | 0.38 |

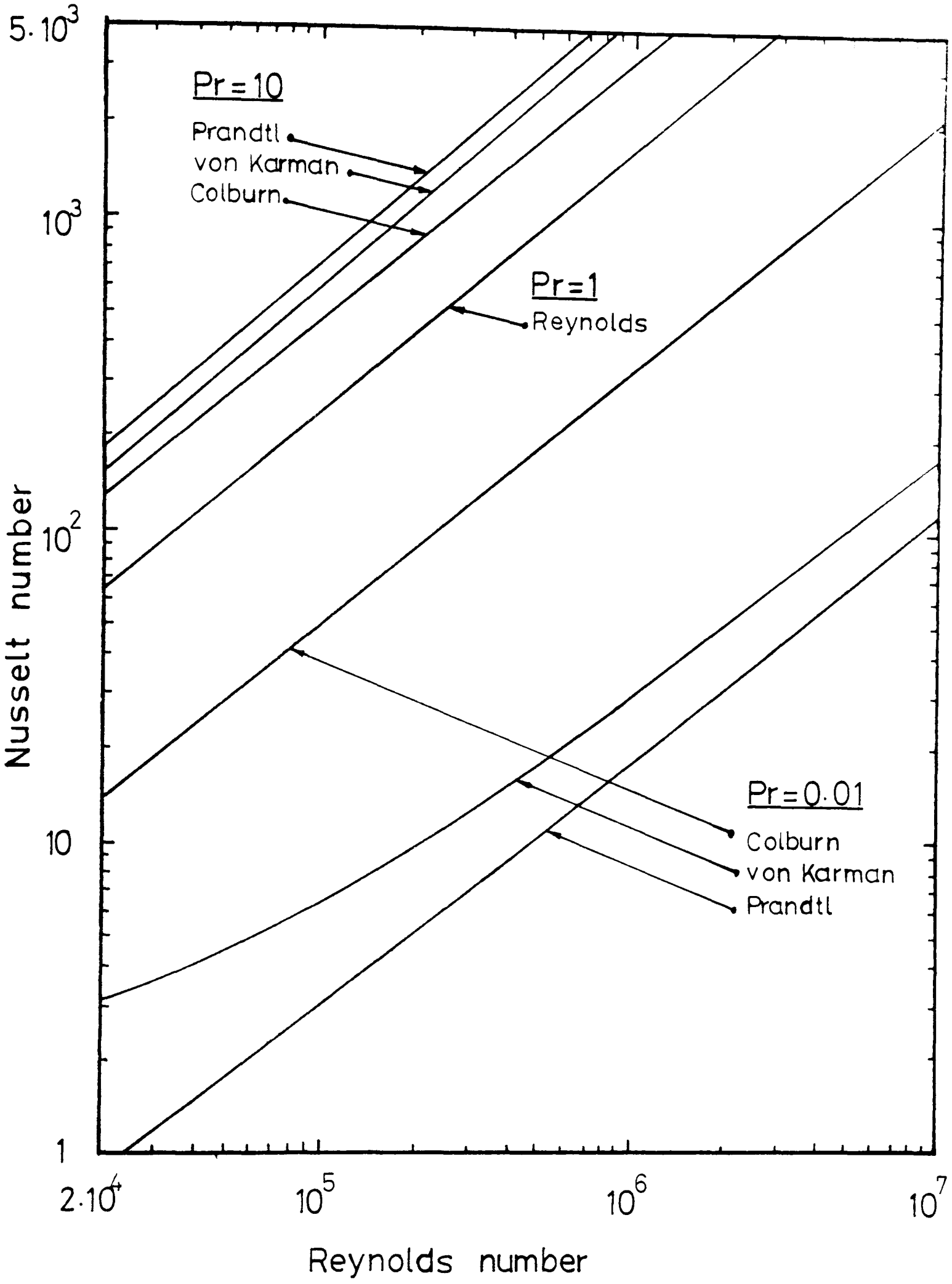


Fig. 1 Comparison of various analogies between heat and momentum transfer.

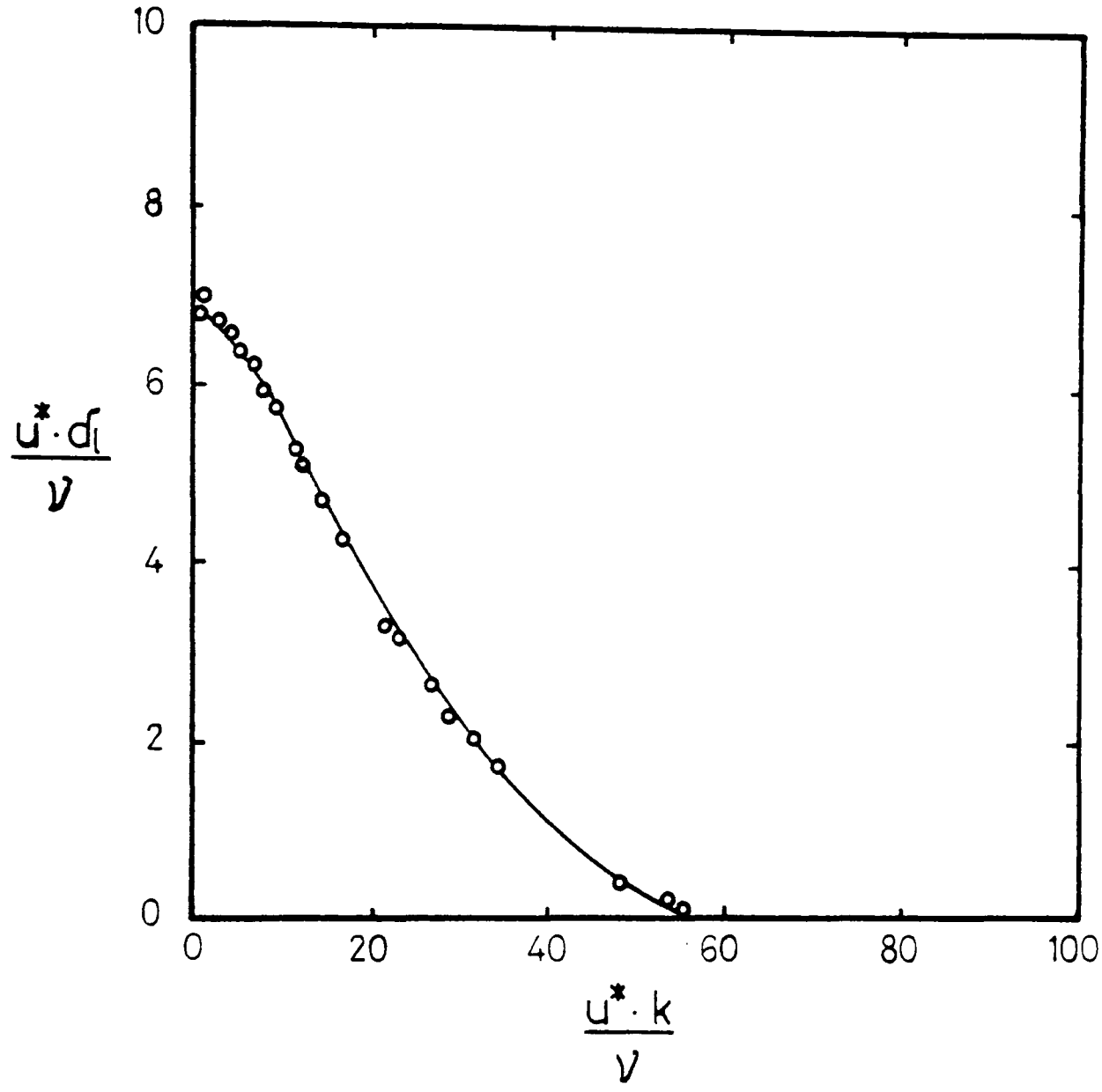


Fig. 2 Effect of wall roughness on the laminar sublayer according to Nikuradse's experiments with uniform sandgrain roughness.

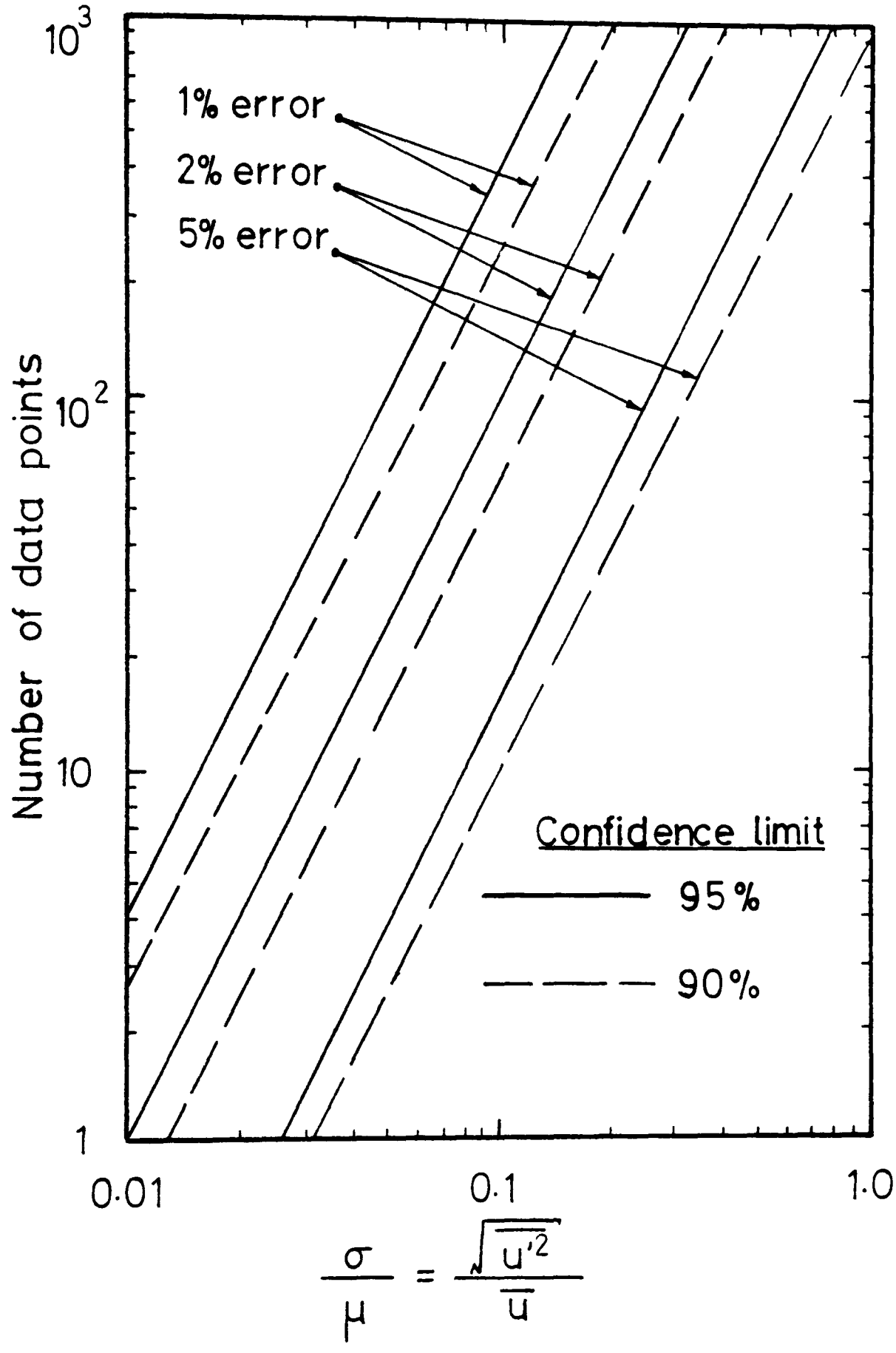


Fig. 3 Statistical error prediction for mean velocity.

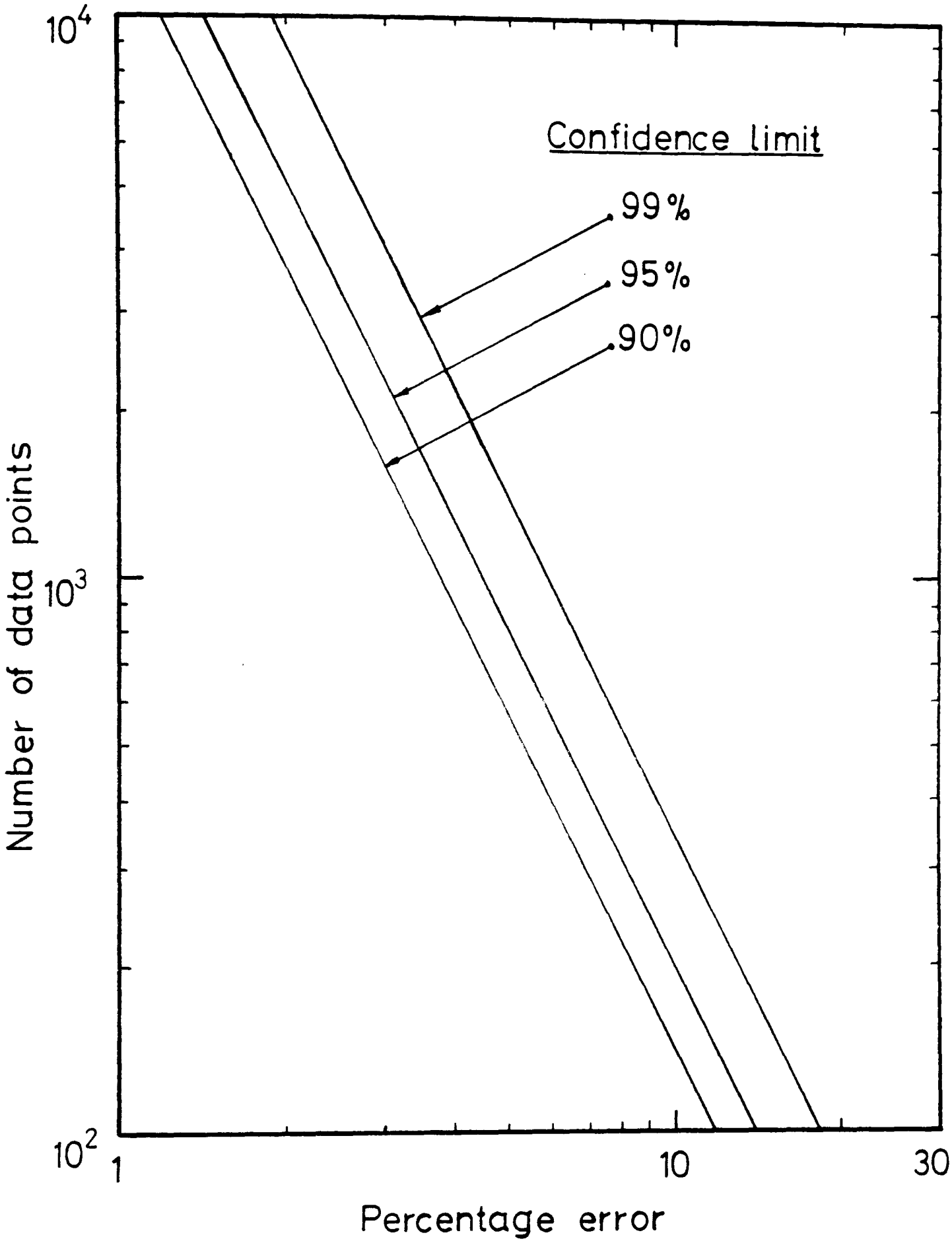


Fig.4 Statistical error prediction for standard deviation.

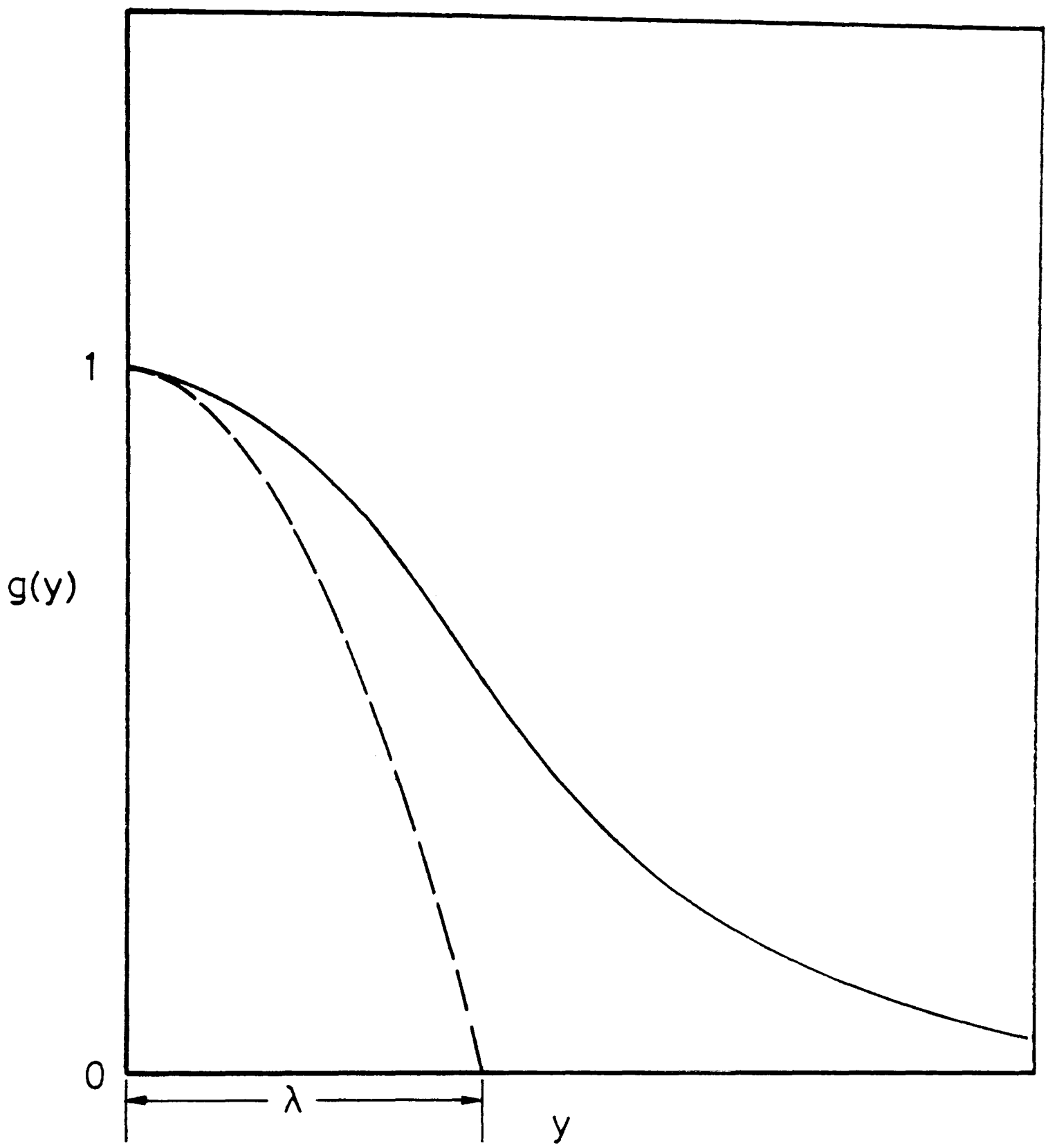


Fig.5 Osculation parabola of the lateral correlation coefficient g(y) and the microscale λ.

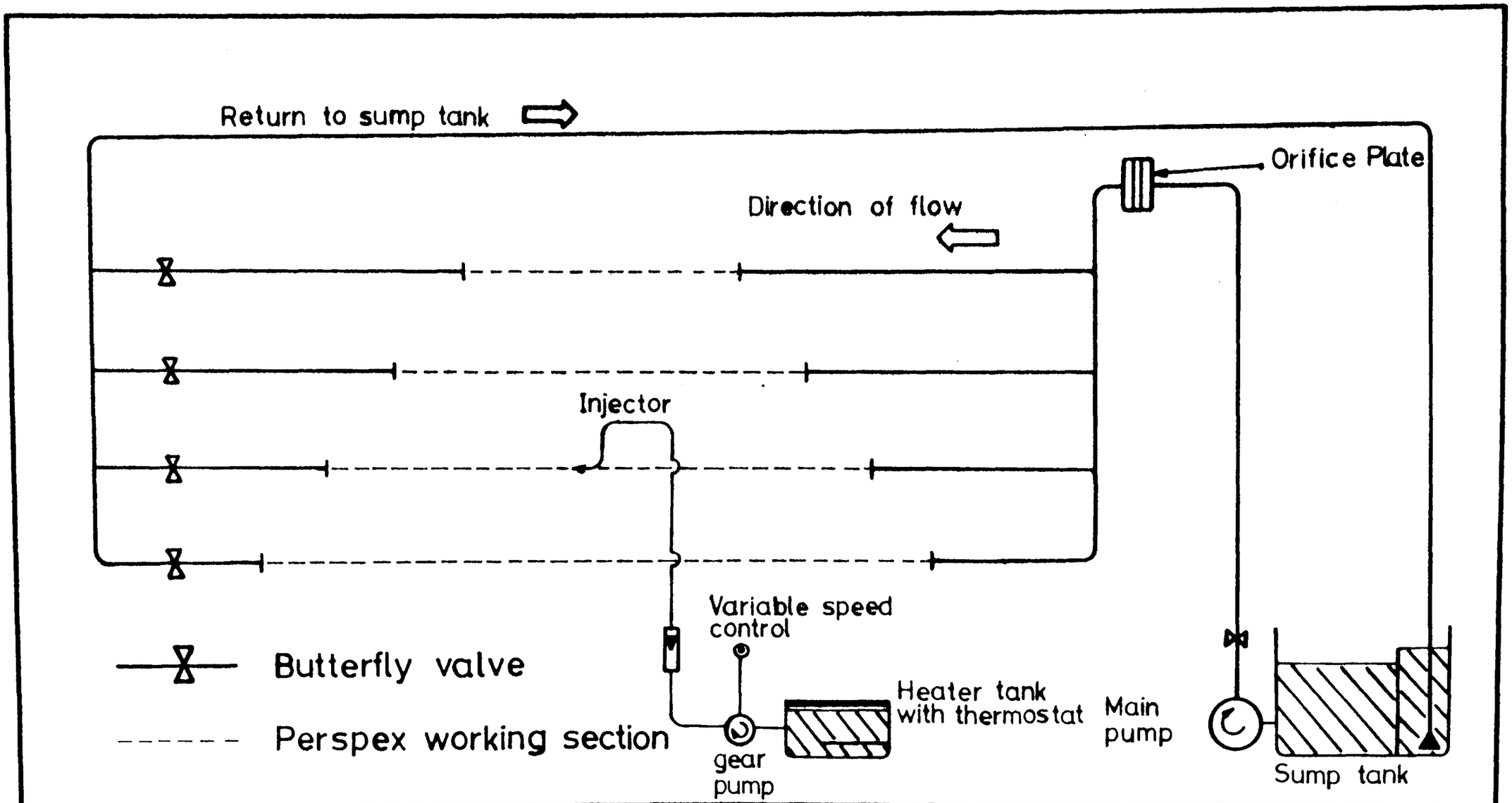


Fig.6 Schematic layout of the experimental facilities.

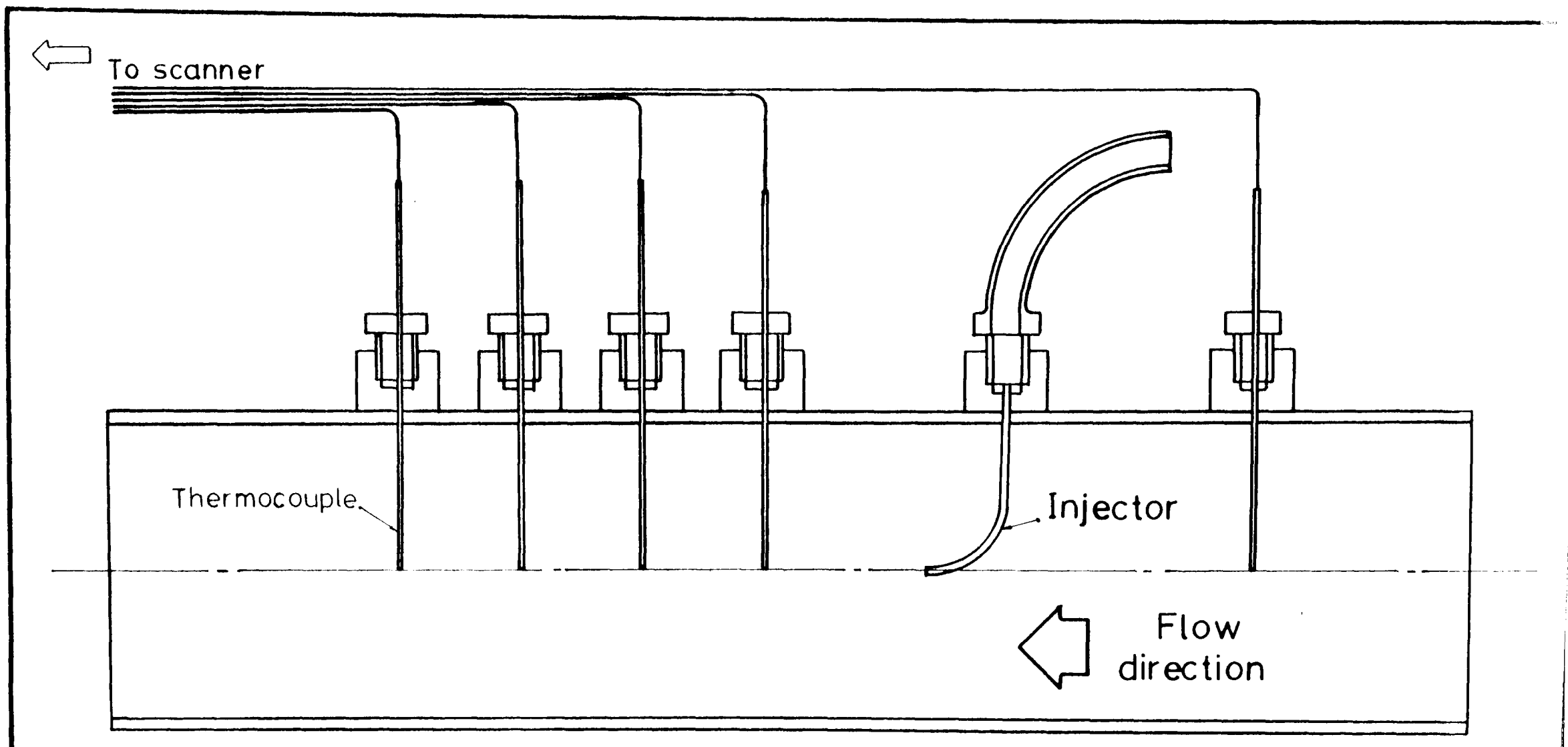


Fig. 7 Perspex working section.

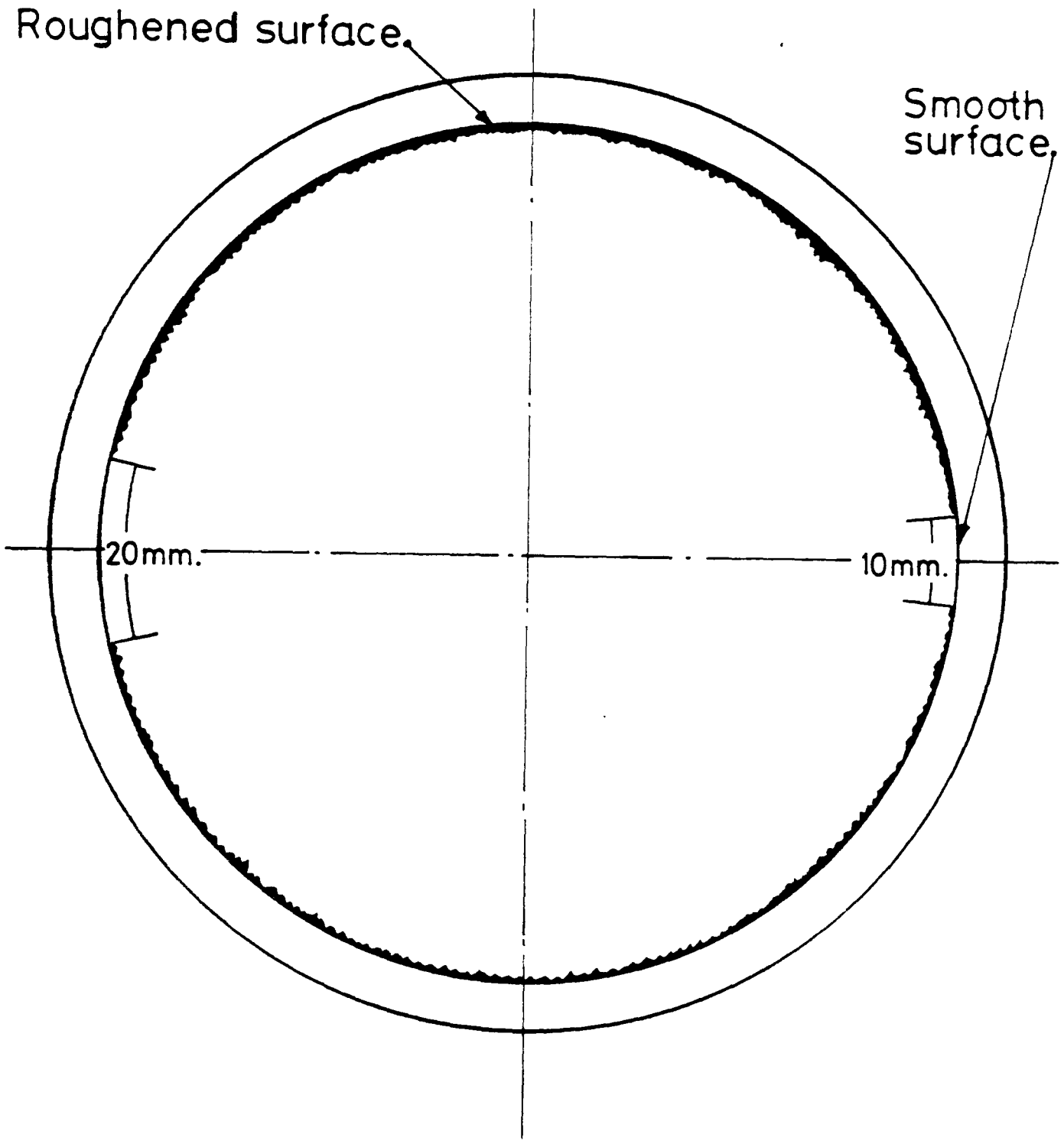


Fig. 8 Cross-section of a typical roughened pipe.

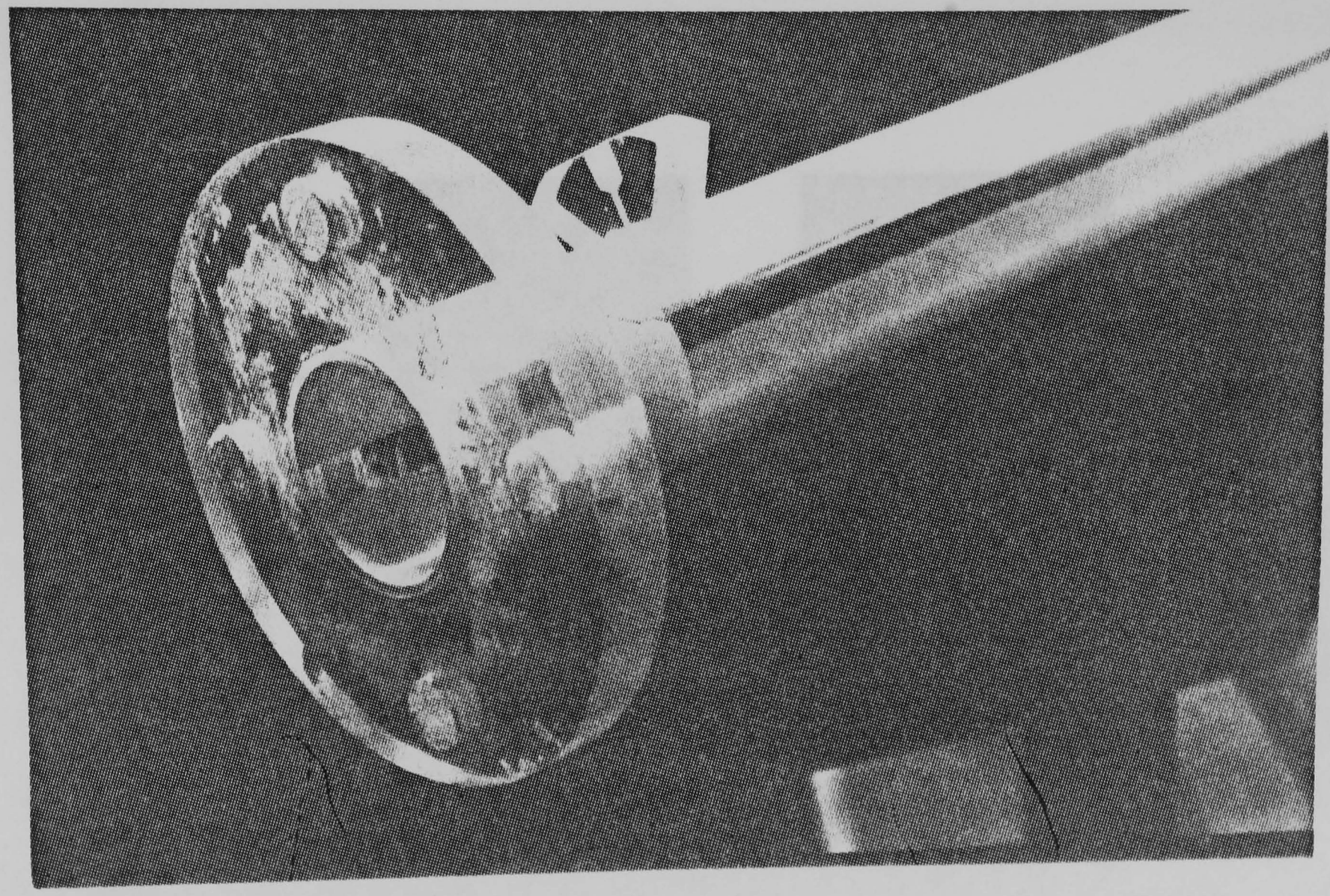

Fig.9 A typical roughened pipe .

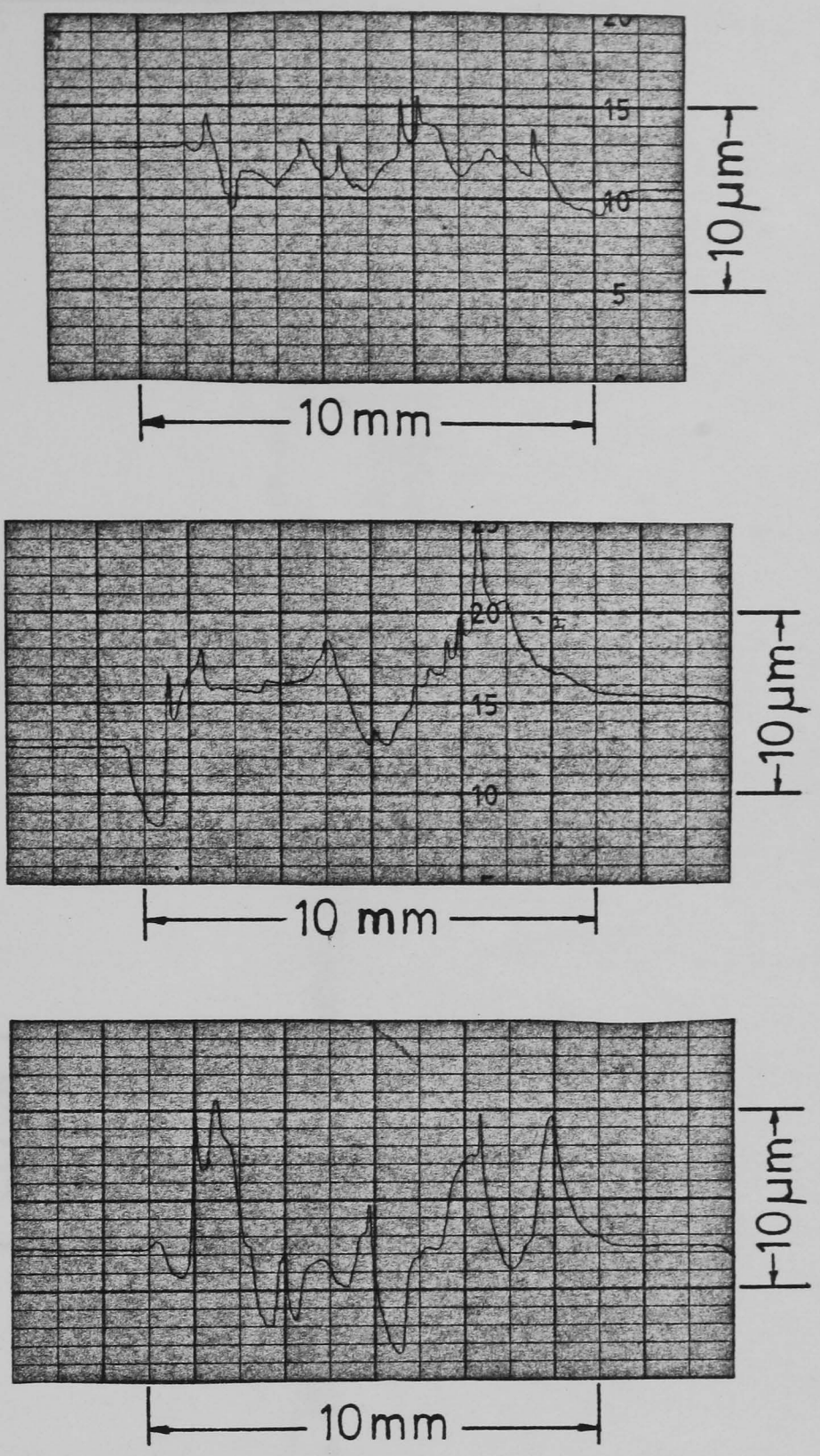


Fig.10(a)-(c) Output of roughness measurements.

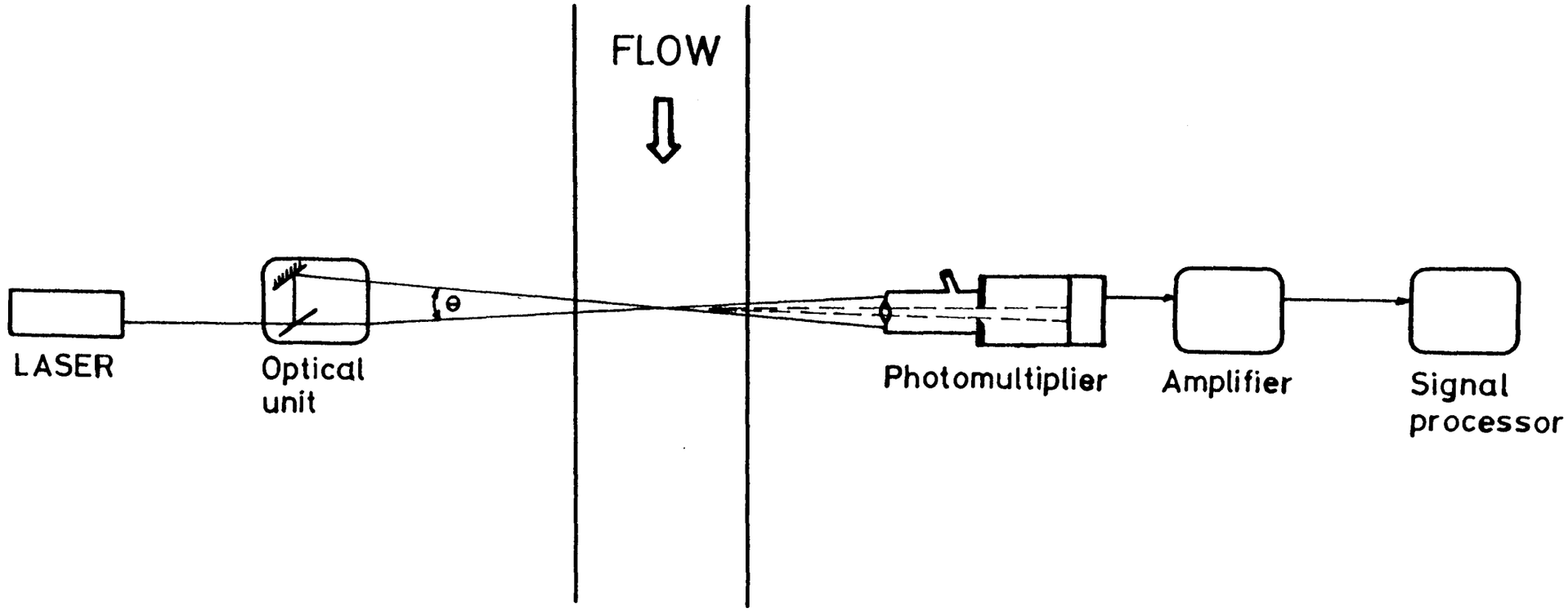


Fig. 11 A differential doppler velocity measurement system.

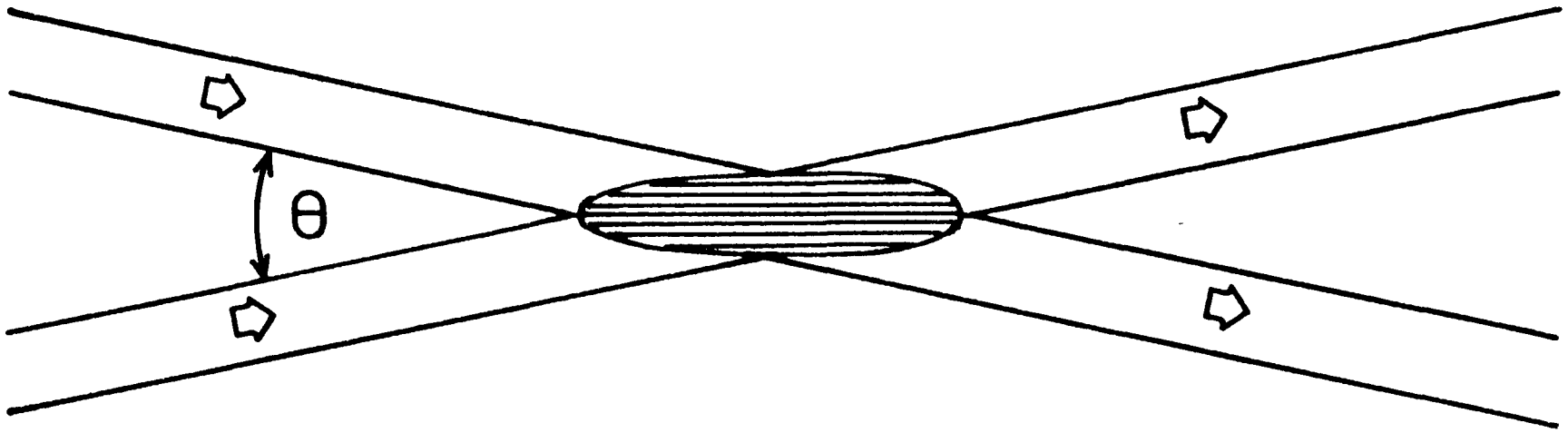


Fig. 12 Fringe pattern produced by crossing beams in the differential doppler technique.

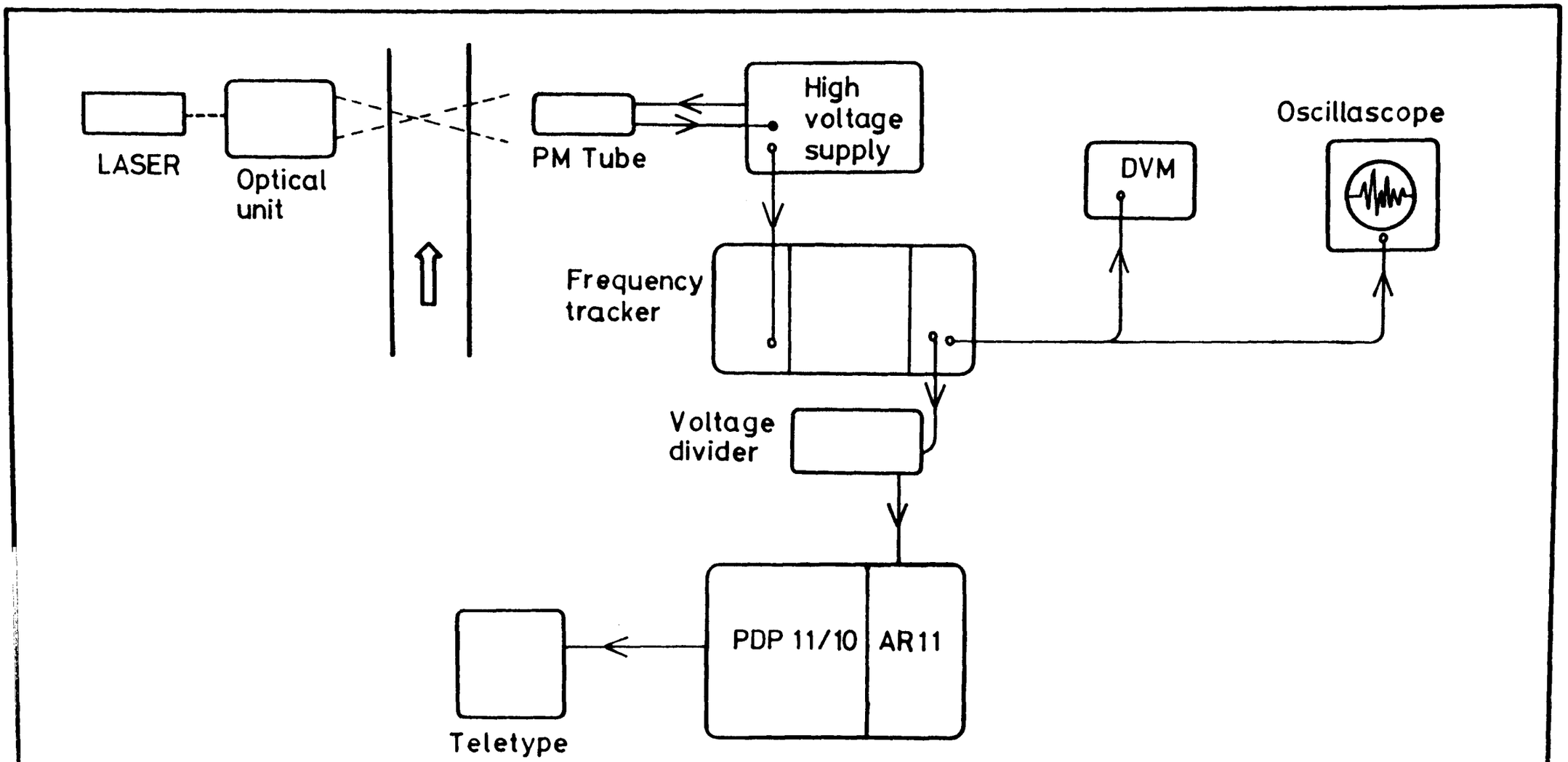


Fig. 13 Arrangement of LDA measurement chain.

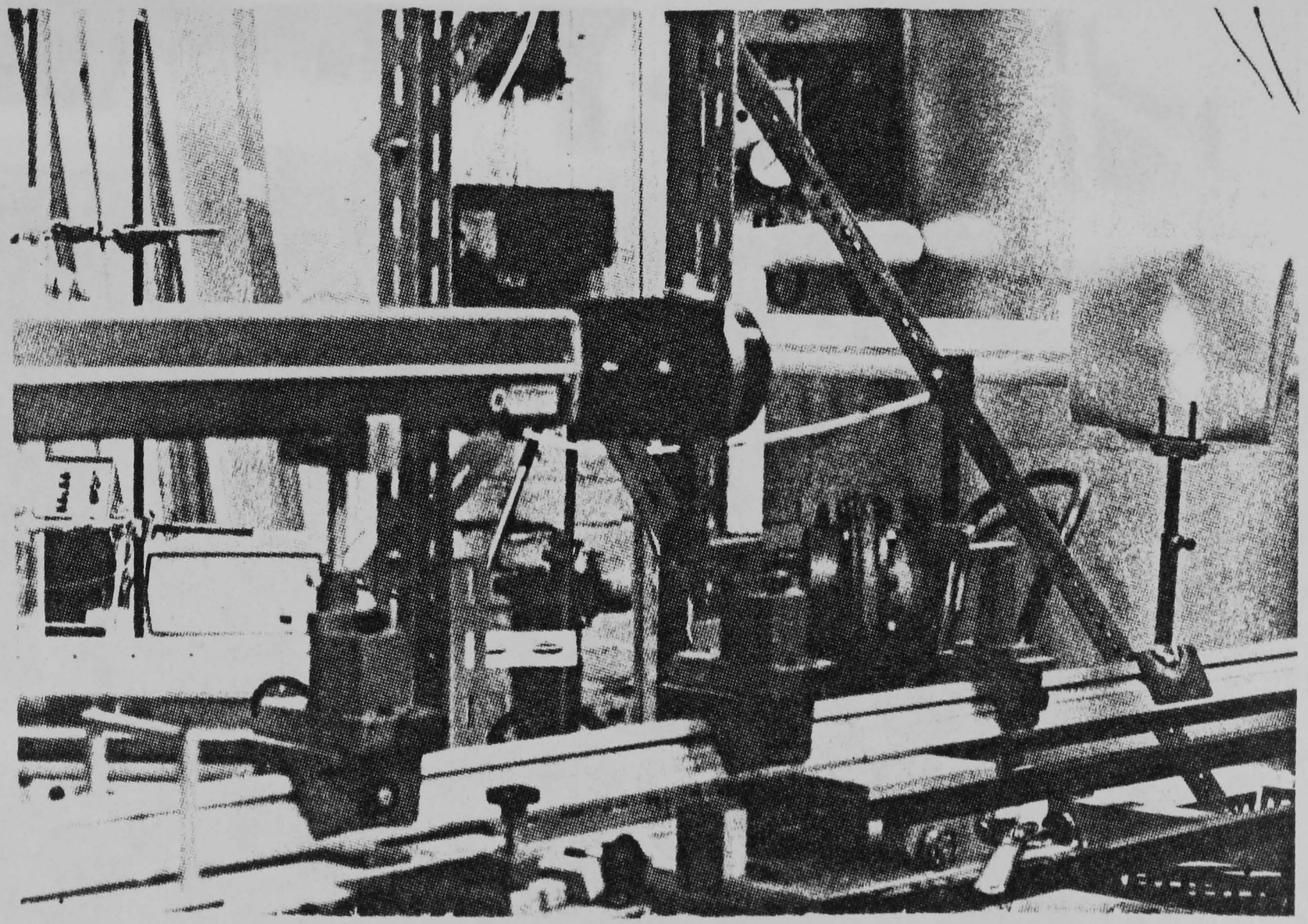

Fig. 14 Screening the intersection volume.

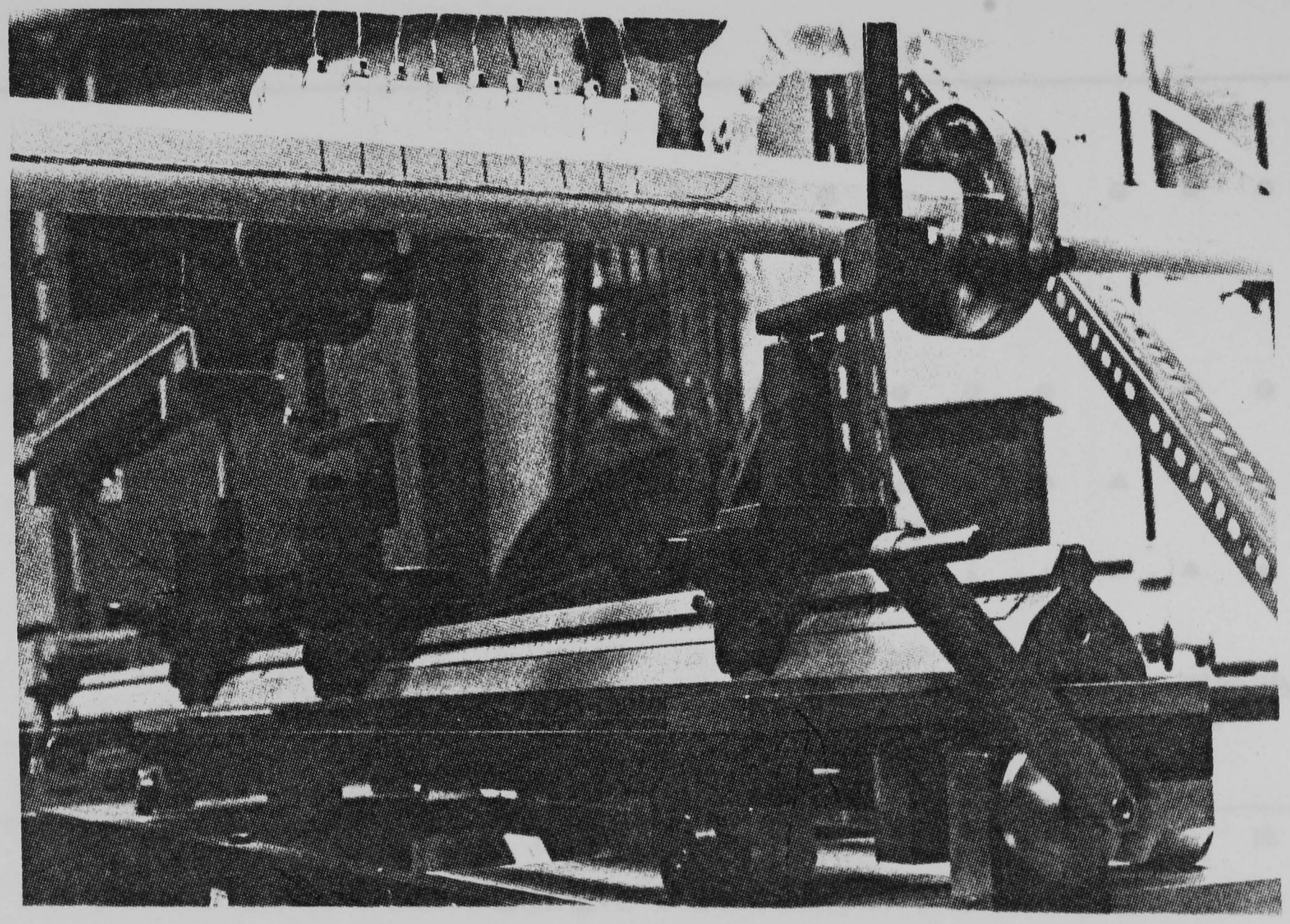

Fig. 15 View of the traversing mechanism.

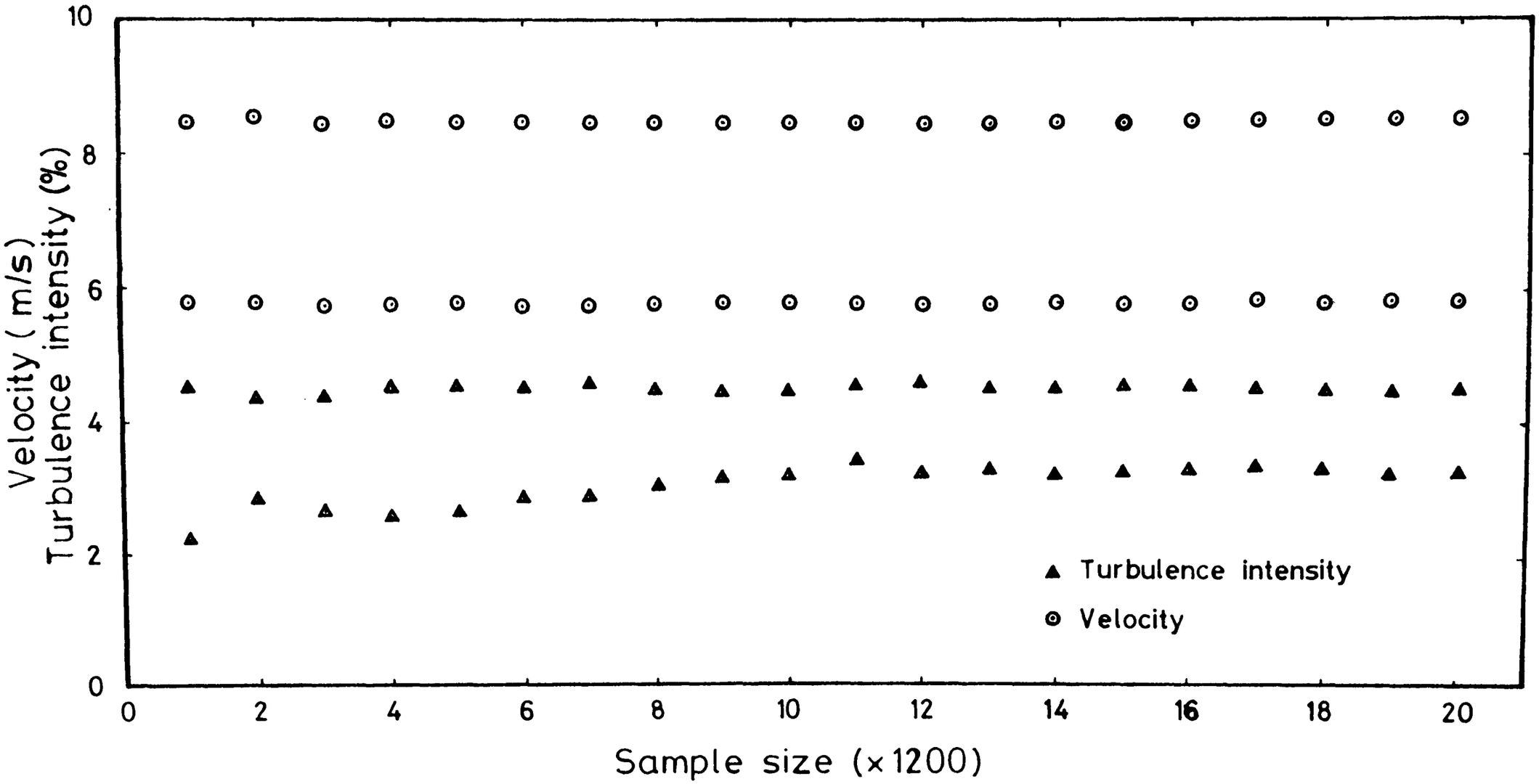


Fig. 16 Convergence of velocity and turbulence intensity measurements.

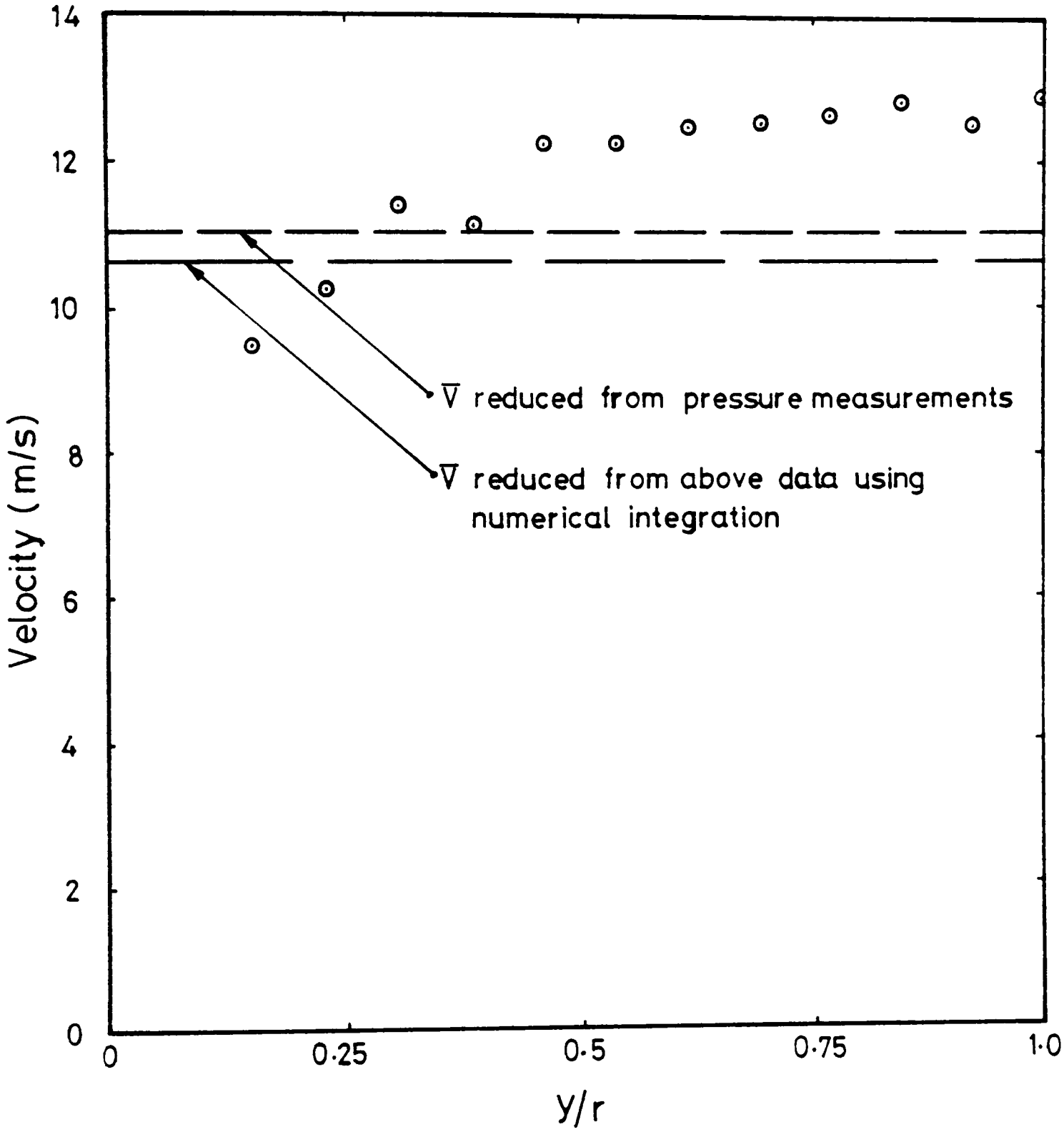


Fig. 17 Comparison between velocity measurements obtained with the LDA and that reduced from pressure drop across the orifice plate.

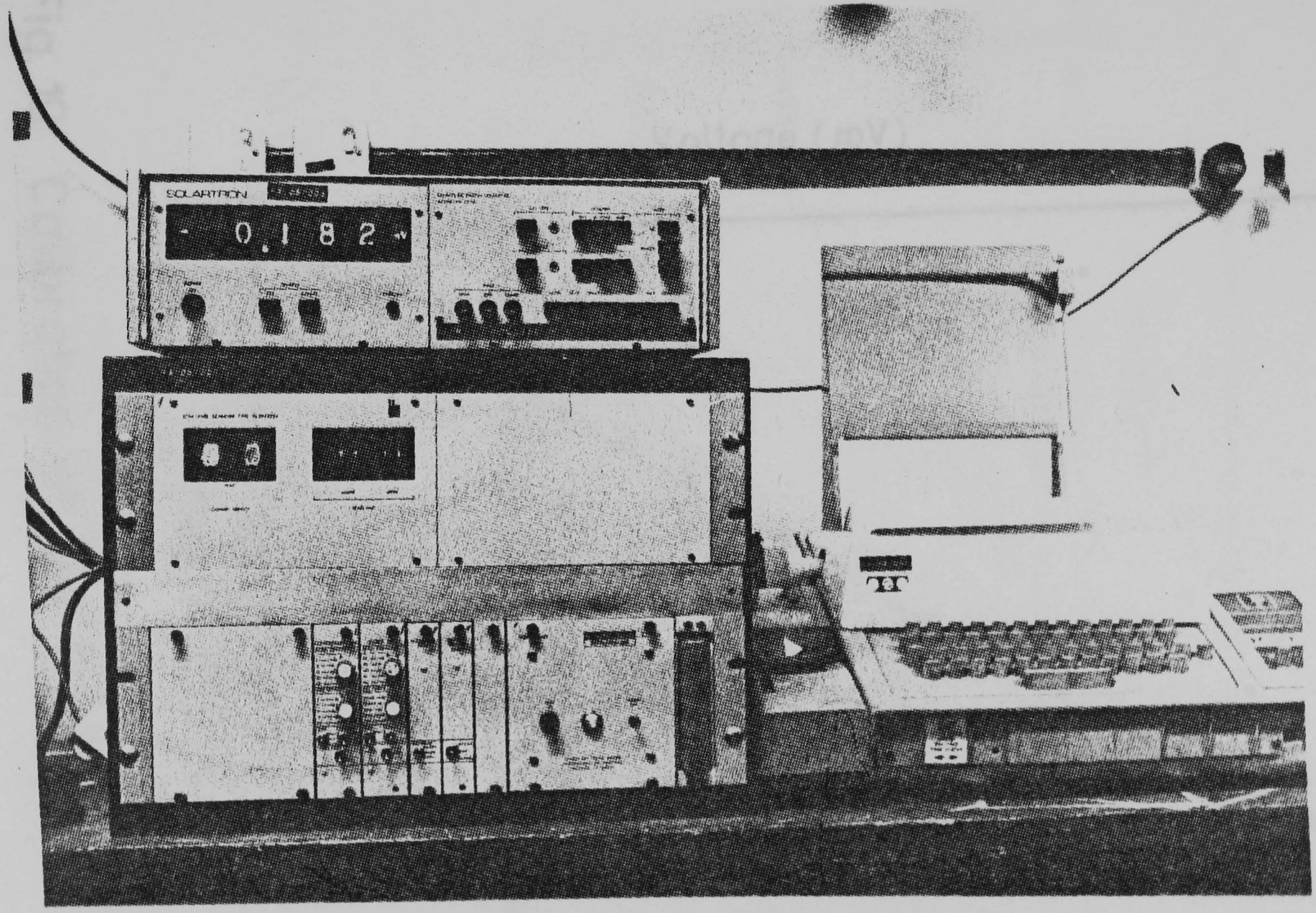


Fig. 18 Data scanner equipment.

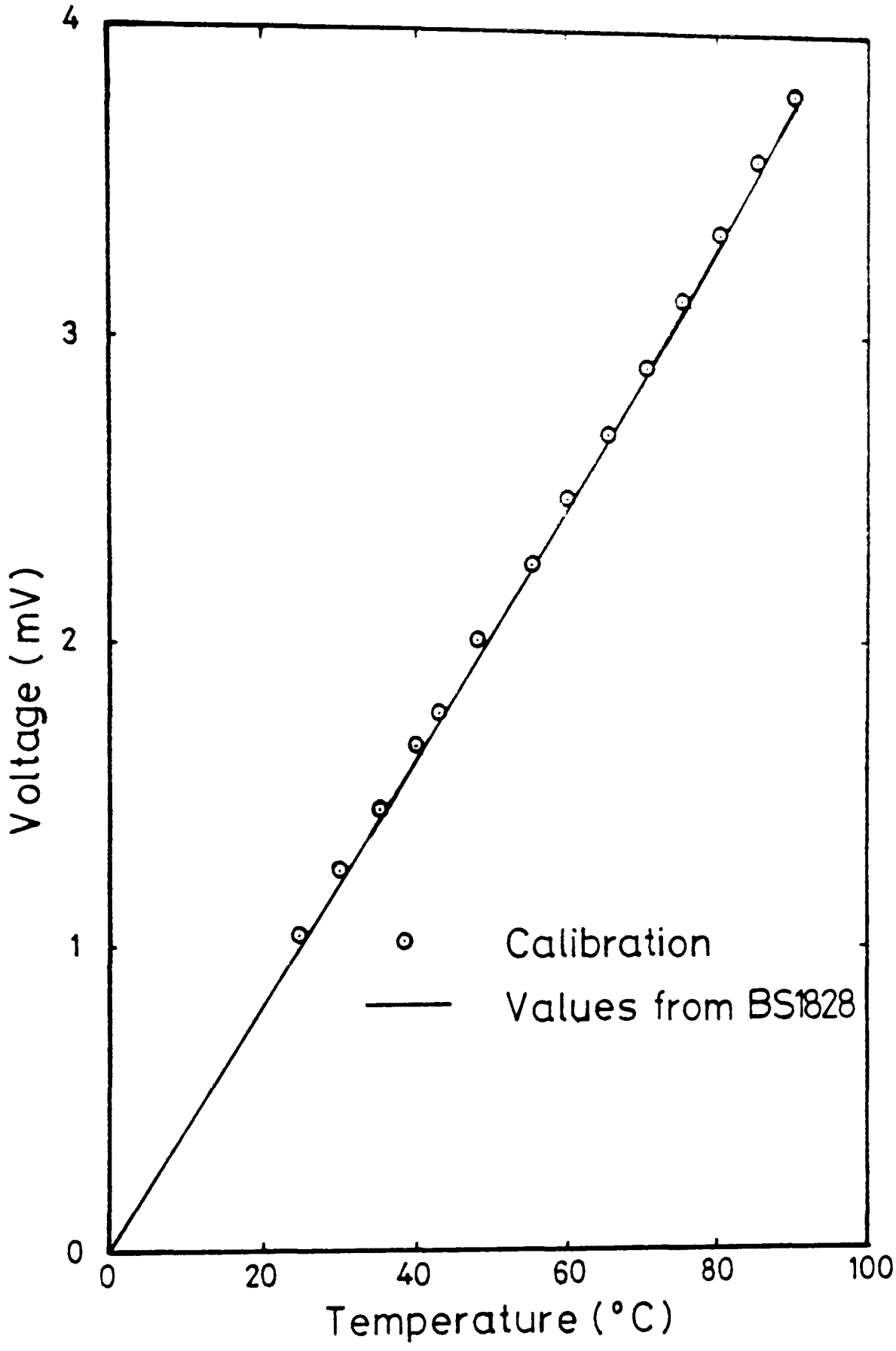


Fig. 19 Calibration of Cu-Con thermocouple.

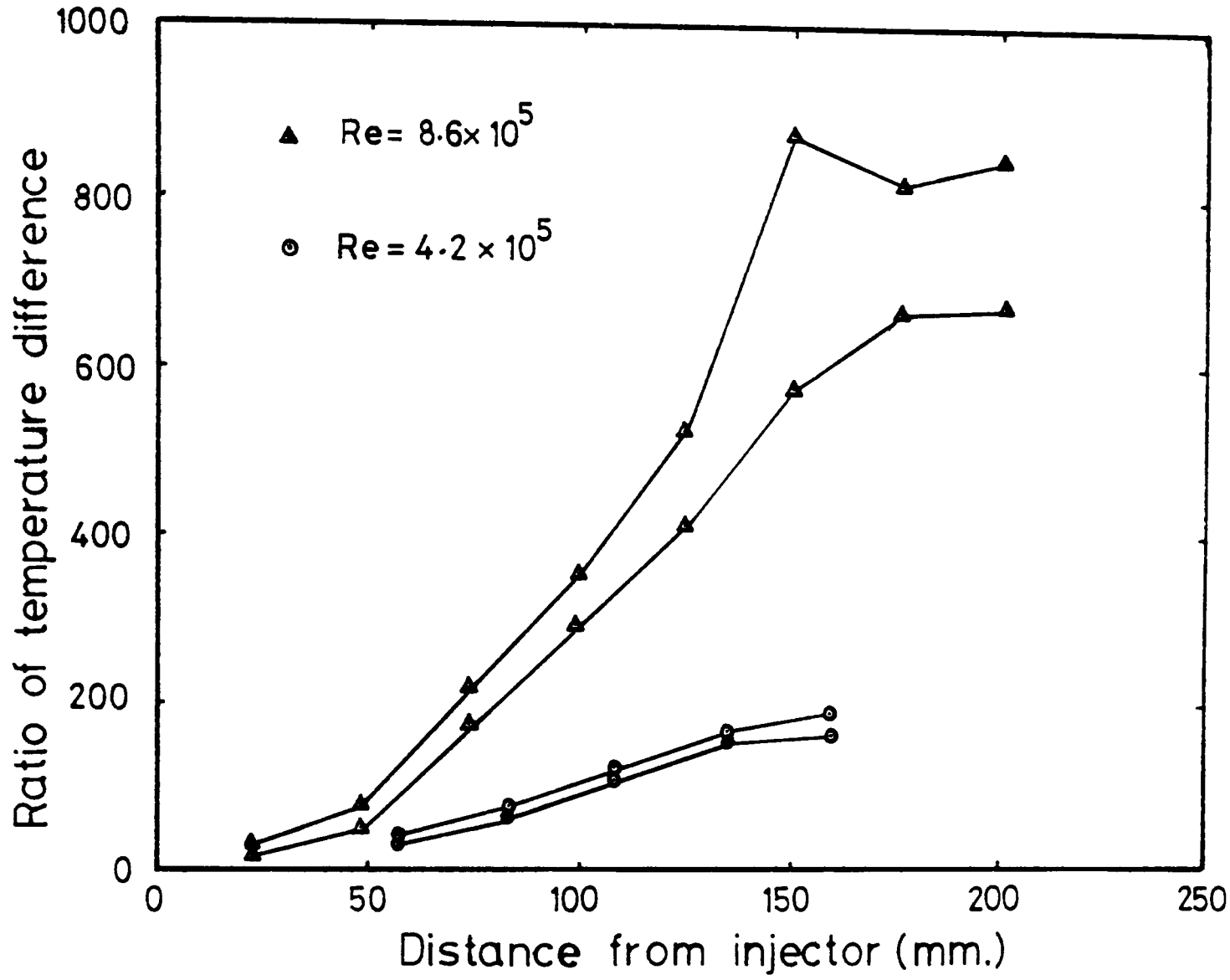


Fig.20 Distribution of temperature difference along the centreline.

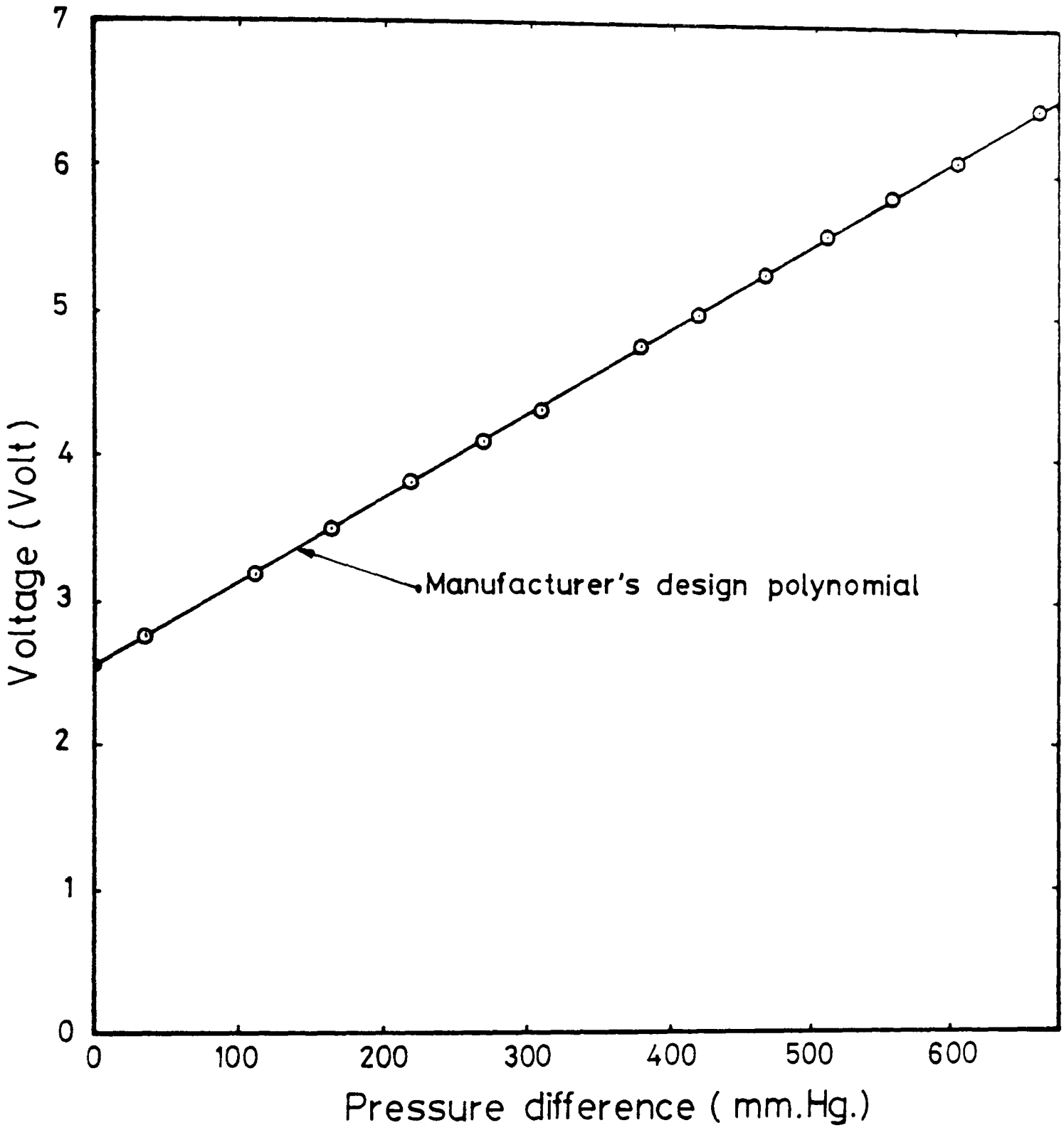


Fig. 21 Calibration of National Semiconductor differential pressure transducer.

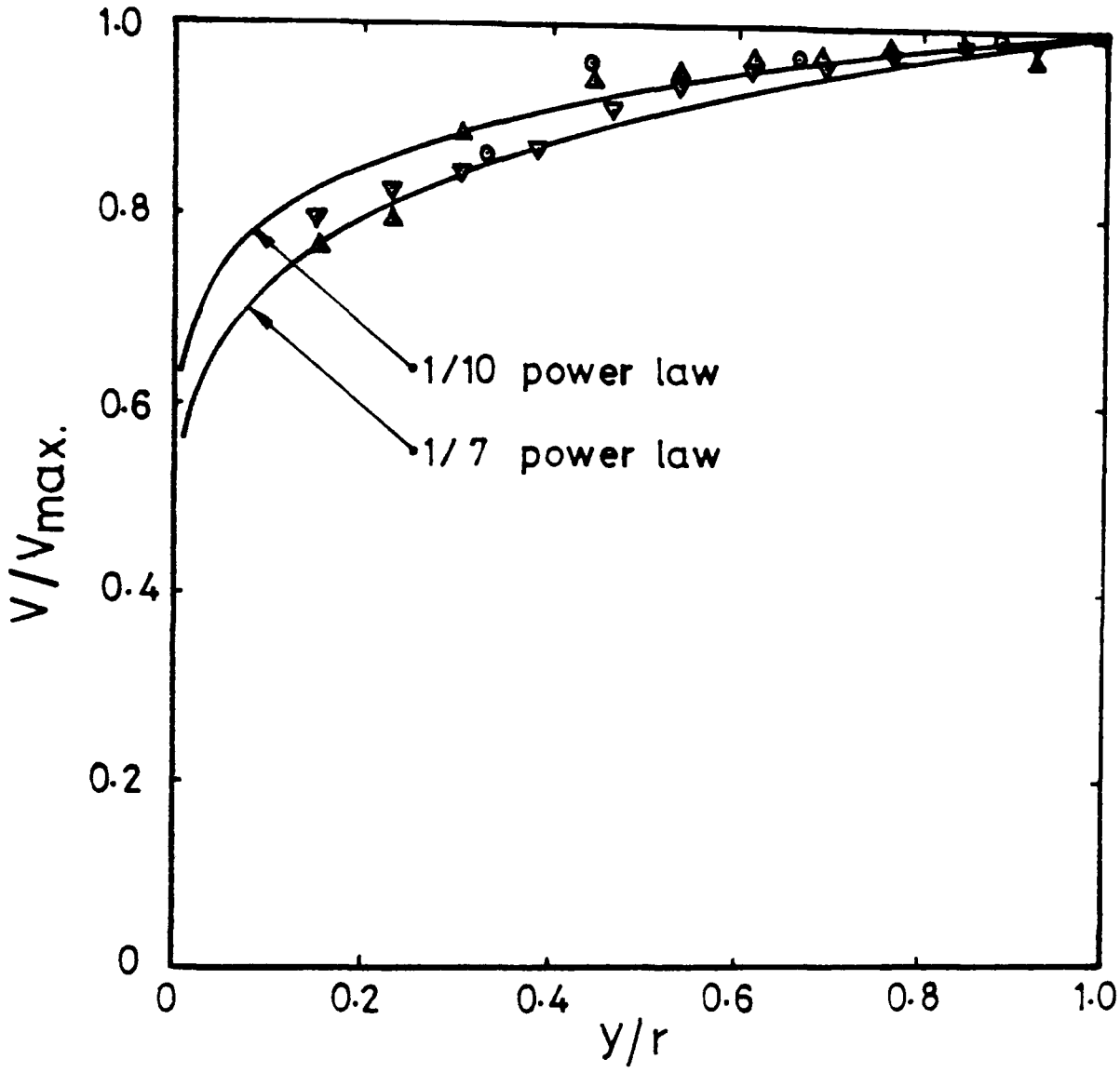


Fig. 22 Radial distribution of velocity measurements.

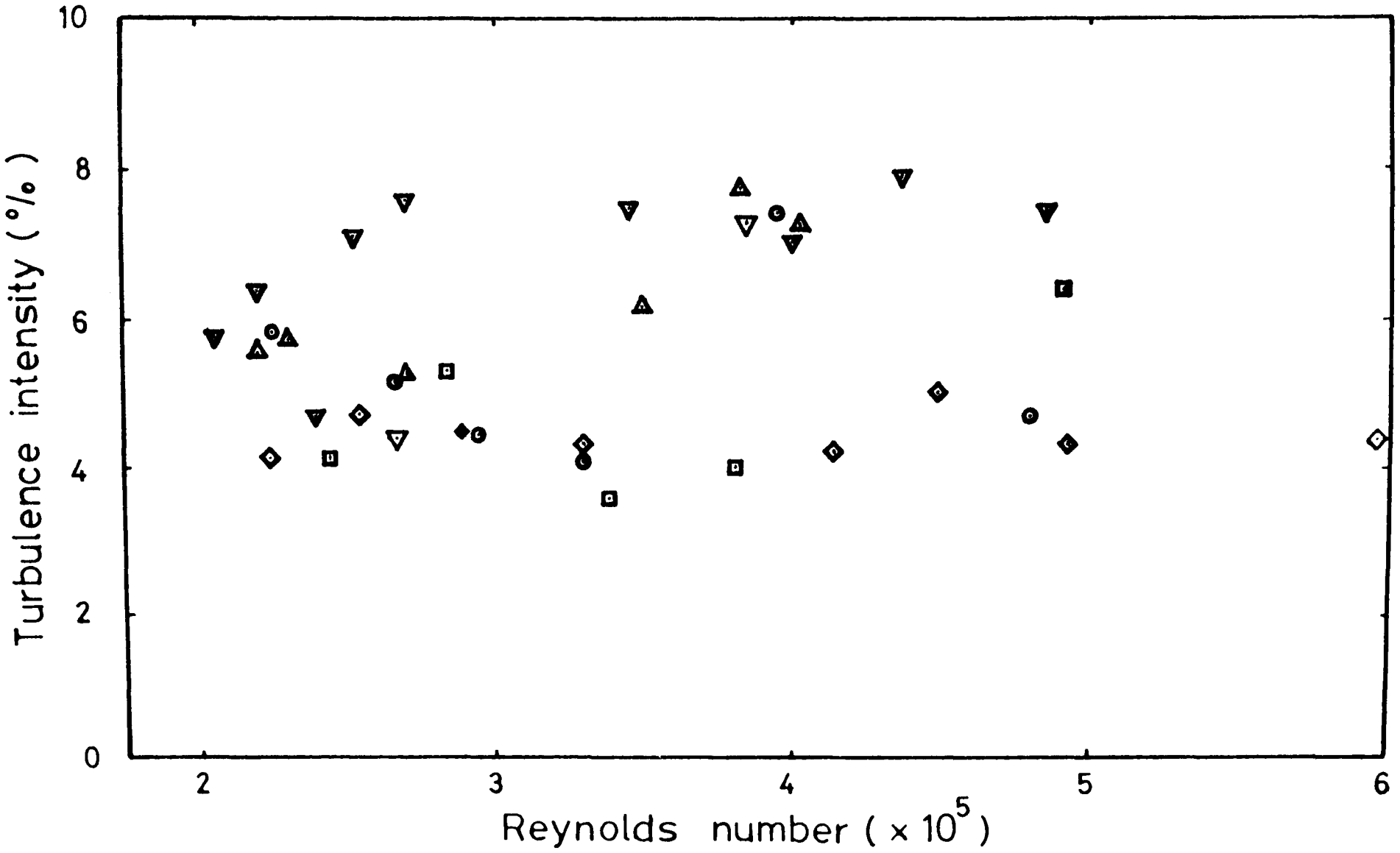


Fig. 23 Variation of turbulence intensity.

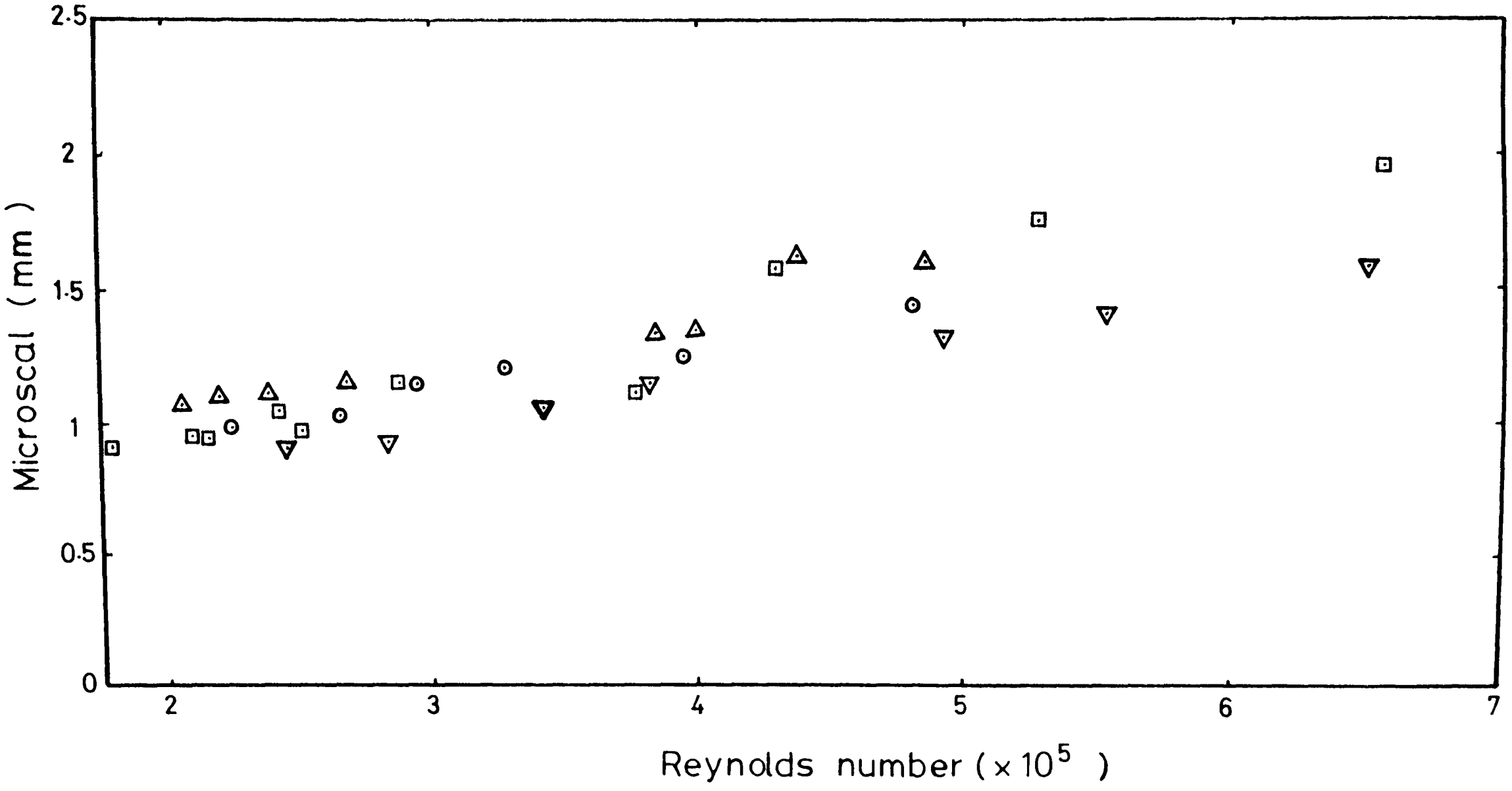


Fig. 24 Variation of microscale.

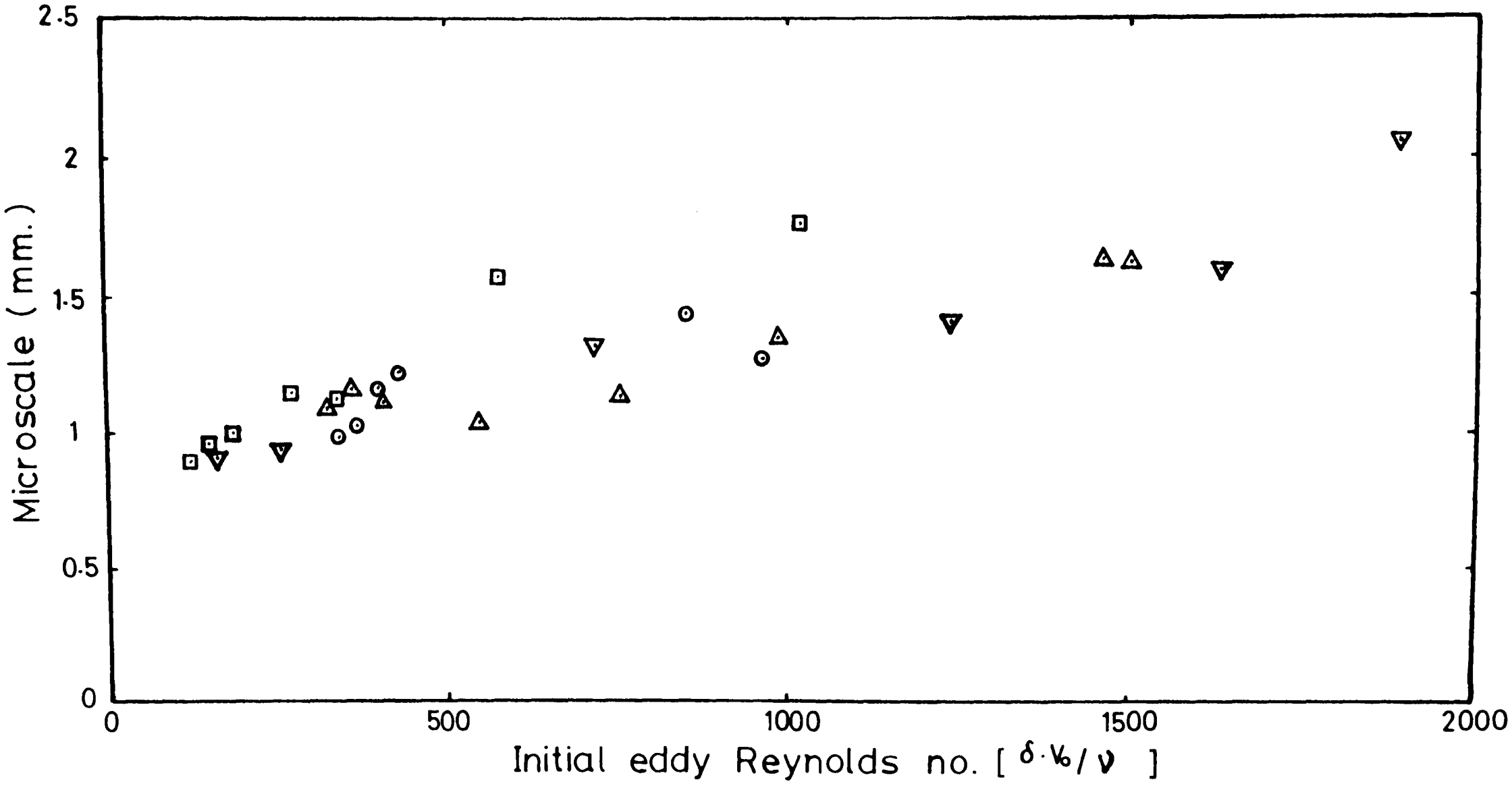


Fig. 25 Relationship between eddy Reynolds no. and microscale.

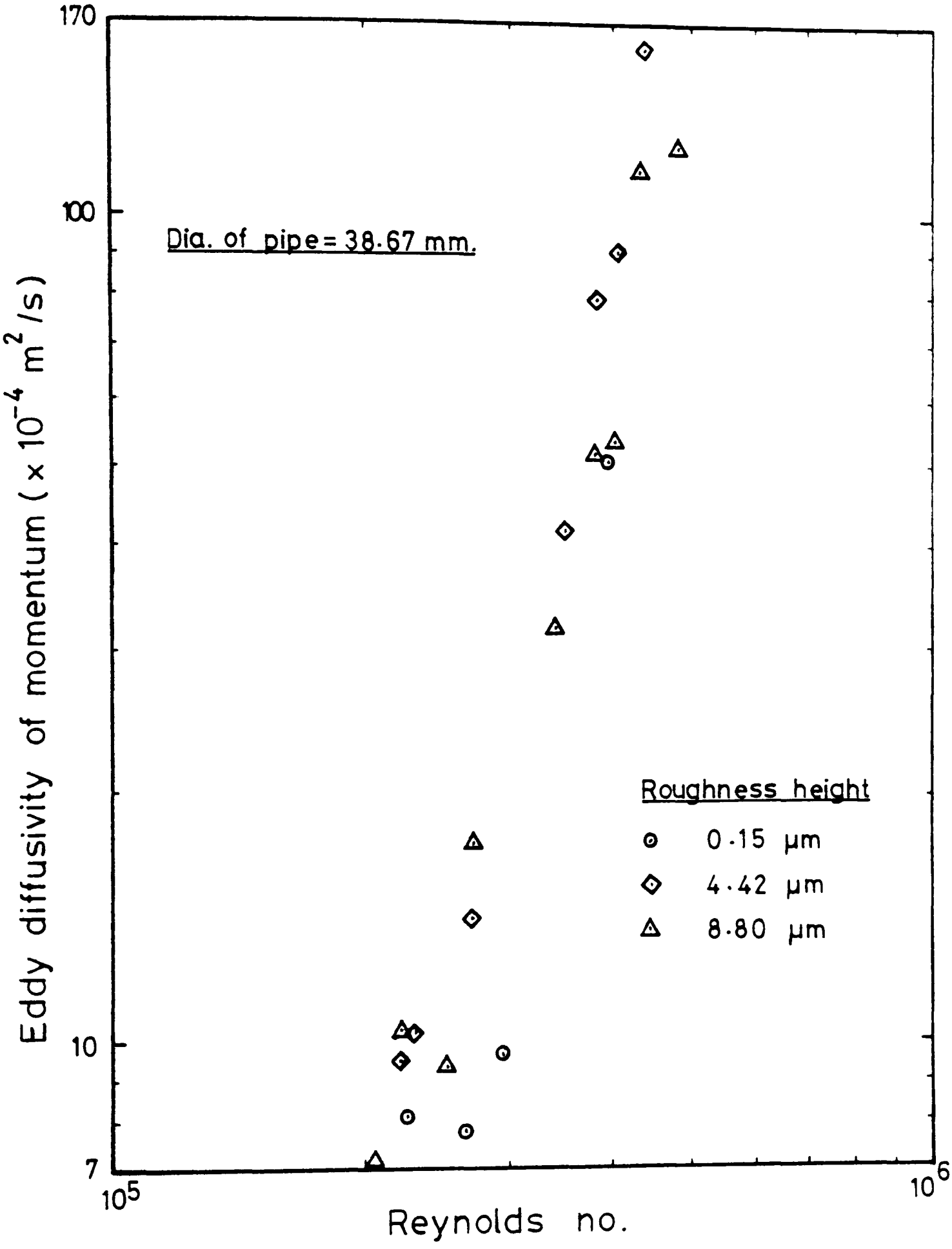


Fig. 26(a) Distribution of eddy diffusivity of momentum.

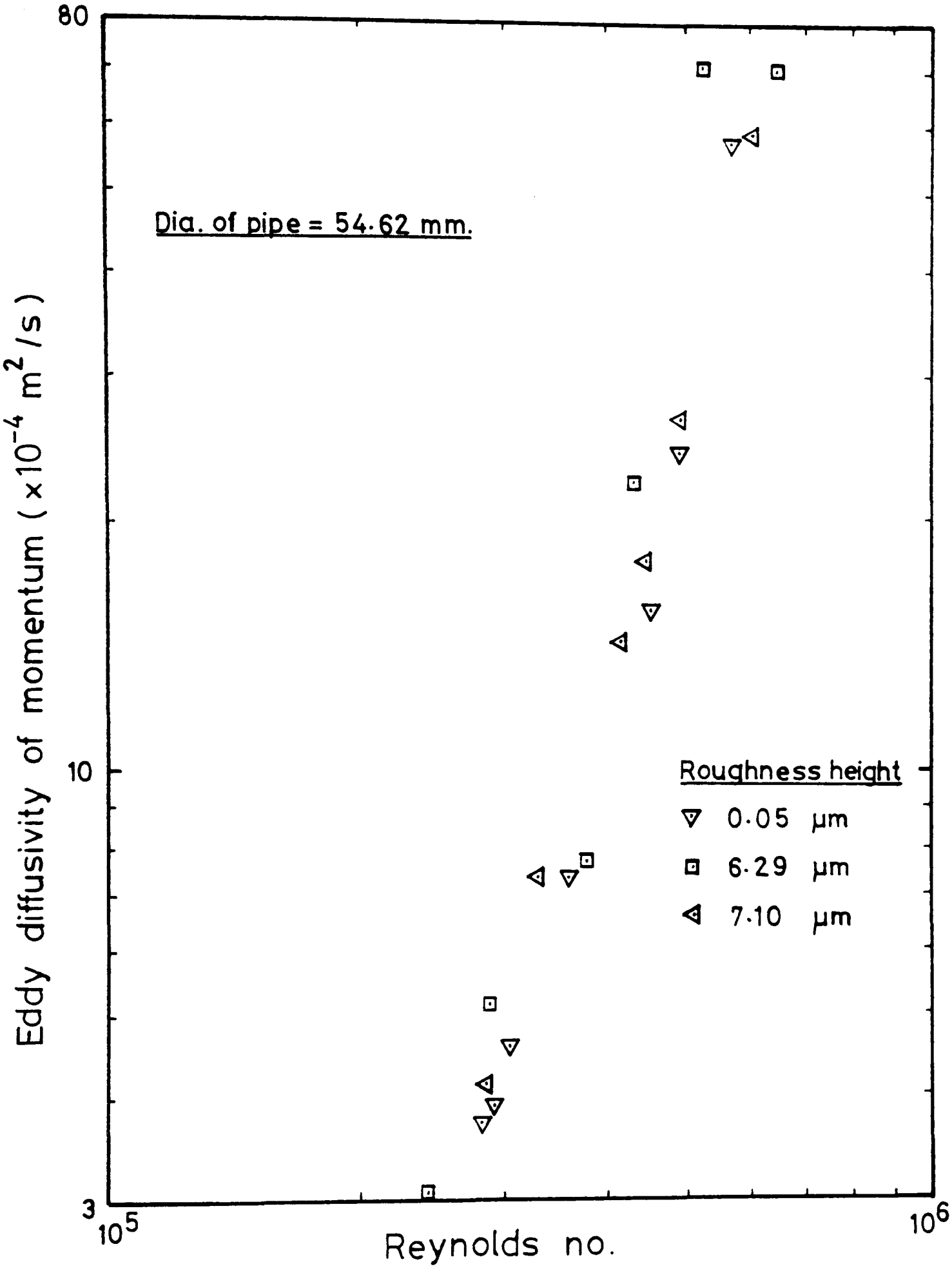


Fig. 26(b) Distribution of eddy diffusivity of momentum.

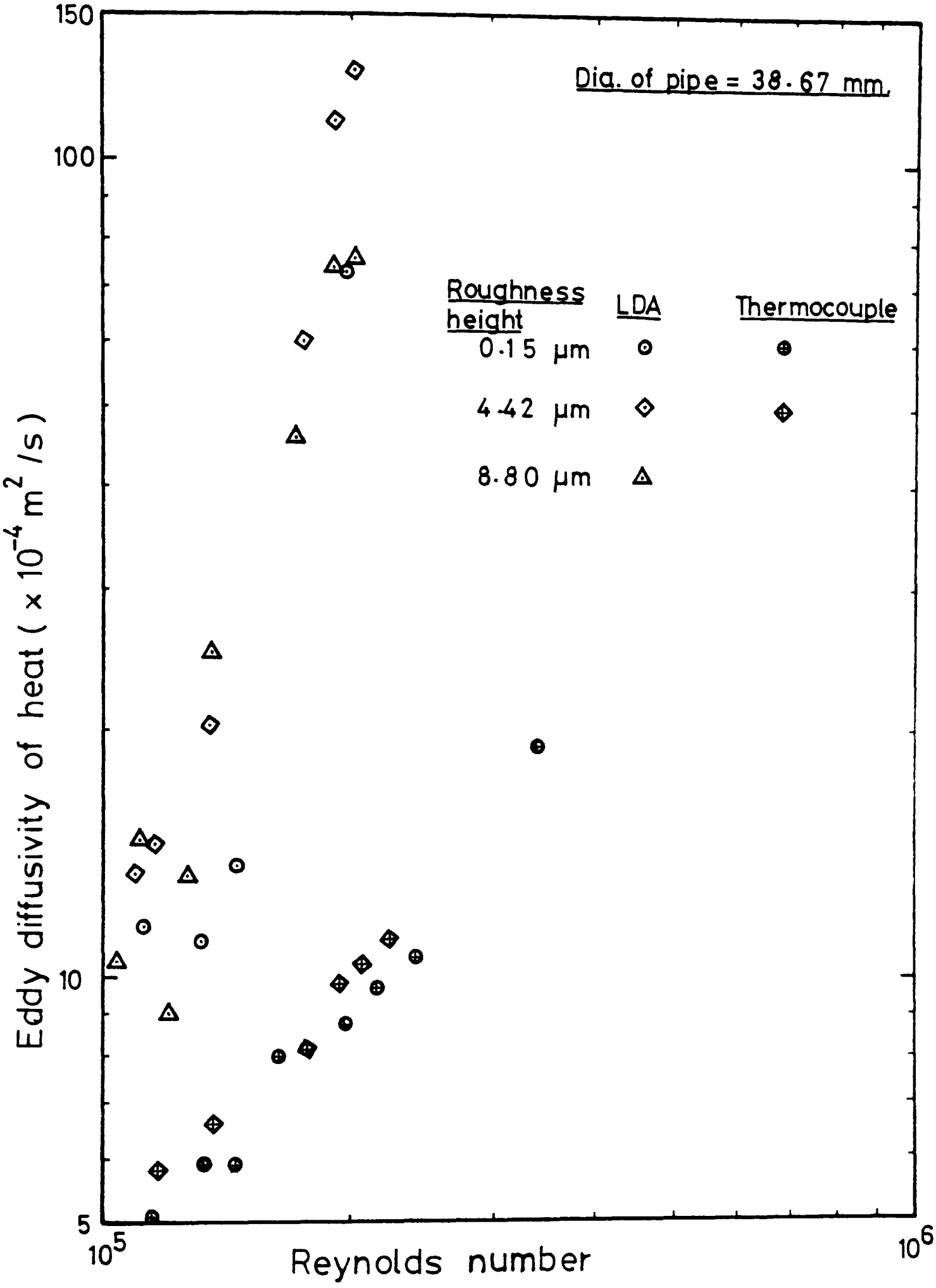


Fig. 27(a) Camparison of eddy diffusivity of heat obtained with the LDA and thermocouples.

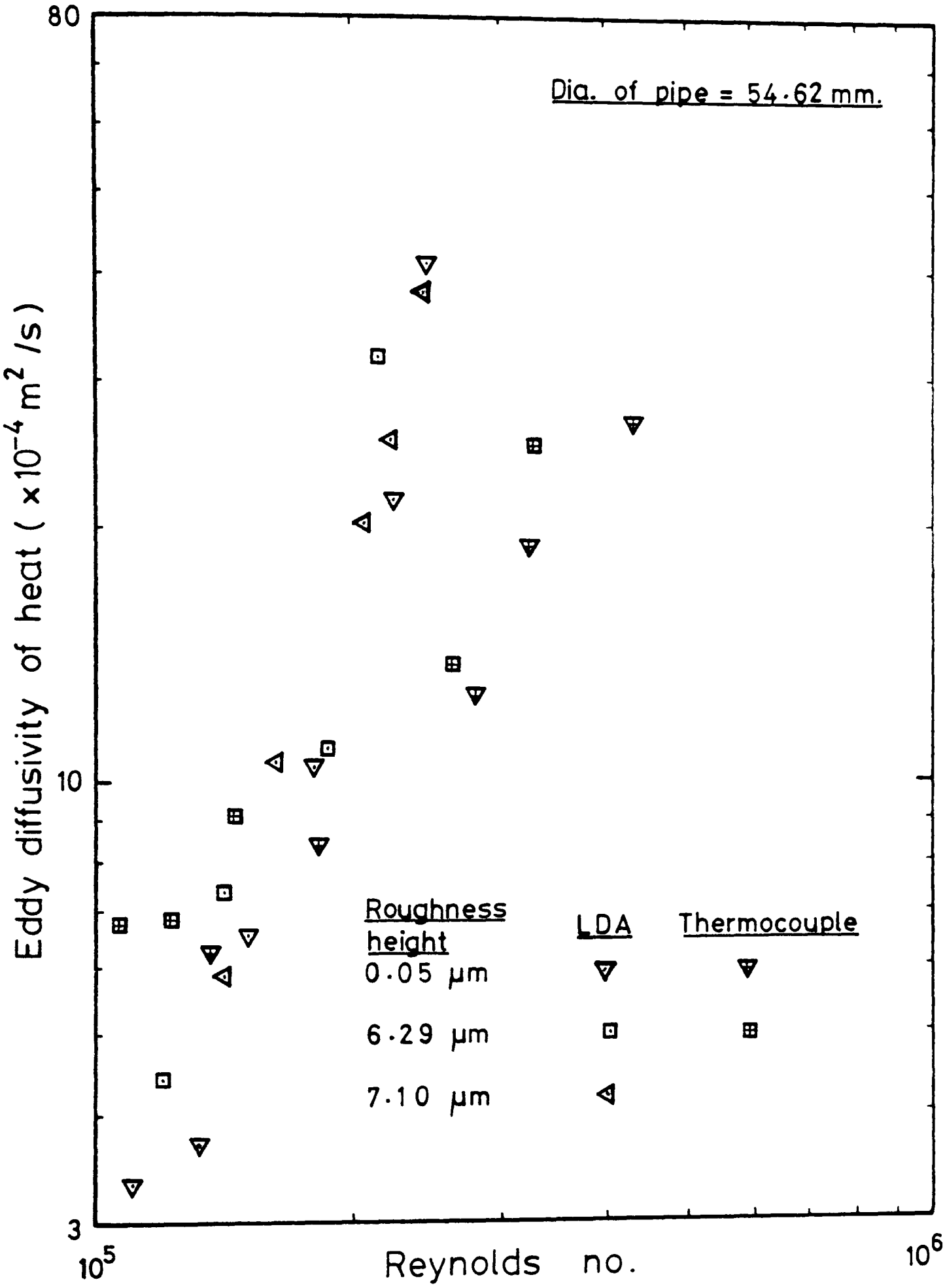


Fig. 27(b) Camparison of eddy diffusivity of heat obtained with the LDA and thermocouples.

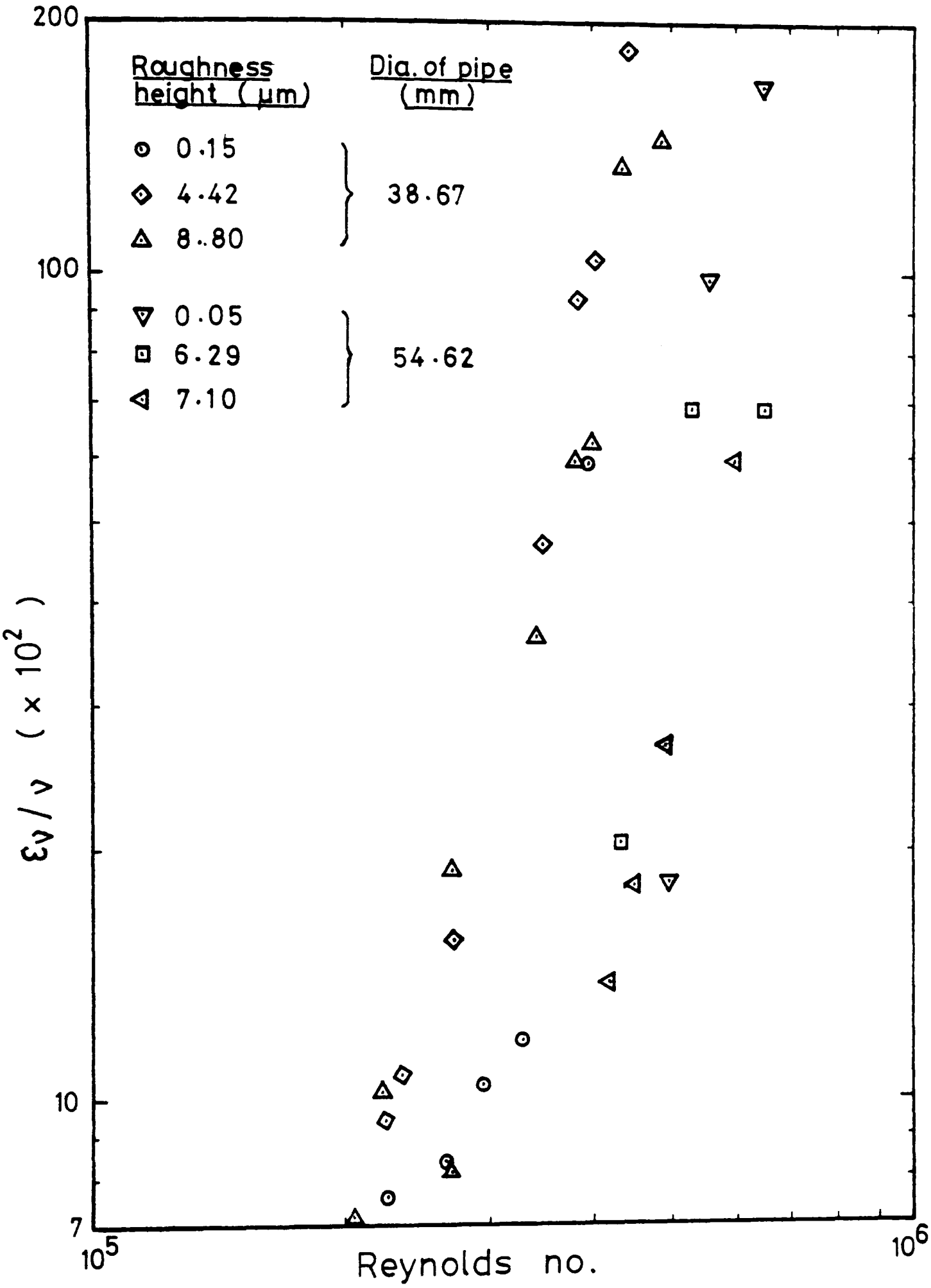


Fig. 28 Distribution of the ratio of eddy diffusivity of momentum to absolute viscosity.

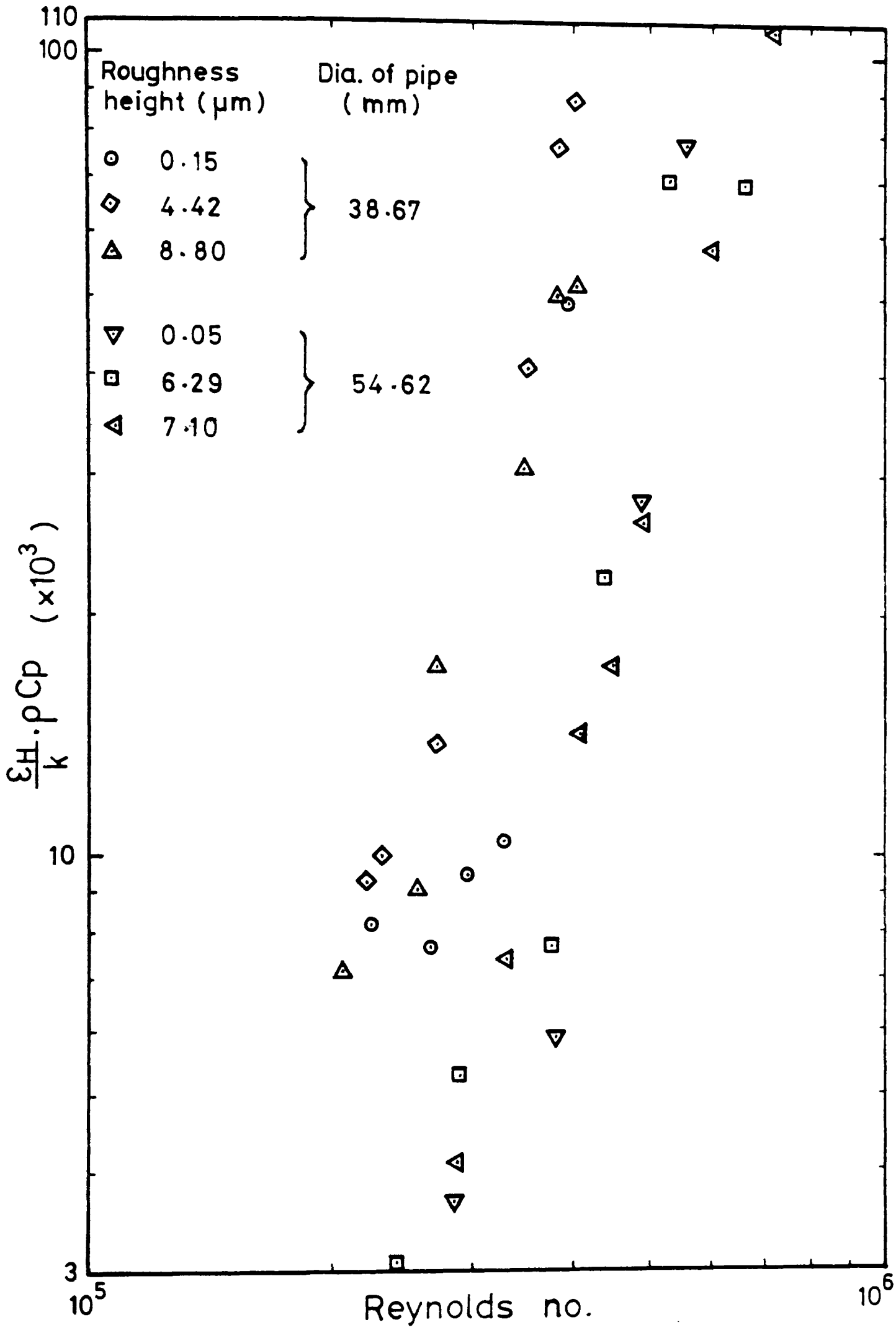


Fig.29 The ratio of eddy diffusivity of heat to thermal diffusivity obtained with the LDA.

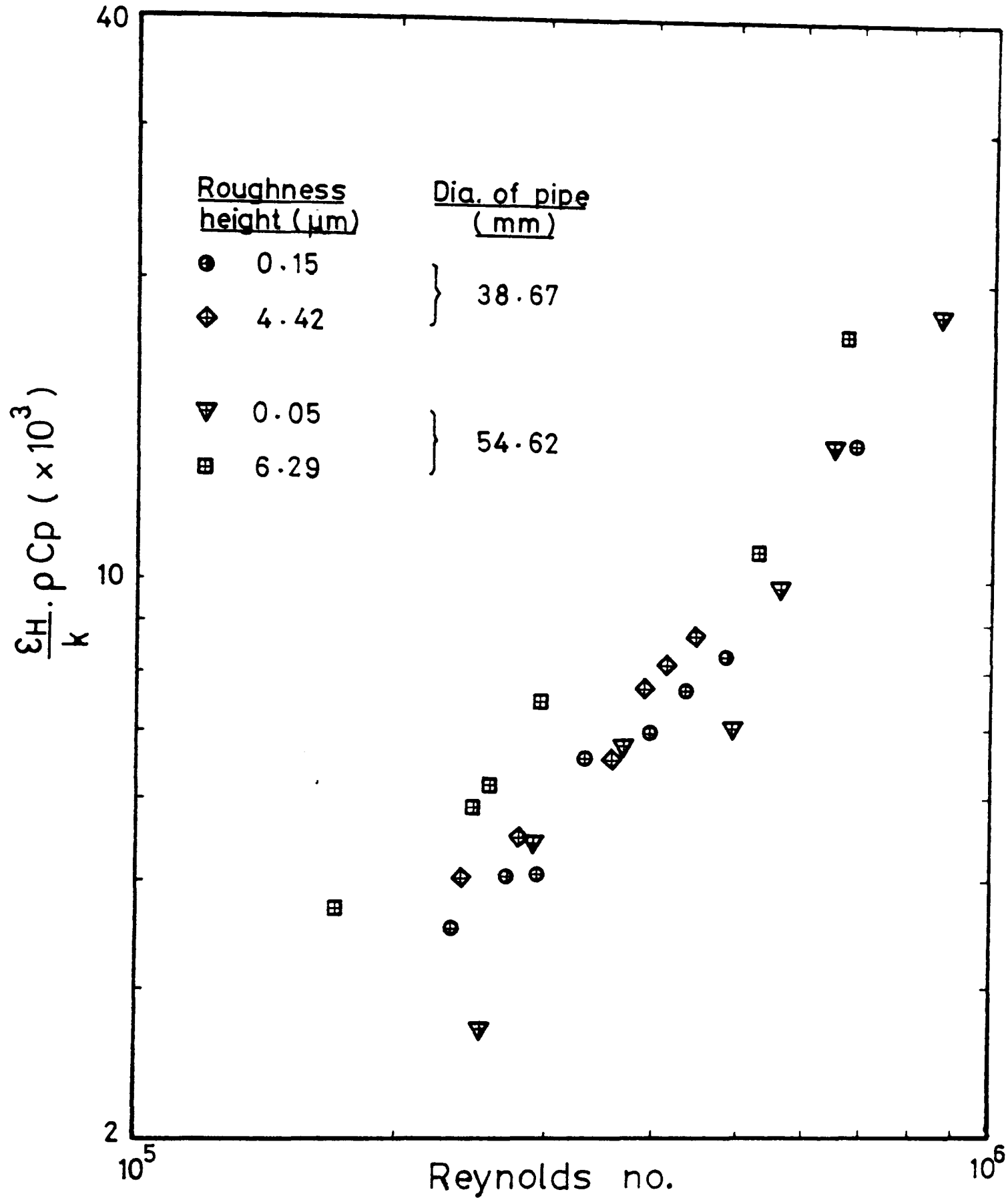


Fig. 30 The ratio of eddy diffusivity of heat to thermal diffusivity obtained with thermocouples.

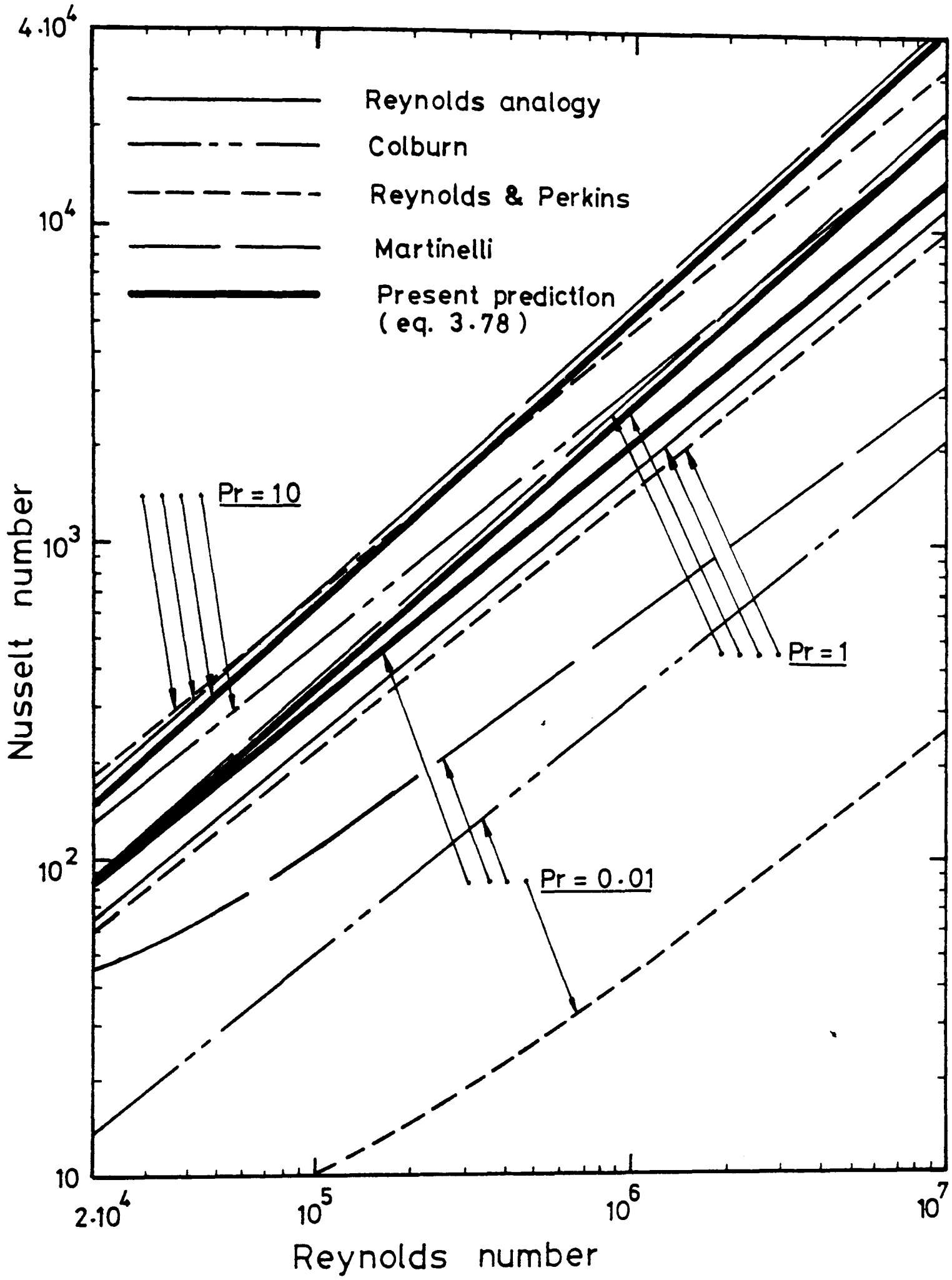


Fig. 31 Overall heat transfer similarity parameter ( comparison with different heat transfer analogies ).

## APPENDIX 1. NAVIER-STOKES EQUATIONS AND REYNOLDS EQUATION OF MOTION

For an incompressible flow, the Navier-Stokes equations may be expressed as:-

$$\frac{\partial}{\partial x_i}(u_i) = 0 \qquad \text{(A1.1)}$$

$$\rho\left[\frac{\partial u_i}{\partial t} + \frac{\partial}{\partial x_j}(u_i u_j)\right] = -.\frac{\partial \rho}{\partial x_i} + \mu \nabla^2 u_i \qquad \text{(A1.2)}$$

As the instantaneous velocity may be expressed in terms of mean and fluctuating velocities:-

$$u_i = \overline{u}_i + u_i' \qquad \text{(A1.3)}$$

Similarly,

$$p = \overline{p} + p'$$

Hence (A1.1) and (A1,2) become:-

$$\frac{\partial}{\partial x_i}(\overline{u}_i + u_i') = 0 \qquad \text{(A1.4)}$$

$$\rho\left[\frac{\partial}{\partial t}(\overline{u}_i + u_i') + \frac{\partial}{\partial x_j}\left\{(\overline{u}_i + u_i')(\overline{u}_j + u_j')\right\}\right] =$$

$$-\frac{\partial}{\partial x_i}(\overline{p} + p') + \mu \nabla^2(\overline{u}_i + u_i') \qquad \text{(A1.5)}$$

The Reynolds rules of averages have the following properties:-

(1) $\overline{f + g} = \overline{f} + \overline{g}$

(2) $\overline{cf} = c.\overline{f}$ (c being a constant)

(3) $\overline{fg} = \overline{f}\,\overline{g}$

(4) $\overline{\text{Lim } fn} = \text{Lim } (\overline{fn})$ (fn being a sequence of function)

Therefore equation (A1.4) may be written as:-

$$\frac{\partial \overline{u}_i}{\partial x_i} + \frac{\partial u_i'}{\partial x_i} = 0$$

Taking the mean value of this equation implies

$$\frac{\partial \overline{u_i}}{\partial x_i} + \frac{\partial \overline{u_i'}}{\partial x_i} = 0$$

As $\overline{u}'_i = 0$, hence the conservation of mass equation may now be written as:-

$$\frac{\partial \overline{u}_i}{\partial x_i} = 0 \qquad \text{(A1.6)}$$

Equation (A1.5) becomes:-

$$\rho \left[ \frac{\partial \overline{u}_i}{\partial t} + \frac{\partial \overline{u}_i'}{\partial t} + \frac{\partial}{\partial x_j} (\overline{u}_i\overline{u}_j + \overline{u}_i u_j' + u_i'\overline{u}_j + u_i'u_j') \right]$$

$$= - \frac{\partial \overline{p}}{\partial x_i} - \frac{\partial p'}{\partial x_i} + \mu\nabla^2 \overline{u}_i + \mu\nabla^2 u_i'$$

Again, taking the mean value of the above equation and putting $\overline{u_i'} = 0$ and $\overline{p'} = 0$,

$$\rho\left[\frac{\partial \overline{u}_i}{\partial t} + \frac{\partial}{\partial x_j} (\overline{u}_i\overline{u}_j) + \frac{\partial}{\partial x_j} (\overline{u_i'u_j'}) \right] = \frac{\partial \overline{p}}{\partial x} + \partial\nabla^2 \overline{u}_i$$

$$\therefore \quad \rho\left[\frac{\partial \bar{u}_i}{\partial t} + \frac{\partial}{\partial x_j}(\bar{u}_i \bar{u}_j)\right] - \rho \frac{\partial}{\partial x_j}(\overline{u_i' u_j'}) = -\frac{\partial \bar{p}}{\partial x} + \mu \nabla^2 \bar{u}_i$$

$$\text{or} \quad \rho\left[\frac{\partial \bar{u}_i}{\partial t} + \frac{\partial}{\partial x_j}(u_i u_j)\right] = -\frac{\partial \bar{p}}{\partial x} + \mu \nabla^2 \bar{u}_i + \frac{\partial}{\partial x_j}(-\rho \overline{u_i' u_j'}) \qquad \text{(A1.7)}$$

Equations (A1.6) and (A1.7) are the Reynolds equations of motion for the turbulent flow in an incompressible fluid.

## APPENDIX 2. MIXING LENGTH THEORY

For simplicity, the mean value of the transferable quantity $\overline{q}$ may be considered to be a function of y only. A body of fluid which originally belongs to a layer y=y moves to a layer y=y+$\ell$. Since the fluid preserves its value of $\overline{q}$ during the turbulent mixing process over the path $\ell$ , at the new layer the fluctuating value of q will be given by:-

$$|q'| = \overline{q}(y+\ell) - \overline{q}(y) \qquad \text{(A2.1)}$$

Expanding $\overline{q}(y+\ell)$ in a Taylor series about y, the above equation becomes:-

$$|q'| = \ell \cdot \frac{d\overline{q}}{dy} + \frac{\ell^2}{2} \cdot \frac{d^2\overline{q}}{dy^2} + \ldots \qquad \text{(A2.2)}$$

As $\ell$ may be considered a small quantity, it yields

$$|q'| = \ell \cdot \frac{d\overline{q}}{dy} \qquad \text{(A2.3)}$$

In actual analysis, further hypothesis about the variation of the mixing length $\ell$ has to be made.

In Prandtl's original mixing length theory, it was assumed that the momentum of the flow was a transportable quantity. Thus, for parallel flow,

$$|u'| = \ell \cdot \frac{d\overline{u}}{dy} \qquad \text{(A2.4)}$$

By further assuming that the vertical velocity fluctuation v' to be proportional to u' and the turbulent shear stress $\rho\overline{u'v}$ proportional to their product, Prandtl obtained the formula for the shearing stress of nearly parallel turbulent flow,

$$\tau = \rho.\ell^2.\left|\frac{d\bar{u}}{dy}\right|.\frac{du}{dy} \qquad \text{(A2.5)}$$

For actual applications, the mixing length is a function of spatial co-ordinates and the constants of proportionality in these cases can only be determined from experimental data.

Taylor pointed out that no physical reason justified the assumption of the conservation of momentum during the turbulent mixing process used by Prandtl. Instead, he suggested the use of the theorem of the conservation of vorticity or conservation of the momentum as a starting point upon which to build up a more adequate model for the mechanism of turbulent flows. On this basis, he developed the vorticity transport theory.

If the vorticity is assumed to be the transportable quantity, then:-

$$|w'| = \ell.\frac{d\bar{w}}{dy} \qquad \text{(A2.6)}$$

For parallel flow and neglecting the viscous term, Reynolds equation reduces to:-

$$\frac{dp}{dx} = -\rho\,\overline{v'w'} \qquad \text{(A2.7)}$$

Hence,

$$\frac{dp}{dx} = -\rho|v'|.\ell\,\frac{d\overline{w}}{dy}$$

leading to

$$\frac{dp}{dx} = -\rho|v'|\,\ell.\,\frac{d^2\overline{u}}{dy^2} \qquad \text{(A2.8)}$$

when the mixing length is independent of y, expression (A2.8) is identical to that obtained by using Prandtl's momentum transport theory. In general, these two theories give different results. Even in the case where the mean velocity distributions given by these two theories are the same, there is a difference between the temperature distribution for the two corresponding cases.

## APPENDIX 3. SOLUTIONS TO EQUATIONS OF MOTION

The equations of motion for a spherical entity moving in a turbulent fluid was given in section 3.1.4 as:-

$$\frac{dU}{dt} = - \frac{9\mu}{2\rho} \frac{1}{r^2} \left(U - y \frac{d\langle u \rangle}{dy}\right) \qquad \text{(A3.1)}$$

$$\frac{dV}{dt} = - \frac{9\mu}{2\rho} \cdot \frac{1}{r^2} \cdot V \qquad \text{(A3.2)}$$

$$\frac{dW}{dt} = - \frac{9\mu}{2\rho} \cdot \frac{1}{r^2} \cdot W \qquad \text{(A3.3)}$$

with initial conditions that $(U,V,W)_{\substack{y=0 \\ t=0}} = (Uo, Vo, Wo)$.

Equations (A3.2) and (A3.3) become:-

$$V = Vo.e^{\frac{-9\mu}{2\rho r^2}t}$$

$$W = Vo.e^{\frac{-9\mu}{2\rho r^2}t}$$

However, for steady flow, $\frac{dV}{dt} = V \frac{dv}{dy}$

$$\therefore \quad \frac{VdV}{dy} = - \frac{9\mu}{2\rho r^2} .V$$

$$\frac{dV}{dy} = - \frac{9\mu}{2\rho r^2}$$

$$V = - \frac{9\mu}{2\rho r^2} .y + C$$

$y=0$ gives $V = Vo$ implies $C = Vo$

$$\therefore \quad V = Vo - \frac{g\mu}{2\rho r^2} \cdot y$$

$$y = \frac{2\rho r^2}{g\mu} (Vo - V)$$

Hence, $$y = \frac{2\rho r^2}{g\mu} Vo \left(1 - e^{-\frac{g\mu}{2\rho r^2} t}\right) \qquad (A3,4)$$

As the minimum value of $e^{-\frac{g\mu}{2\rho r^2}t}$ is 0, there is a maximum value of y given by:-

$$y^* = \frac{2\rho r^2}{g\mu} . Vo \qquad (A3,5)$$

$$\therefore \quad y = y^* \left(1 - e^{-\frac{g\mu}{2\rho r^2} t}\right) \qquad (A3,6)$$

or $$e^{-\frac{g\mu}{2\rho r^2} t} = 1 - y/y^* \qquad (A3.7)$$

Equation (A3.1) becomes:-

$$\frac{dU}{dt} = -\frac{g\mu}{2\rho r^2} \left[ U - \frac{2\rho r^2}{g\mu} Vo \left(1 - e^{-\frac{g\mu}{2\rho r^2} t}\right) . \frac{d\langle u\rangle}{dy} \right]$$

$$= -\frac{g\mu}{2\rho r^2} U + Vo \frac{d\langle u\rangle}{dy} \left(1 - e^{-\frac{g\mu}{2\rho r^2} t}\right)$$

$$\therefore \quad \frac{dU}{dt} + \frac{g\mu}{2\rho r^2} U = Vo \frac{d\langle u\rangle}{dy} - Vo \frac{d\langle u\rangle}{dy} . e^{-\frac{g\mu}{2\rho r^2} t} \qquad (A3.8)$$

Since the ordinary differential equation $\frac{dy}{dx} + P(x)y = Q(x)$ gives the solution of the form

$$y . e^{\int P dx} = \int Q . e^{\int P dx} dx + C \qquad (A.3.9)$$

Therefore equation (A3.8) becomes:-

$$Ue^{\frac{g\mu}{2\rho r^2} t} = \int \left(Vo \frac{d\langle u\rangle}{dy} e^{\frac{g\mu}{2\rho r^2} t} - Vo \frac{d\langle u\rangle}{dy}\right) dt + C$$

$$= Vo \frac{d\langle u\rangle}{dy} \cdot \frac{2\rho r^2}{9\mu} e^{\frac{9\mu}{2\rho r^2} t} - Vo \frac{d\langle u\rangle}{dy} t + C$$

$t = 0$ gives $U = Uo$ implies

$$C = Uo - Vo \frac{d\langle u\rangle}{dy} \cdot \frac{2\rho r^2}{9\mu}$$

$$\therefore \quad U = Uo\, e^{-\frac{9\mu}{2\rho r^2} t} - Vo \frac{d\langle u\rangle}{dy} \frac{2\rho r^2}{9\mu} \left( e^{-\frac{9\mu}{2\rho r^2} t} - 1 \right) -$$

$$- Vo \frac{d\langle u\rangle}{dy} t.e^{\frac{9\mu}{2\rho r^2} t}$$

As $e^{-\frac{9\mu}{2\rho r^2} t} = 1 - y/y^*$

$$-\frac{9\mu}{2\rho r^2} t = \ell n\, (1 - y/y^*)$$

and $$t = -\frac{2\rho r^2}{9\mu} .\ell n\, (1 - y/y^*)$$

$$\therefore \quad U = Uo\, (1 - y/y^*) + Vo \frac{d\langle u\rangle}{dy} \cdot \frac{2\rho r^2}{9\mu} \cdot \frac{y}{y^*}$$

$$+ \quad Vo \frac{d\langle u\rangle}{dy} (1 - y/y^*) \cdot \frac{2\rho r^2}{9\mu} .\ell n\, (1 - y/y^*)$$

As $Vo \frac{2\rho r^2}{9\mu} = y^*$

$$U = Uo\, (1 - y/y^*) + y \cdot \frac{d\langle u\rangle}{dy} + y^* \frac{d\langle u\rangle}{dy} (1 - y/y^*) .\ell n\, (1 - y/y^*)$$

As $y^*$ represents the mathematical maximum value of $y$, it would be more appropriate to look at the physical maximum of $y$. By considering the mean distance that an entity travels from the plane $y = 0$ before its momentum is entirely dissipated, $\lambda^*$ may be put in place of $y^*$. Hence, the solutions to equations of motion (A3.1) to (A3.3) may be expressed as:-

$$U = U_o\,(1 - y/\lambda^*) + \frac{d\langle u\rangle}{dy}\left[\, y + \lambda^*\,(1 - y/\lambda^*)\,\ell n\,(1 - y/\lambda^*)\right] \qquad \text{(A3.10)}$$

$$V = V_o\,(1 - y/\lambda^*) \qquad \text{(A3.11)}$$

$$W = W_o\,(1 - y/\lambda^*) \qquad \text{(A3.12)}$$

## APPENDIX 4. SOLUTIONS TO THE EQUATION OF THERMAL ENERGY TRANSPORT

The equation of thermal energy transport for a spherical entity moving in a turbulent fluid was given in section 3.1.5 as:-

$$\frac{dT}{dt} = - \frac{3\,k}{\rho Cp} \frac{1}{r^2} \left(T - y \frac{d<Tf>}{dy}\right) \qquad (A4.1)$$

with initial condition that $T_{y=0,\ t=0} = To$.

Using equation (A3.6) in Appendix 3, and putting $a = \frac{3\,k}{\rho Cp r^2}$ and $b = \frac{9\mu}{2\rho r^2}$, the above equation becomes:-

$$\frac{dT}{dt} = - a\left[ T - y^* \left(1 - e^{-bt}\right) \frac{d<Tf>}{dy} \right]$$

$$= - a\,T + a y^* \frac{d<Tf>}{dy} \left(1 - e^{-bt}\right)$$

$$\therefore \quad \frac{dT}{dt} + aT = a\, y^* \frac{d<Tf>}{dy} \left(1 - e^{-bt}\right) \qquad (A4.2)$$

Using the standard result of (A3.9), the solution of the above equation becomes:-

$$T.e^{at} = \int a\, y^* \frac{d<Tf>}{dy} e^{at} \left(1 - e^{-bt}\right) dt + C$$

$$= a\, y^* \frac{d<Tf>}{dy} \cdot \frac{1}{a} e^{at} - a\, y^* \frac{d<Tf>}{dy} \frac{1}{(a-b)} e^{(a-b)t} + C$$

$$= y^* \frac{d<Tf>}{dy} \left[e^{at} - \left(\frac{a}{a-b}\right) e^{(a-b)t}\right] + C$$

t=0 gives T=0 implies:-

$$C = To - y^* \frac{d<Tf>}{dy} \left[ 1 - \left(\frac{a}{a-b}\right)\right]$$

$$= To + y^* \frac{d<Tf>}{dy} \left(\frac{b}{a-b}\right)$$

$$\therefore \quad T.e^{at} = y^* \frac{d<Tf>}{dy}\left[ e^{at} - \left(\frac{a}{a-b}\right)e^{(a-b)t}\right] + To + y^* \frac{d<Tf>}{dy} \left(\frac{b}{a-b}\right)$$

$$\text{or} \quad T = y^* \frac{d<Tf>}{dy}\left[ 1 - \left(\frac{a}{a-b}\right)e^{-bt} + \left(\frac{b}{a-b}\right)e^{-at}\right] + To\, e^{-at}$$

$$= y^* \frac{d<Tf>}{dy} + y^* \frac{d<Tf>}{dy}\left[\left(\frac{b}{a-b}\right)e^{-at} - \left(\frac{a}{a-b}\right)e^{-bt}\right] + To\, e^{-at}$$

However, equation (A3.6) implies $y^* = y + y^* e^{-bt}$

$$\therefore \quad T = y \frac{d<Tf>}{dy} + y^* \frac{d<Tf>}{dy}\left[ \left(\frac{b}{a-b}\right)e^{-at} + e^{-bt} - \left(\frac{a}{a-b}\right)e^{-bt}\right] + To\, e^{-at}$$

$$= y \frac{d<Tf>}{dy} + y^* \frac{d<Tf>}{dy}\left[ \left(\frac{b}{a-b}\right)e^{-at} - \left(\frac{b}{a-b}\right)e^{-bt}\right] + To\, e^{-at}$$

$$= y \frac{d<Tf>}{dy} + y^* \frac{d<Tf>}{dy} \left(\frac{b}{a-b}\right)(e^{-at} - e^{-bt}) + To\, e^{-at}$$

As $y^* = \frac{2\rho r^2}{9\mu}$ . $Vo = \frac{Vo}{b}$

Hence $$T = y. \frac{d<Tf>}{dy} + \frac{Vo}{a-b}. \frac{d<Tf>}{dy}(e^{-at} - e^{-bt}) + To\, e^{-at}$$

Since $e^{-bt} = (1 - y/y^*)$, it may be deduced that $e^{-at} = (1 - y/y^*)^{a/b}$. Therefore, the above equation becomes:-

$$T = To\,(1 - y/y^*)^{a/b} + y. \frac{d<Tf>}{dy} + \frac{Vo}{(a-b)}. \left[ (1 - y/y^*)^{a/b} - (1 - y/y^*)\right]\frac{d<Tf>}{dy} \qquad (A4.3)$$

Again, considering the mean distance that an entity travels from the plane y=0 before its thermal energy is entirely dissipated, $\lambda^*$ may be put in place in $y^*$. Hence, the solution to the equation of thermal energy transport (A4.1) may be expressed as:-

$$T = To\,(1 - y/\lambda^*)^{a/b} + y \frac{d<Tf>}{dy} + \frac{Vo}{(a-b)}\left[ (1 - y/\lambda^*)^{a/b} - (1 - y/\lambda^*)\right]\frac{d<Tf>}{dy} \qquad (A4.4)$$

where $a = \frac{3\,k}{\rho Cpr^2}$ and $b = \frac{9\mu}{2\rho r^2}$ .

## APPENDIX 5. JAYNES' FORMALISM OF INFORMATION THEORY

As Jaynes' formalism of information theory and statistical mechanics gave good estimates for the probabilities of random variables, the method of application is summarised as follows:-

(a) Enumerate each microstate and assign a symbol for its probability.

(b) Enumerate what is known about the "averages" associated with the system.

(c) Express the averages in the form of equations, as follows:-

$$\langle g_r \rangle = \sum_i p_i g_r(x_i) = \int_{-\infty}^{\infty} p_i g_r(x_i) di \qquad (A5.1)$$

where x is a property that serves to identify a state and $x_i$ is the value of x identified with state i. $g_r(x)$ is a function of x. $\langle g_r \rangle$ is a known average.

(d) Making use of the equations that represent the averages and the additional equation,

$$\sum_i p_i = \int_{-\infty}^{\infty} p_i d_i = 1$$

(e) Maximise the entropy

$$S = K.\sum_i p_i \ln p_i = -K \int_{-\infty}^{\infty} p_i \ln p_i \, d_i$$

(f) The resulting probability distribution is thus given by:-

$$p_i = \exp\left[ - \alpha - \beta_r g_r(x_i) \right]$$

(g) The "zeroth" Langrangian multiplier is given by:-

$$\alpha = \ln\left\{ \sum_i \exp\left[ -\beta_r g_r(x_i) \right] \right\} = \ln \left\{ \int_{-\infty}^{\infty} e^{-\beta_r g_r(x_i)} d_i \right\}$$

(h) The expected values, $\langle g_r \rangle$ are given by:-

$$\langle g_r \rangle = - \frac{\partial \alpha}{\partial \beta_r}$$

(i) The variance in $g_r$ is given by:-

$$\sigma^2(g_r) = \frac{\partial^2 \alpha}{\partial \beta_r^2}$$

(j) The entropy or uncertainty is given by:-

$$S_{max} = K.\alpha + K.\sum_r \beta_r \langle g_r \rangle = K.\alpha + K. \int_{-\infty}^{\infty} \beta_r \langle g_r \rangle \, dr$$

(k) If the function $g_r$ (but not $g_1, g_2, \ldots g_{r-1}, g_{r+1}$) depends upon another parameter, say Y, i.e.

$g_r = g_r(X,Y)$, then

$$\left\langle \frac{\partial g_r}{\partial Y} \right\rangle = \frac{1}{\beta_r} \frac{\partial \alpha}{\partial Y}$$

As indicated by Tribus {126} that there was no way of proving Jaynes' formalism, it should be taken as an axiom for a system of inductive logic. It represents the best that one can do under the rules for rational thinking that have been postulated. If the output conclusions do not agree with observations, one is forced to conclude that the input information is incorrect. If the output information is vague, one concludes that the input data are insufficient. If the output conclusions are correct, it may then be concluded that the input data are sufficient for estimating the probability distributions of random variables.

## APPENDIX 6. CORRECTION OF LASER DOPPLER ANEMOMETER READINGS DUE TO REFRACTION

Consider the laser beams from the optical unit of the LDA entering the perspex working section as shown in Figure A6.1. From the figure,

$$AP = \frac{a}{2} - b \tan i_1 \quad ,$$

$$= \frac{a}{2} - b \tan \frac{\Theta}{2}$$

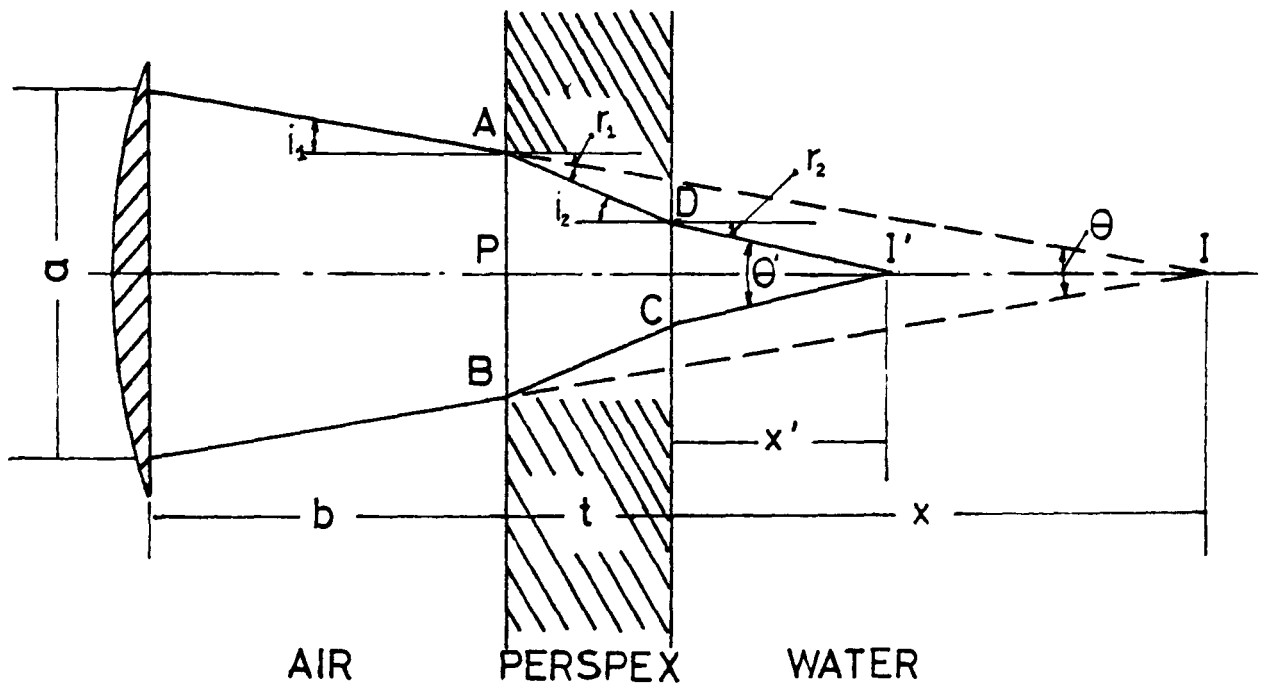


Figure A6.1 REFRACTION OF LASER BEAMS

$$DQ = x \tan r_2$$

$$= x \tan \frac{\Theta'}{2}$$

However, AP may also be expressed as:-

$$AP = t.\tan i_2 + DQ$$

Hence, $t.\tan i_2 + x \tan \frac{\Theta'}{2} = \frac{a}{2} - b \tan \frac{\Theta}{2}$ (A6.1)

$$x \tan \frac{\Theta'}{2} = \frac{a}{2} - b \tan \frac{\Theta}{2} - t \tan i_2$$

$$\therefore \quad x = (\frac{a}{2} - b \tan \frac{\Theta}{2} - t \tan i_2)/ \tan \frac{\Theta'}{2} \quad \text{(A6.2)}$$

$$\text{or} \quad x = (\frac{a}{2} - t \tan i_2)/\tan \frac{\Theta'}{2} - b. \frac{\tan \frac{\Theta}{2}}{\tan \frac{\Theta'}{2}}, \quad \text{(A6.3)}$$

For a particular beam separation distance, a and $\Theta$ are constants. t is also constant as it is the thickness of the perspex pipe wall.

When the optical unit (lens) is moved a distance $\delta b$ towards the pipe, the corresponding distance moved by the intersection point away from the pipe wall is thus $\delta x$. As equation (A6.3) relates the distance of the optical unit from the outer pipe wall to the distance of the intersection point from the inner pipe wall, the following expression holds:-

$$(x + \delta x) = (\frac{a}{2} - t \tan i_2)/\tan \frac{\Theta'}{2} - (b - \delta b) \frac{\tan \frac{\Theta}{2}}{\tan \frac{\Theta'}{2}},$$

(A6.4)

Equations (A6.3) and (A6.4) give:-

$$\delta x = \frac{\delta b \cdot \tan \frac{\Theta}{2}}{\tan \frac{\Theta'}{2}} \quad \text{(A6.5)}$$

However, when light beam travels from one medium with refractive index $n_1$ into another medium with refractive index $n_2$, the following relation holds:-

$$\eta_1 \sin I = \eta_2 \sin R$$

where I and R are the angles of incidence and refraction respectively. Hence,

$$\eta_a \sin i_1 = \eta_p \sin r_1 \qquad \text{(A6.6)}$$

$$\eta p \sin i_2 = \eta_w \sin r_2 \qquad \text{(A6.7)}$$

where a, p and w denote air, perspex and water respectively. As $i_2 = r_1$ , equations (A6.6) and (A6.7) give:-

$$\eta_a \sin i_1 = \eta_w \sin r_2$$

or $$\eta_a \sin \frac{\Theta}{2} = \eta_w \sin \frac{\Theta'}{2}$$

$$\therefore \quad \frac{\Theta'}{2} = \sin^{-1}\left[\frac{\eta_a}{\eta_w} \sin \frac{\Theta}{2}\right]$$

$$\tan \frac{\Theta'}{2} = \tan\left[\sin^{-1}\left(\frac{\eta_a}{\eta_w} \sin \frac{\Theta}{2}\right)\right] \qquad \text{(A6.8)}$$

Therefore, equation (A6.5) becomes:-

$$\delta x = \delta b. \tan \frac{\Theta}{2} . \cot\left[\sin^{-1}\left(\frac{\eta_a}{\eta_w} \sin \frac{\Theta}{2}\right)\right]$$

As $\eta_a$ and $\eta_w$ may generally be expressed as 1 and 1.33 respectively,

Hence, $$\delta x = \delta b . \tan \frac{\Theta}{2} . \cot\left[\sin^{-2}\left(\frac{1}{1.33} \sin \frac{\Theta}{2}\right)\right] \qquad \text{(A6.9)}$$

In addition, as the formula $V = \frac{f_D . \lambda_a}{2\sin\frac{\Theta}{2}}$ is only valid for measurements in air (vacuum).

For measurements in water as shown in Figure (A6.1), the velocity may be expressed as:-

$$V = \frac{f_D.\lambda_w}{2\sin\frac{\Theta'}{2}} \qquad \text{(A6.10)}$$

However, the laws of refraction are given by:-

$$\lambda_a.\eta_a = \lambda_p.\eta_p = \lambda_w.\eta_w$$

and $\eta_a.\sin\frac{\Theta}{2} = \eta_p.\sin r_1 = \eta_w.\sin\frac{\Theta'}{2}$

Equation (A6.10) becomes:-

$$V = \frac{f_D.\lambda_a.\eta_a/\eta_w}{2\sin\frac{\Theta}{2}.\eta_a/\eta_w}$$

Hence, $V = \frac{f_D.\lambda_a}{2\sin\frac{\Theta}{2}}$ (A6.11)

where $\frac{\Theta}{2}$ is the half intersection angle of the laser beam before introducing into the flow.

## APPENDIX 7. PROGRAM TO ESTABLISH THE OPTIMUM SAMPLE SIZE

```
00100   REM  ***   PROGRAM TO TEST CONVERGENCE OF RESULTS   ***
00200   DIM A(600),Z(1200)
00300   PRINT "INPUT AMBIENT TEMPERATURE IN DEGREE C."
00400   INPUT T
00500   REM  ***   CALCULATE THE VISCOSITY OF WATER   ***
00600   REM  ***       FROM TEMPERATURE READING       ***
00700   REM
00800   X=((2*((273.15+T)/273.15))-2.3661)/.366099
00900   N6=(.352*X**8)-(.533*X**7)+(.124*X**6)-(.357*X**5)
01000   N7=(1.231*X**4)-(2.044*X**3)+(3.161*X**2)-(4.581*X)
01100   N=(N6+N7+5.478)*1E-7
01200   PRINT "INPUT FREQ. RANGE,TAN T/2,PIPE DIA.,V CONSTANT"
01300   INPUT F,R,P,V
01400   PRINT "NO. OF SAMPLES    U (M/S)     T.I. (%)      RE."
01500   FOR I=1 TO 15
01600   B=0
01700   G=0
01800   REM  ***   COMMENCE SAMPLING   ***
01900   CALL "USE"(A)
02000   CALL "RTS"(A,0,1,1200,2)
02100   CALL "SETR"(3,1,4)
02200   FOR J=0 TO 1199
02300   CALL "RDB"(A,Z(J))
02400   IF Z(J)>0 THEN 2700
02500   IF Z(J)=-2 THEN 2800
02600   PRINT "BAD DATA AT EVENT";J
02700   B=B+Z(J)
02800   NEXT J
02900   C=B/1200
03000   K=(.0209049*C)-10.7307
03100   REM  ***   CALCULATE THE STANDARD DEVIATION   ***
03200   FOR J=0 TO 1199
03300   E2=E1-K
03400   E3=E2**2
03500   G=G+E3
03600   NEXT J
03700   H=SQR(G/1200)
03800   REM  ***   DEDUCE MEAN VELOCITY, TURBULENCE   ***
03900   REM  ***    INTENSITY AND REYNOLDS NUMBER     ***
04000   U1=H/K*100
04100   U1=(K*F/V*632.8E-7)/(2*SIN(ATN(R))
04200   S1=H/K*100
04300   U2=U2+U1
04400   S2=S2+S1
04500   U=U2/I
04600   S=S2/I
04700   R=U*P/N
04800   PRINT L*1200,U,S,R
04900   NEXT I
00100   END
```

## APPENDIX 8. PROGRAM TO CALCULATE MEAN VELOCITY FROM 12,000 SAMPLES USING THE ENSEMBLED OR TIME AVERAGED TECHNIQUE

```
00100   REM  ***   PROGRAM TO CALCULATE MEAN VELOCITY   ***
00200   PRINT "INPUT VOLTAGE OF T1"
00300   INPUT T1
00400   T1=-.218622*(T1**2)+17.2125*T1-.370868
00500   X=((2*((273.15+T1)/273.15))-2.3661)/.366099
00600   N6=(.352*X**8)-(.533*X**7)+(.124*X**6)-(.357*X**)
00700   N7=1.231*X**4)-(2.044*X**3)+(3.161*X**2)-(4.581*X)
00800   N1=(N6+N7+5.478)*1E-7
00900   C7=.011446*(T1**2)-.85239*T1+4194.73
01000   K1=(T1+273.15)/273.15
01100   K2=2839.5*K1-1800.7*(K1**2)
01200   K3=525.77*(K1**3)-73.44*(K1**4)
01300   K4=(K3+K2-922.47)/1000
01400   P9=N1*1000*C7/K4
01500   PRINT T1,N1,P9,C7,K4
01600   PRINT "FREQ. RANGE,TAN T/2,PIPE DIA.,V CONSTANT"
01700   INPUT M,R,F1,N
01800   Y1=0
01900   Y2=0
02000   Y3=0
02100   DIM A(600),Z(1200),D(1200)
02200   FOR K1=1 TO 10
02300   CALL "USE"(A)
02400   CALL "RTS"(A,0,1,1200,2)
02500   CALL "SETR"(3,1,4)
02600   FOR I=0 TO 1199
02700   CALL "RDB"((A,Z(I))
02800   IF Z(I)>0 THEN 3100
02900   IF Z(I)=-2 THEN 3200
03000   PRINT "BAD DATA AT EVENT";I
03100   B=B+Z(I)
03200   NEXT I
03300   C=B/1200
03400   K=(.0209049*C)-10.7307
03500   P=K*M/N
03600   S=ATN(R)
03700   T=(P*632.8E-7)/(2*SIN(S))
03800   FOR I=0 TO 1199
03900   E1=(.0209049*Z(I))-10.7307
04000   E2=E1-K
04100   F=E2**2
04200   G=G+F
04300   D(I)=E2
04400   NEXT I
```

```
04500    H=G/1200
04600    J=SQR(H)
04700    W=J*100/K
04800    L4=T*F1/N1
04900    PRINT "MEAN VELOCITY IS                    ";T;"M/S"
05000    PRINT "TURBULENCE INTENSITY IS             ";W;"%"
05100    PRINT "CENTRE LINE REYNOLDS NUMBER IS ";L4
05200    PRINT
05300    B=0
05400    G=0
05500    Y1=Y1+T
05600    Y2=Y2+W
05700    Y3=Y3+L4
05800    NEXT K1
05900    Y1=Y1/10
06000    Y2=Y2/10
06100    Y3=Y3/10
06200    PRINT "ENSEMBLE AVERAGED RESULTS FOR 12000 SAMPLES:-"
06300    PRINT
06400    PRINT "          MEAN VELOCITY =";Y1;"M/S"
06500    PRINT "    TURBULENCE INTENSITY =";Y2;"%"
06600    PRINT "       FLOW REYNOLDS NO. =";Y3
06700    END
```

## APPENDIX 9. SUBROUTINE FOR THE INFLEXION COUNTING TECHNIQUE

```
00100   REM  *** INFLEXION COUNTING SUBPROGRAM   ***
00200   P2=0
00300   G1=H*F/V
00400   G2=G1*6.328E-7/2*SIN(ATN(P))
00500   FOR I=0 TO 1197
00600   B1=Z(I+1)-Z(I)
00700   B2(Z(I+2)-Z(I+1)
00800   P1=SGN(B1)+SGN(B2)
00900   IF P1=-2 THEN 1200
01000   IF P1=2 THEN 1200
01100   P2=P2+1
01200   NEXT I
01300   P4=P2/.48
01400   RETURN
```

## APPENDIX 10. PROGRAM TO DERIVE A POLYNOMIAL FOR EACH THERMOCOUPLE

```
00100    REM  ***   PROGRAM TO FIT BEST POLYNOMIAL   ***
00200    DIM T(22)
00300    PRINT "WHICH THERMOCOUPLE ?"
00400    INPUT P
00500    FOR I=1 TO 22
00600    READ T(I)
00700    NEXT I
00800    N=22
00900    A1=N\A2=0\A3=0
01000    B1=0\B2=0\B3=0
01100    C1=0\C2=0\C3=0
01200    D1=0\D2=0\D3=0
01300    FOR I=1 TO 22
01400    READ X
01500    A2=A2+X
01600    A3=A3+(X**2)
01700    B1=B1+X
01800    B2=B2+(X**2)
01900    B3=B3+(X**3)
02000    C1=C1+(X**2)
02100    C2=C2+(X**3)
02200    C3=C3+(X**4)
02300    Y=T(I)
02400    D1=D1+Y
02500    D2=D2+(Y*X)
02600    D3=D3+(Y*(X**2))
02700    NEXT I
02800    E1=((B2*C3)-(B3*C2))*A1
02900    E2=((B1*C3)-(B3*C1))*A2
03000    E3=((B1*C2)-(B2*C1))*A3
03100    E4=E1-E2+E3
03200    F1=((B3*D3)-(D2*C3))*A2
03300    F2=((B2*D3)-(D2*C2))*A3
03400    F3=((B2*C3)-(B3*C2))*D1
03500    E5=F1-F2+F3
03600    S1=E5/E4
03700    G1=((B3*D3)-(D2*C3))*A1
03800    G2=((B1*D3)-(D2*C1))*A3
03900    G3=((B1*C3)-(B3*C1))*D1
04000    E6=-G1+G2-G3
04100    S2=E6/E4
04200    H1=((B2*D3)-(D2*C2))*A1
04300    H2=((B1*D3)-(D2*C1))*A2
04400    H3=((B1*C2)-(B2*C1))*D1
04500    E7=H1-H2+H3
04600    S3=E7/E4
04700    PRINT "POLYNOMIAL FOR THERMOCOUPLE NO.";P;"IS"
04800    PRINT
04900    PRINT "T = ";S3;"V**2 + ";S2;"V + ";S1
05000    PRINT
05100    END
```

## APPENDIX 11. THEORETICAL PREDICTION OF TEMPERATURE LOSS ALONG INJECTION TUBE

A simplified model of the actual temperature variation may be assumed to be as illustrated in Figure A10.1. The heat transfer process on the inside of the tube may be assumed to be satisfied by the empirical equation as:-

$$Nu = 0.0155.Pr^{0.5}\ Re^{0.83} \qquad (A11.1)$$

Hence, the heat transfer coefficient on the inner surface of the tube is $h = \frac{Nu.\alpha}{2r_1}$

$$\text{or } h_{in} = \frac{0.00775 Pr^{0.5}\ Re^{0.83}.}{r_1} \qquad (A11.2)$$

where $r_1$ is the internal radius of the tube.

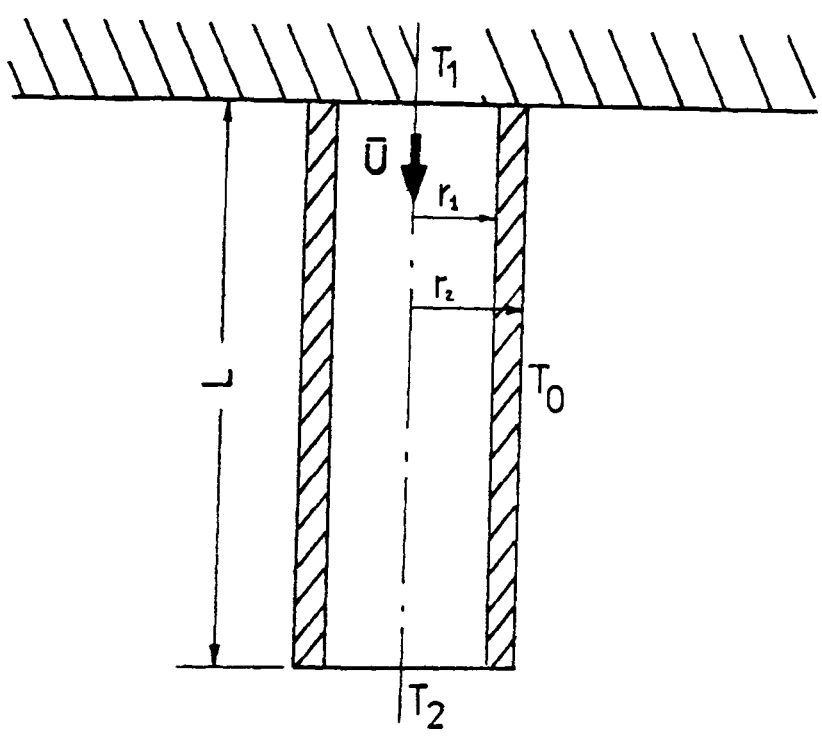


Figure 11.1 SIMPLIFIED MODEL OF INJECTION TUBE

On the other surface of the tube, it becomes an external flow situation. Hence, the above heat transfer coefficient is not expected to be valid. The heat transport similarity parameter however may be assumed to be:-

$$Nu = 0.193 \times Pr^{0.33} . Re^{0.618}$$

Again, this is an empirical formula quoted by Reynolds & Perkins {50}. The heat transfer coefficient on the outer surface may therefore be expressed as:-

$$h_{out} = \frac{0.0965\ Pr^{0.33} . Re^{0.613}}{r_2} \qquad (A11.3)$$

where $r_2$ is the half the outside diameter of the tube.

With the overall heat transfer process, Kay & Nedderman {44} suggested that the temperature distribution could be represented by:-

$$(T_2 - T_o) = (T_1 - T_o).\exp.(- \frac{h}{mCp} .\pi DL) \qquad (A11.4)$$

where D could be taken as $2r_1$, L being the total length of the injection tube, m being the mass flow rate of the injector and h being the overall heat transfer coefficient which could be expressed as:-

$$\frac{1}{h} = \frac{1}{h_{in}} + \frac{r_1}{k} \ln(\frac{r_2}{r_1}) + \frac{r_1}{r_2} . \frac{1}{h_{out}} \qquad (A11.5)$$

The middle term on the right in equation (A11.5) represents the conduction term across the injection tube wall. Hence, k is the thermal conductivity of the stainless steel hypodermic tube.

Therefore, the actual temperature of the injection fluid at the point of injection may be expressed as:-

$$T_2 = T_o + (T_1 - T_o) e^{(- \frac{h}{mCp} \pi DL)} \qquad (A11.6)$$

where $T_1$ is the temperature of injection fluid at the upstream end of the injection tube, $T_o$ is the ambient temperature of the main fluid stream and m may be expressed as:-

$$m = \rho . \frac{\pi . D^2}{4} . U \qquad (A11.7)$$

## APPENDIX 12. PROGPAM TO EVALUATE THE EDDY DIFFUSIVITY OF HEAT FROM THERMOCOUPLE READINGS

```
00100    REM  ***   PROGRAM FOR THE PROCESSING OF    ***
00200    REM  ***         THERMOCOUPLE READINGS      ***
00300    DIM T(14),V(14),H(14),R(10),E(10)
00400    DIM X5(10)
00500    DIM G6(10,11),X6(40),Y6(40),O6(20)
00600    DIM B6(20),C6(20),H1(14),S1(14)
00700    DIM E7(14)
00800    READ A7,T9
00900    READ D,J,J1,L
01000    READ K9
01100    FOR K=1 TO T9-2
01200    READ X5(K)
01300    NEXT K
01400    FOR A9=1 TO A7
01500    READ R9,M
01600    READ U,U9
01700    PRINT R9
01800    PRINT "RUN NO.  ",R9
01900    PRINT "VELOCITY OF JET IS ";U;"M/S"
02000    PRINT "VELOCITY OF MAIN FLOW IS  ";U9;"M/S"
02100    C3=U*J*J/16
02200    A=0
02300    R8=0
02400    N8=0
02500    P8=0
02600    P9=0
02700    FOR A8=1 TO M
02800    FOR I=1 TO A9
02900    READ V(I)
03000    NEXT I
03100    T(1)=-.218622*V(1)**2+17.2125*V(1)-.370868
03200    T(2)=-.220018*V(2)**2+17.2620*V(2)-.451493
03300    T(3)=-.211522*V(3)**2+17.1575*V(3)-.307668
03400    T(4)=-.218163*V(4)**2+17.2232*V(4)-.417665
03500    T(5)=-.210146*V(5)**2+17.1660*V(5)-.318308
03600    T(6)=-.218138*V(6)**2+17.2077*V(6)-.342309
03700    T(7)=-.208166*V(7)**2+17.1485*V(7)-.193740
03800    T(8)=0
03900    T(9)=-.207287*V(9)**2+17.1727*V(9)-.343504
04000    T(10)=-.215007*V(10)**2+17.2124*V(10)-.467030
04100    T(11)=-.212972*V(11)**2+17.2206*V(11)-.471656
04200    T(12)=-.220443*V(12)**2+17.2473*V(12)-.473862
04300    T(13)=0
04400    T(14)=-.218622*V(14)**2+17.2125*V(14)-.370868
04500    I=1
04600    X=((2*((273.15+T(I))/273.15))-2.3661)/.366099
04700    N6=(.352*X**8)-(.533*X**7)+(.124*X**6)-(.357*5**5)
04800    N7=(1.231*X**4)-(2.044*X**3)+(3.161*X**2)-(4.581*X)
```

```
04900    N=(N6+N7+5.478)*1E-7
05000    C7=.011446*T(I)**2-.85239*T(I)+4149.73
05100    K1=(T(I)+273.15)/273.15
05200    K2=2839.5*K1-1800.7*(K1**2)
05300    K3=525.77*(K1**3)-73.44*(K1**4)
05400    K=(K3+K2-922.47)/1000
05500    P=N*1000*C7/K
05600    F=N/P
05700    R1=J*U/N
05800    N1=.0155*R1**.83*P**.33
05900    HE=N2*K/J1
06000    H3=J/K9*LOG(J1/J)
06100    H4=1/((1/H1)+(J/J1/H2)+H3
06200    J2=J
06300    M1=1000*U*3.14159*J2*J2/4
06400    E1=-H4*3.14159*J2*L/M1/C7
06500    T2=T(2)
06600    T(2)=T(1)+(T(2)-T(1))*EXP(E1)
06700    H(I)=T(2)-T(1)
06800    FOR I=2 TO T9-1
06900    H(I)=T(I+1)-T(1)
07000    NEXT I
07100    FOR I=1 TO T9-2
07200    R(I)=H(I)/H(I+1)
07300    NEXT I
07400    REM  ***   LEAST SQUARE ROUTINE   ***
07500    F6=0
07600    D6=1
07700    N6=T9-2
07800    N4=N6-1
07900    FOR K=0 TO 14
08000    X6(K)=X5(K+1)
08100    Y6(K)=R(K+1)
08200    NEXT K
08300    FOR I6=0 TO 2*D6:C6(I6)=0:NEXT
08400    FOR I6=0 TO D6:B6(I6)=0:NEXT
08500    FOR K6=0 TO N4:S6=1
08600    FOR I6=0 TO 2*D6:C6(I6)=C6(I6)+S6
08700    IF I6<=D6 THEN B6(I6)=B6(I6)+S6*Y6(K6)
08800    S6=S6*X6(K6):NEXT I6:NEXT K6
08900    FOR I6=0 TO D6:FOR J6=0 TO D6
09000    G6(I6,J6)=C6(I6+J6):NEXT J6:G6(I6,D6+1)=B6(I6)
09100    NEXT I6
09200    FOR I6=0 TO D6-1
09300    FOR J6=I6+1 TO D6:IF G6(J6,I6)=0 THEN 9800
09400    FOR K6=I6+1 TO D6
09500    G6(J6,K6)=G6(J6,K6)-G6(I6,K6)*G6(J6,I6)/G6(I6,I6)
09600    NEXT K6
09700    G6(J6,D6+1)=G6(J6,D6+1)-G6(I6,D6+1)*G6(J6,I6)/G6(I6,I6)
```

```
09800    NEXT J6:NEXT I6
09900    O6(D6)=G6(D6,D6+1)/G6(D6,D6)
10000    FOR I6=0 TO D6-1:K6=D6-I6-1:L6=K6+1
10100    FOR J6=L6 TO D6
10200    G6(K6,D6+1)=G6(K6,D6+1)-O6(J6)*G6(K6,J6)
10300    NEXT J6
10400    O6(K6)=G6(K6,D6+1)/G6(K6,K6)
10500    NEXT I6
10600    S7=0
10700    FOR K6=0 TO N4
10800    S6=1
10900    Z6=0
11000    FOR I6=0 TO D6
11100    Z6=Z6+O6(I6)*S6
11200    S6=S6*X6(K6)
11300    NEXT I6
11400    E6(K6)=Z6-Y6(K6)
11500    E7(K6)=E6(K6)**2
11600    S7=S7+E7(K6)
11700    NEXT K6
11800    S9=S7/(N6-2)
11900    IF S9<1.0 THEN 12800
12000    IF (ABS(E6(0)/Y6(0))+ABS(E6(N4)/Y6(N4)))<.1 THEN 12800
12100    N4=N4-1
12200    IF E7(0)<E7(N4+1) THEN 8300
12300    FOR K=0 TO N4
12400    X6(K)=X6(K+1)
12500    Y6(K)=Y6(K+1)
12600    NEXT K
12700    GOTO 8300
12800    H1(A8)=C3*O6(1)-F
12900    R7=U9*D/N
13000    A=A+H1(A8)
13100    R8=R8+R7
13200    P8=P8+P
13300    NEXT A8
13400    A=A/M
13500    R8=R8/M
13600    P8=P8/M
13700    P9=R8*P8
13800    N8=N2*P8
13900    PRINT "          EDDY DIFFUSIVITY IS ";A;"M**2/S"
14000    PRINT "           REYNOLDS NUMBER IS ";R8
14100    PRINT "      N-D FACTOR FOR HEAT IS ";N8
14200    PRINT "            PRANDTL NUMBER IS ";P8
14300    PRINT "             PECLET NUMBER IS ";P9
14400    NEXT A9
14500    END
```

## APPENDIX 13. PROGRAM FOR ON-LINE SAMPLING AND PROCESSING OF VELOCITY, TURBULENCE INTENSITY, MICROSCALE AND EDDY DIFFUSIVITY OF MOMENTUM AND HEAT

```
00100   REM  ***   PROGRAM FOR ON-LINE SAMPLING AND   ***
00200   REM  ***       PROCESSING OF LDA READINGS     ***
00300   PRINT "INPUT VOLTAGE OF T1"
00400   INPUT T1
00500   T2=-.216324*(T1**2)+17.1919*T1-.330355
00600   X=((2*((273.15+T2)/273.15))-2.3661)/.366099
00700   N6=(.352*X**8)-(.533*X**7)+(.124*X**6)-(.357*X**5)
00800   N7=(1.231*X**4)-(2.044*X**3)+(3.161*X**")-(4.581*X)
00900   N1=(N6+N7+5.478)*1E-7
01000   C7=>011446*(T2**2)-.85239*T2+4194.73
01100   K1=(T2+273.15)/273.15
01200   K2=2839.5*K1-1800.7*(K1**2)
01300   K3=525.77*(K1**3)-73.44*(K1**4)
01400   K4=(K3+K2-922.47)/1000
01500   P9=N1*1000*C7/K4
01600   PRINT T2,N1,P9,C7,K4
01700   PRINT "INPUT FREQ. RANGE,TAN T/2,PIPE DIA.,V CONSTANT"
01800   INPUT M,R,F1,N
01900   Y1=0\Y2=0\Y3=0\Y4=0\Y5=0\Y6=0\Y7=0\Y8=0
02000   DIM A(600),Z(1200),D(1200)
02100   FOR K1=1 TO 10
02200   CALL "USE"(A)
02300   CALL "RTS"(A,0,1,1200,2)
02400   CALL "SETR"(3,1,4)
02500   FOR I=0 TO 1199
02600   CALL "RDB"(A,Z(I))
02700   IF Z(I)>0 THEN 3000
02800   IF Z(I)=-2 THEN 3100
02900   PRINT "BAD DATA AT EVENT";I
03000   B=B+Z(I)
03100   NEXT I
03200   C=B/1200
03300   K=(.0209049*C)-10.7307
03400   P=K*M/N
03500   S=ATN(R)
03600   T=(P*6.328E-7)/(2*SIN(S))
03700   FOR I=0 TO 1199
03800   E1=(.0209049*Z(I))-10.7307
03900   E2=E1-K
04000   F=E2**2
04100   G=G+F
04200   D(I)=E2
04300   NEXT I
04400   H=G/1200
04500   J=SQR(H)
04600   W=J*100/K
04700   G1=J*M/N
04800   G2=G1*6.328E-7/(2*SIN(S))
```

```
04900    FOR I=0 TO 1197
05000    B1=Z(I+1)-Z(I)
05100    B2=Z(I+2)-Z(I+1)
05200    P1=SGN(B1)+SGN(B2)
05300    IF P1=-2 THEN 5600
05400    IF P1=2 THEN 5600
05500    P2=P2+1
05600    NEXT I
05700    P4=P2/.48
05800    PRINT P4
05900    P2=0
06000    L1=T*1000/(3.14159*P4)
06100    L2=(L1**2)*(G2**2)/(162*N1*1E6)
06200    L3=(L1**2)*G2/(18*N1*1000)
06300    L4=T*F1/N1
06400    L6=(L1**2)*(G2**2)/(36*N1*1E6)*(P9/(1+3*P9))
06500    PRINT "MEAN VELOCITY IS                    ";T;"M/S"
06600    PRINT "TURBULENCE INTENSITY IS             ";W;"%"
06700    PRINT "CENTRELINE REYNOLDS NUMBER IS       ";L4
06800    PRINT "ENTITY REYNOLDS NUMBER IS           ";L5
06900    PRINT "MICROSCALE IS                       ";L1;"MM."
07000    PRINT "EDDY VISCOSITY IS                   ";L2;"M**2/S"
07100    PRINT "MEAN EDDY DISTANCE IS               ";L3;"MM."
07200    PRINT "EDDY DIFFUSIVITY OF HEAT IS         ";L6;"M**2/S"
07300    PRINT
07400    PRINT
07500    B=0
07600    G=0
07700    Y1=Y1+T
07800    Y2=Y2+W
07900    Y3=Y3+L4
08000    Y4=Y4+L5
08100    Y5=Y5+L1
08200    Y6=Y6+L2
08300    Y7=Y7+L3
08400    Y8=Y8+L6
08500    NEXT K1
08600    Y1=Y1/10
08700    Y2=Y2/10
08800    Y3=Y3/10
08900    Y4=Y4/10
09000    Y5=Y5/10
09100    Y6=Y6/10
09200    Y7=Y7/10
09300    Y8=Y8/10
09400    M9=Y6/Y1/F1
09500    N9=Y8*P9/N1
09600    P8=Y3*P9
09700    PRINT "ENSEMBLE AVERAGED RESULTS FOR 12000 SAMPLES:-"
```

```
09800    PRINT
09900    PRINT "              MEAN VELOCITY ="$Y1$"M/S"
10000    PRINT "                  MICROSCALE ="$Y5$"MM."
10100    PRINT "    TURBULENCE INTENSITY ="$Y2$"%"
10200    PRINT "       FLOW REYNOLDS NO. ="$Y3
10300    PRINT "       EDDY REYNOLDS NO. ="$Y4
10400    PRINT "DIFFUSIVITY OF MOMENTUM ="$Y6$"M**2/S"
10500    PRINT "N-D FACTOR FOR MOMENTUM ="$M9
10600    PRINT "     DIFFUSIVITY OF HEAT ="$Y8$"M**2/S"
10700    PRINT "           PRANDTL NUMBER ="$P9
10800    PRINT "     N-D FACTOR FOR HEAT ="$N9
10900    PRINT "           PECLET NUMBER ="$P8
11000    PRINT "           EDDY DISTANCE ="$Y7$"MM."
11100    END
```

## APPENDIX 14. ERROR ANALYSIS

The evaluation of error limits must be based, to some extent, on the experimenter's judgement; hence, such an evaluation is necessarily somewhat subjective. Nevertheless, an attempt has been made to set limits which are compatible with the observed degree of agreement among redundant measurements and the degree of reproducibility among repeated measurements. The error limits discussed in this Appendix are taken to represent a high confidence coefficient for the reported values of the respective measurements.

The equation used for the determination of the velocity, using the LDA, was:-

$$\bar{u} = \frac{f_D, \lambda}{2 \sin\frac{\Theta}{2}} \qquad (A14.1)$$

$$\therefore \quad \frac{d\bar{u}}{\bar{u}} = \frac{d\, f_D}{f_D} + \frac{d\lambda}{\lambda} - \frac{d\,(\sin\frac{\Theta}{2})}{\sin(\frac{\Theta}{2})} \qquad (A14.2)$$

As indicated by the instruction manual of the LDA supplied by DISA, the doppler frequency is measured in general with an accuracy of 1% and the wavelength of laser light is given with an accuracy of 0.04%. In order to estimate the accuracy involved in the measurements of the beam intersection angle, consider the geometry formed by the laser beam as in Figure A14.1, As the angle $\Theta$ was in general of the order of $5^o$, it could be assumed that:-

$$\sin\frac{\Theta}{2} \approx \tan\frac{\Theta}{2} = \frac{b/2}{a}$$

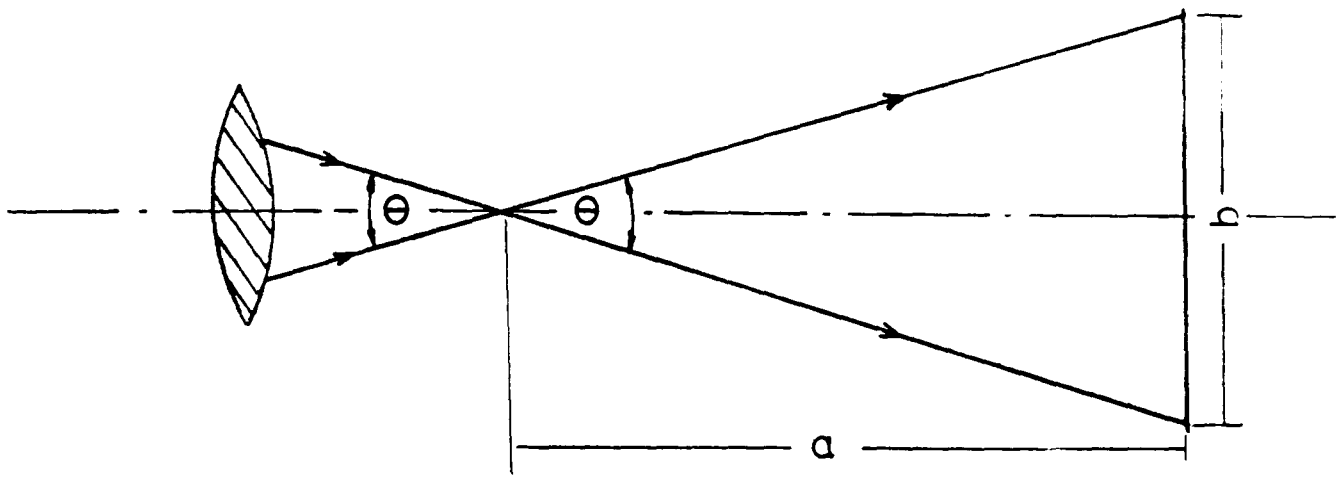


Figure A14.1 Intersection of laser beam

$$\therefore \quad \frac{d\left(\sin\frac{\Theta}{2}\right)}{\sin\frac{\Theta}{2}} = \frac{db}{b} - \frac{da}{a}$$

As a and b could be measured with an accuracy of about 0.5%, the order of magnitude associated with the error in the measurement of $\sin\frac{\Theta}{2}$ could then be assumed to be of 1%. Hence, the overall accuracy of velocity measurements may be expressed as:-

$$\frac{d\bar{u}}{\bar{u}} = O(1\%) + O(0.04\%) + O(1\%)$$

$$\therefore \quad \frac{d\bar{u}}{\bar{u}} \approx O(2\%)$$

Statistically, the error associated with sampling 12,000 data for the velocity measurement, as shown in section 2.3, was considerably less than 1%. Hence, the combined accuracy of the velocity measurements, using the LDA, may be taken as 2 per cent, i.e.:-

$$\frac{d\bar{u}}{\bar{u}} = O(2\%) \qquad \text{(A14.3)}$$

The equation used for the determination of the microscale was:-

$$\delta = \frac{\bar{u}}{\pi.N} \qquad \text{(A14.4)}$$

where N was the number of maxima and minima of u fluctuations per unit time. The above equation yields:-

$$\frac{d\delta}{\delta} = \frac{d\overline{u}}{\overline{u}} - \frac{dN}{N}$$

Although there was no direct way of evaluating the accuracy of N, the large values of N suggested a value of $\frac{dN}{N}$ comparatively smaller than 1%. Therefore, the accuracy of the microscale measurements could be taken to be the same order as the measurements of velocity.

$$\therefore \quad \frac{d\delta}{\delta} = O(2\%) \qquad \text{(A14.5)}$$

The equation used for the evaluation of eddy diffusivity of momentum was given by:-

$$\varepsilon_\nu = \frac{1}{162} \cdot \nu \cdot \delta^2 \cdot V_o^2 \qquad \text{(A14.6)}$$

where $Vo^2 = \overline{u'^2}$ and $\delta$ was the microscale.

$$\therefore \quad \frac{d\varepsilon\nu}{\varepsilon\nu} = 2. \frac{d\delta}{\delta} + 2\frac{dVo}{Vo} - \frac{d\nu}{\nu}$$

As u' was obtained in the same way as $\overline{u}$ using the LDA, the accuracy in their evaluation could be considered equal. Hence:-

$$\frac{dVo}{Vo} = \frac{du'}{u'} = \frac{d\overline{u}}{\overline{u}} = O(2\%)$$

For the accuracy of the evaluation of viscosity, although the eighth order Chebyshev polynomial was expected to give very accurate values of viscosity, temperature change during a test would lead to an error in the evaluation of viscosity. With a temperature change of $3^oC$, which was found to be the maximum rise in ambient temperature during one single test, the error associated with the evaluation of viscosity was found to be about 10%. Hence, the combined accuracy with eddy diffusivity of momentum could be expressed as:-

$$\frac{d\varepsilon_\nu}{\varepsilon_\nu} = 2.O(2\%) + 2.O(2\%) + O(10\%)$$

$$\therefore \quad \frac{d\varepsilon_\nu}{\varepsilon_\nu} = O(20\%) \qquad \text{(A14.7)}$$

The equation for the eddy diffusivity of heat was given by:-

$$\varepsilon_H = \frac{1}{36\nu} \left(\frac{Pr}{1 + 3\,Pr}\right) \cdot \delta^2 \cdot Vo^2 \qquad \text{(A14.8)}$$

$$\therefore \quad \frac{d\varepsilon_H}{\varepsilon_H} = 2.\frac{d\delta}{\delta} + 2.\frac{dVo}{Vo} - \frac{d\nu}{\nu} + \frac{dPr}{Pr} - \frac{3dPr}{1+3Pr}$$

As 3Pr>>1, it could be assumed that $\frac{3dPr}{1+3Pr} \approx \frac{dPr}{Pr}$. However, as the Prandtl number was evaluated using the expression, $Pr = \frac{\mu.Cp}{k} = \frac{\nu.\rho\,Cp}{k}$ and the variation of $\rho$, Cp and k were small over a temeprature difference of $3^oC$, it could be assumed that:-

$$\frac{dPr}{Pr} = \frac{d\nu}{\nu}$$

$$\therefore \quad \frac{d\varepsilon_H}{\varepsilon_H} = 2.\frac{d\delta}{\delta} + 2.\frac{dVo}{Vo} + 3.\frac{d\nu}{\nu}$$

$$= 2.O(2\%) + 2.O(2\%) + 3.O(10\%)$$

Hence, the overall accuracy of the eddy diffusivity of heat derived from LDA measurements could be taken as 40%.

$$\therefore \quad \frac{d\varepsilon_H}{\varepsilon_H} = O(40\%) \qquad \text{(A14.9)}$$

For the heat transfer measurements using the thermocouples, the total diffusivity of heat was given by:-

$$\varepsilon_T = \frac{\bar{u}.d^2}{16x} \frac{\Delta\Theta}{\Delta T} \qquad \text{(A14.10)}$$

where $\Delta\Theta = Tf - Ta$ and $\Delta T = T - Ta$.

$$\therefore \quad \frac{d_{\varepsilon T}}{\varepsilon T} = \frac{d\bar{u}}{\bar{u}} + 2.\frac{d\ d}{d} - \frac{dx}{x} + \frac{d\Delta\Theta}{\Delta\Theta} - \frac{d\Delta T}{\Delta T} \qquad (A14.11)$$

Assume the accuracy associated with each temperature measurement to be of the order x%.

$$\therefore \quad \frac{dTf}{Tf} = \frac{dTa}{Ta} = \frac{dT}{T} = x\%.$$

$$\therefore \quad dTf = Tf.x\%$$
$$dTa = Ta.x\%$$
$$dT = T.x\%$$

$$dTf - dTa = (Tf - Ta).x\%$$

and $dT - dTa = (T - Ta)x\%$

$$\therefore \quad \frac{d\Delta\Theta}{\Delta\Theta} = \frac{(Tf - Ta)}{(Tf - Ta)} . x\%$$

and $$\frac{d\Delta T}{\Delta T} = \frac{(T - Ta)}{(T - Ta)}.x\%$$

As the accuracy associated with the temperature measurement, with careful calibration, could be assumed to be of the order of 1%, the accuracy associated with the measurements of diameter d and distance x could be taken to be about 0.5%. Hence:-

$$\frac{d\varepsilon T}{\varepsilon T} = \bigcirc(2\%) + 2.\bigcirc(0.5\%) + \bigcirc(0.5\%) + \bigcirc(1\%) + \bigcirc(1\%)$$

$$= \bigcirc(5.5\%)$$

In addition, an error band of 5% was imposed for the evaluation of $\frac{\Delta\Theta}{\Delta T}/x$, as indicated in section 5.4. Hence the overall accuracy of total diffisuvity of heat obtained using the thermocouples could be taken as 10%. The eddy diffusivity of heat could be expressed as:-

$$\varepsilon_H = \varepsilon_T - \frac{k}{\rho Cp} \qquad \text{(A14.12)}$$

As the total diffusivity of heat is in general much larger than the molecular diffusivity of heat, in addition the variations of k, $\rho$ and Cp could be assumed to be small compared with the overall accuracy of $\varepsilon_T$, hence the accuracy of the eddy diffusivity of heat obtained using the thermocouples could also be taken as 10%.

$$\therefore \quad \frac{d\varepsilon H}{\varepsilon_H} = O(10\%) \qquad \text{(A14.13)}$$

For the Reynolds number of the flow, it could be expressed as:-

$$Re = \frac{\bar{u}.D}{\nu} \qquad \text{(A14.14)}$$

giving $$\frac{dRe}{Re} = \frac{d\bar{u}}{\bar{u}} + \frac{dD}{D} - \frac{d\nu}{\nu}$$

$$\therefore \quad \frac{dRe}{Re} = O(2\%) + O(0.5\%) + O(10\%)$$

Therefore, the accuracy associated with the Reynolds number evaluated with measurements using the LDA could be taken as:-

$$\frac{dRe}{Re} = O(12.5\%) \qquad \text{(A14.15)}$$

## APPENDIX 15. DERIVATION OF DIMENSIONLESS PARAMETERS

The Buckingham Π method presents a general approach of dimensional analysis which may be used even in problems for which the governing equations have not been formulated. Assume, first of all, the important parameters in heat transfer are as follows, with their dimensions given:-

| | | |
|---|---|---|
| diameter of pipe | D | $[L]$ |
| mean velocity of the fluid | u | $[LT^{-1}]$ |
| absolute viscosity of fluid | $\mu$ | $[ML^{-1}T^{-1}]$ |
| specific heat | Cp | $[L^2T^{-2}\Theta^{-1}]$ |
| eddy diffusivity of heat | $\varepsilon_H$ | $[L^2T^{-1}]$ |
| thermal conductivity | k | $[ML\ T^{-3}\theta^{-1}]$ |
| density | $\rho$ | $[ML^{-3}]$ |

A dimensionless parameter must be of the form:-

$$D^{x_1}.u^{x_2}.\mu^{x_3}.Cp^{x_4}.\ \varepsilon_H{}^{x_5}.k^{x_6}.\ \rho^{x_7}$$

Hence, the product, $[L]^{x_1}.[\ LT^{-1}]^{x_2}.[ML^{-1}T^{-1}]^{x_3}.[L^2T^{-2}\ \Theta^{-1}]^{x_4}.$ $[L^2T^{-1}]^{x_5}.[ML\ T^{-3}\Theta^{-1}]^{x_6}.[ML^{-3\ x_7}]$ is dimensionless. The dimensions of length, time, mass and temperature may be equated to zero respectively and obtain the following four equations for the unknown exponents.-

For the dimension of length $[L]$,

$$x_1 + x_2 - x_3 + 2x_4 + 2x_5 + x_6 - 3x_7 = 0 \qquad (A15.1)$$

For the dimension of time, $[T]$,

$$-x_2 - x_3 - 2x_4 - x_5 - 3x_6 = 0 \qquad (A15.2)$$

For the dimension of mass $[M]$,

$$x_3 + x_6 + x_7 = 0 \qquad (A15.3)$$

For the dimension of temperature $[\theta]$,

$$-x_4 \quad -x_6 \quad = 0 \qquad \text{(A15.4)}$$

As there are seven unknowns with four equations, it is necessary to have three exponents chosen arbitrarily. Equations (A15.1) to (A15.4) become:-

$$x_6 = -x_4$$

$$x_7 = -x_3 - x_6$$
$$= -x_3 + x_4$$

$$x_5 = -x_2 - x_3 - 2x_4 - 3x_6$$
$$= -x_2 - x_3 - 2x_4 + 3x_4$$
$$= -x_2 - x_3 + x_4$$

$$x_1 = -x_2 + x_3 - 2x_4 - 2x_5 - x_6 + 3x_7$$
$$= -x_2 + x_3 - 2x_4 + 2x_2 + 2x_3 - 2x_4 + x_4 - 3x_3 + 3x_4$$
$$= x_2$$

Hence, the dimensionless parameter becomes:-

$$D^{x_2}.u^{x_2}.\mu^{x_3}\ Cp^{x_4}.\ \varepsilon_H{}^{-x_2-x_3+x_4}.k^{-x_4}.\rho^{-x_3+x_4}$$

The three arbitrary exponents can be disposed by setting each in turn equal to 1 and simultaneously setting the remaining two exponents equal to zero. Thus, for

$$x_2 = 1, \quad x_3 = x_4 = 0$$

$D.u.\varepsilon_H{}^{-1}$ is non-dimensional

for $x_3 = 1$, $x_2 = x_4 = 0$

$\mu.\varepsilon_H^{-1}.\rho^{-1}$ is non-dimensional

for $x_4 = 1$, $x_2 = x_3 = 0$

$Cp.\varepsilon_H.k^{-1}\rho$ is non-dimensional

For turbulent momentum transfer, it may be assumed that the important parameters are:-

| | | |
|---|---|---|
| diameter of pipe | D | $[L]$ |
| mean velocity of the fluid | u | $[LT^{-1}]$ |
| absolute viscosity of the fluid | $\mu$ | $[ML^{-1}T^{-1}]$ |
| eddy diffusivity of momentum | $\varepsilon_\nu$ | $[L^2T^{-1}]$ |
| density | $\rho$ | $[ML^{-3}]$ |

The dimensionless parameter must be of the form:-

$$d^{y_1}u^{y_2}\mu^{y_3}.\ \varepsilon_\nu^{y_4}.\ \rho^{y_5}$$

Hence, the product, $[L]^{y_1}.[LT^{-1}]^{y_2}.[ML^{-1}T^{-1}]^{y_3}.[L^2T^{-1}]^{y_4}.[ML^{-3}]^{y_5}$ is dimensionless. As previously, equate the dimensions to obtain three equations for the unknown exponents:

For the dimension of length $[L]$,

$$y_1 + y_2 - y_3 + 2y_4 - 3y_5 = 0 \qquad (A15.5)$$

For the dimension of time $[T]$,

$$- y_2 - y_3 - y_4 = 0 \qquad (A15.6)$$

For the dimension of mass [ M] ,

$$y_3 + y_5 = 0 \qquad \text{(A15.7)}$$

$$\therefore \quad y_5 = -y_3$$

$$y_4 = -y_2 - y_3$$

$$y_1 = -y_2 + y_3 - 2y_4 + 3y_5$$

$$= -y_2 + y_3 + 2y_2 + 2y_3 - 3y_3$$

$$= y_2$$

Hence, the dimensionless parameter becomes:-

$$D^{y_2}.u^{y_2}\mu^{y_3}.\varepsilon_\nu{}^{-y_2-y_3}.\rho^{-y_3}$$

Again, by setting each of the exponents in turn equal to 1, non-dimensional parameters may be obtained. Thus:-

For $y_2 = 1$, $y_3 = 0$

$$D.u.\varepsilon_\nu{}^{-1} \text{ is non-dimensional}$$

For $y_3 = 1$, $y_2 = 0$

$$\mu.\varepsilon_\nu{}^{-1}\rho^{-1} \text{ is non-dimensional}$$

So far, five non-dimensional similarity parameters have been established associated with turbulent heat and momentum transfer. They could be expressed in terms of the eddy diffusivities of heat and momentum as:-

$$\Pi_1 = \frac{\varepsilon_H}{uD} \qquad \text{(A15.8)}$$

$$\Pi_2 = \frac{\varepsilon_H}{\mu}.\rho = \frac{\varepsilon_H}{\nu} \qquad \text{(A15.9)}$$

$$\Pi_3 = \frac{\varepsilon_H}{k/\rho Cp} \qquad \text{(A15.10)}$$

$$\Pi_4 = \frac{\varepsilon_\nu}{uD} \qquad \text{(A15.11)}$$

$$\Pi_5 = \frac{\varepsilon_\nu}{\mu}.\rho = \frac{\varepsilon_\nu}{\nu} \qquad \text{(A15.12)}$$